

The author(s) shown below used Federal funds provided by the U.S. Department of Justice and prepared the following final report:

**Document Title: Forensic Glass Analysis by LA-ICP-MS:
Assessing the Feasibility of Correlating
Windshield Composition and Supplier**

**Author: Abbegayle J. Dodds, Edward M. “Chip” Pollock,
and Donald P. Land**

Document No.: 232134

Date Received: October 2010

Award Number: 2004-IJ-CX-K007

This report has not been published by the U.S. Department of Justice. To provide better customer service, NCJRS has made this Federally-funded grant final report available electronically in addition to traditional paper copies.

**Opinions or points of view expressed are those
of the author(s) and do not necessarily reflect
the official position or policies of the U.S.
Department of Justice.**

**Forensic glass analysis by LA-ICP-MS:
Assessing the feasibility of correlating windshield composition and supplier**

Award No: 2004-IJ-CX-K007

FINAL TECHNICAL REPORT

Abbegayle J. Dodds¹⁻³, Edward M. “Chip” Pollock³, and Donald P. Land^{1,2}

¹Department of Chemistry, and ²Graduate Group in Forensic Science;
University of California, Davis

³Sacramento County District Attorney’s Laboratory of Forensic Services

Contact:

Robert A. Jarzen, Director
Sacramento County DA
Laboratory of Forensic Services
4800 Broadway, Suite 200
Sacramento, CA 95820
(916) 874-9240 *tel*
(916) 874-9620 *fax*
jarzenb@saccounty.net

Literature Review

Introduction

Glass fragments represent a valuable class of trace evidence. Like other traces materials, they are easily transferred from source to suspect, and are easily unnoticed by the suspect bearing them; further, glass fragments are particularly durable. Most glass products readily shatter when broken, distributing glass fragments to objects and persons in their path. Because there is a limited radius of distribution, glass transfers generally represent primary transfers resulting from contact or close proximity with the broken glass product (1). While secondary and environmental transfers do occur, they are rare (2-4); this suggests that most individuals bearing glass fragments were near the glass product(s) distributed on their person when the breaking event occurred. The persistence of these transfers is largely dependent on the retention of the material to which the transfer is deposited (1), whether the transfer was passive or forcible, and the ability of glass to withstand environmental effects. Common items of clothing (cotton and woolen materials) show a high retention for glass, passively or forcibly transferred. Certain materials, such as wood, soft polymers and metals, retain glass transfers only if forcible contact is made between the material and the glass source. Because glass fragments are often minute and transparent, it is usually difficult for a suspect to see the evidence and remove it. Glass fragments persist on a suspect's clothing or in soft materials for extended periods of time since glass is resistant to environmental degradation.

Classical methods of forensic glass examination are based primarily on variation within the physical properties of glass. Color, density, surface characteristics and optical properties have been relied upon for the comparison of unknown glass fragments with

control glasses (5-7). Surface characteristics and optical properties deserve attention in particular. Similarities in peculiar surface contamination or patterns of erosion between reference and questioned items are highly associative; like fracture edge matching, however, comparing original surfaces requires recovery of abnormally large questioned fragments.

The most common technique for comparing reference and questioned items is by refractive index (RI) comparison (5-7). RI measurement is excellent for distinguishing glasses by type and limited sample is required for multiple measurements. Historically speaking, RI measurement had limited application for classifying glass fragments because RI varied greatly among and within the traditional classes of glass (e.g., tableware, architectural glass, automotive glass, etc). Modern improvements in glass manufacture have decreased the RI variation within a particular class of glass (8). Modern glass has been observed to have a fairly consistent RI that corresponds to the type of glass in question; this makes RI an excellent tool for classifying glass but limits the utility of RI measurement for forensic individualization (7, 9-11). Some have proposed the measurement of RI at multiple wavelengths (called “dispersion analysis”) to enhance individualization by RI. It is rare that dispersion analysis enhances the discriminating power of RI (6).

The first reports of chemical analysis for the forensic discrimination of glass were published in the early 1970s. Initial analyses were made with the intention of classifying glass by type, using a wide variety of instrumental techniques including: neutron activation analysis (NAA), direct current arc source atomic emission spectrometry (AES), atomic absorption spectrometry (AAS), spark-source mass spectrometry, and x-ray

fluorescence (10-18). The inorganic constituents targeted by these methods were in the part-per-million (or $\mu\text{g g}^{-1}$) to part-per-hundred (or dg g^{-1}) concentration levels. Over twenty elements were shown to have application in differentiating between sheet, container and tableware classes of glass (10).

Due to the cumbersome operation of NAA, the semi-quantitative nature of spark source mass spectrometry and x-ray fluorescence, and the limitation of single element quantitation inherent to AA, forensic researchers incorporated inductively coupled plasma source AES in the late 1970s and 1980s. Using this technology, Catterick and Hickman showed the potential to discriminate glasses by type having sample sizes of 500 μg or less (9). They also reported that no correlation existed between chemical composition and RI, indicating that chemical data can be used in conjunction with RI for increased distinction of glasses by type. The increased discrimination of elemental data used in conjunction with RI data was also suggested by Koons, Peters and Rebbert (17). In a separate report, Koons and Buscaglia (19) estimated the random occurrence of two fragments being indistinguishable in RI and elemental composition to be $10^{-13} - 10^{-15}$. This would indicate that chemical data in tandem with RI measurement could facilitate individualization of glass with a high degree of certainty.

Discrimination among glasses using chemical data alone was first suggested by the results of Catterick and Hickman; they showed the discrimination potential of certain elements in discriminating glass samples that fell into the same general class (9). Koons, Fiedler and Rawalt (20) demonstrated the differentiation of sheet glass produced by separate manufacturing plants using six elements. Zurhaar and Mullings (21) argue that the quantitation of 15 – 25 elements provides a unique elemental profile for a particular

glass sample. They further report that 85 – 95% of window glass samples manufactured in the US and Australia are easily distinguished when a greater suite of elements are analyzed. While the uniqueness of a particular elemental profile can be argued (22), there has been a marked increase in the discrimination of glasses within a class by increasing the number of elements quantified and targeting trace elements ($\leq \mu\text{g g}^{-1}$ in concentration, 23).

Until the advent of ICP-source mass spectrometry (ICP-MS), the ability to perform simultaneous, multielement quantitation was not available for the forensic analysis of glass. While ICP-AES is capable of performing multielement quantitation, this technique does not offer simultaneous, multielement data collection. Nor is ICP-AES able to detect low-level elements, especially following acid digestion and sample dilution. Zurhaar and Mullings (21) were the first to apply ICP-MS to the glass matrix for forensic analysis. Parouchais, *et al* (24) used the principles of analysis set forth by Zurhaar and Mullings to propose improved sample preparation protocol for glass analysis by ICP-MS. In the work following, Suzuki, *et al* (25) were able to show the superior discriminatory capabilities of elemental data collected by ICP-MS for bottle glass; Montero, *et al* (26) similarly showed a high level of discrimination available for vehicle float glass using ICP-MS.

Forensic Glass Analysis by ICP-MS

The ICP-MS is a highly sensitive instrument capable of performing rapid, simultaneous, multielement analysis. This technique offers exceptionally low detection limits ($< \text{pg mL}^{-1}$) compared to other techniques for elemental analysis, and can be used

to detect over 70 isotopes. The ICP-MS has three main components: (1) the sample introduction mechanism, which is variable to accommodate gaseous, liquid, and solid samples, (2) the plasma and MS interface region, and (3) the mass analyzer and detector. Following sample introduction, the sample is injected into the plasma and undergoes desolvation and atomization. The resulting atoms are then ionized in the high-energy environment of the plasma; ions are transported through the MS interface region due to a sequential decrease in pressure. They are then mass-filtered and detected by a quadrupole or time-of-flight (TOF) mass spectrometer. Most commercial instruments are equipped with a quadrupole MS.

One of the many benefits of ICP-MS is the number of sample types that may be accommodated. The ICP-MS has been adapted for gaseous, liquid and solid samples, though the original design was intended for liquid sample introduction (called solution nebulization, SN). Early applications of ICP-MS to glass analysis involved lengthy dissolution protocols so that glass could be introduced using SN (21, 23-27). Advances in solid sampling for ICP-MS have been realized in the past decade, and now several reports regarding solid sampling for ICP-MS exist. The majority of forensic applications involve the use of laser ablation (LA) sample introduction (8, 28-30).

SN is the most common sample introduction technique for ICP-MS (31-35) and has wide application in forensic science (21, 36-40). It was the first method of introduction for the forensic analysis of glass (21, 23, 24). In fact, it is the only sampling technique for which an American Standards for Materials and Testing (ASTM) method exists (27). A multitude of sample types are appropriate for SN; matrix-matched calibration and quality control standards are easily obtained. One practical benefit of SN

is the decreased cost over other introduction techniques. Further, current instrumental configurations facilitate highly automated and rapid analysis. Automated instrument optimization and analysis are available, enabling high sample throughput with little analyst intervention. By comparison to solid sampling, less instrument maintenance is required using liquid sample introduction. This is because liquid samples leave fewer deposits on the sampler and skimmer cones and ion lens. While there are a few exceptions, liquid samples tend to be “cleaner” overall (31).

The main drawback of SN introduction is that it is difficult to adapt to solid sample types (31-35). This is especially true of the glass matrix. For the forensic analysis of glass, a costly, time-intensive and potentially hazardous digestion using hydrofluoric acid (HF) is required. This digestion is open-vessel and is followed by two days of sample preparation (27). This process provides many opportunities for contamination and dilution errors; worse, it is a destructive technique.

The existing digestion protocol facilitates only a narrow range of sample masses because the final dilution volumes are relatively small. The minimal suggested sample size, 500 μg , is atypical of glass fragments received as evidence. Glass fragments of only several micrograms in mass are more frequently recovered than those of several hundred micrograms. Having trace elements at 1 – 100 parts-per-million, routine casework fragments push the lower sample size limits for SN-ICP-MS using the established forensic methodology. Finally, the resulting sample volumes might prevent the analyst from performing replicate analyses with certain devices for SN sample introduction. Nonetheless, SN introduction remains the most frequently used sample introduction technique for forensic glass analysis by ICP-MS.

Only a handful of forensic applications exist for LA-ICP-MS, including methods for glass, paint, and bulk metal materials (8, 28-30). Glass analysis stands out as the prominent and best-developed forensic application of both ICP-MS and LA-ICP-MS. Since the application of the LA sampling technique to ICP-MS, forensic analysts have been able to push the lower limits regarding sample size while providing comparable or greater statistical information than was previously available (29, 30).

Due to the diminutive sample size requirements for LA sampling, typical casework sample sizes are easily accommodated. For example, to perform triplicate analyses of a single questioned glass fragment an optimal sample volume of $3 \times 10^6 \mu\text{m}^3$ is preferred; this corresponds to a fragment 300 μm in length, 100 μm in width and 100 μm in depth. In terms of mass, such a fragment is approximately 7 μg . To examine glass by SN-ICP-MS, many would argue that the minimum sample mass is 500 μg but some agencies require 2000 μg – of which 100% is consumed by digestion and analysis. If a traditional-flow (1 mL min^{-1}) nebulizer is used, only one analysis can be performed for a particular digest. This presents a limitation in that statistics cannot be applied to the result. Alternatively, only 0.9 μg glass is consumed during a triplicate analysis using LA. This is roughly 12% of a 7- μg fragment. The limited sample consumption of this technique enables the analyst to perform replicate analyses while preserving the majority of the sample. A benefit to the minimal sample consumed during LA analysis is that when fragments larger than the minimum are recovered (15 μg or more), there is enough sample for additional analyses to be conducted independently. To analyze fragments by SN-ICP-MS, the criminalist performing elemental analysis would be required to obtain permission prior to digestion and analysis; additional scientific experts would be then

able to view the analysis conducted by the criminalist but they would not be able to conduct an independent analysis.

Sample preparation requirements for LA introduction are greatly reduced over those required for SN introduction. For glass analysis by LA-ICP-MS, the samples need only to be cleaned and mounted on a glass slide. There is little opportunity for contamination and no dilution error – both advantages of analyzing the sample “as it is.” This benefit was much lauded by Lundell in 1933 (41), who asserts that valuable analyte information can be lost when removed from the original sample matrix. The field of criminalistics similarly fosters the ideology of *in situ* analysis – physical evidence examinations are always performed in such a manner as to provide highly discriminating data while preserving the character and quantity of the sample to the extent possible.

Currently, the primary analytical limitation of LA is calibration; for some applications, internal standardization is an equally limiting factor. The issue of calibration stems from the fact that well characterized matrix-matched calibration standards are not readily available for many sample matrices. To overcome this issue many have attempted liquid calibration by SN or LA, while many others use the solid National Institute of Standards (NIST) standard reference glasses 610 and 612 for single point calibration (31, 42-46). The use of a single calibrant has been done following the validation of linear response in analyte: internal standard. Alternatively, it is done under the assumption that LA sampling does not alter the many decades of linear response available from ICP-MS. However, this assumption may not be valid for some analytes in certain matrices (47). As Akbar Montaser aptly put, calibration remains the “Achilles’ heel of the laser ablation technique” (31).

Internal standardization is not easily incorporated into solid sampling techniques for ICP-MS. Unlike samples in solution, internal standard spikes are not easily added to solid samples. Instead, it is desired to use an isotope for which analytical response is representative of most or all analytes, that is naturally occurring in the sample, and that is easy to quantify. Generally speaking, this entails the use of a mid-mass isotope (31, 42). Isotopes of silicon have been used for analytes in a variety of matrices including glass (30, 48).

The FBI and forensic research groups have been the primary users of ICP-MS for forensic glass analysis in recent years. To date, less than a dozen state-run crime laboratories own an ICP-MS and among these, the majority makes use of SN sample introduction. The central reason behind the slow integration of ICP-MS to routine casework is the cost of purchasing and maintaining this instrumentation. Modern ICP-MS instruments cost approximately \$300,000 and consume high purity argon at a rate costing operators anywhere from \$12,000 to \$15,000 per year. When the additional cost of a LA unit is considered (approximately \$125,000) criminalists are skeptical of such a purchase. Many crime labs struggle to make instrument purchases equal to that of the LA system alone. Nonetheless, the criminalistics community is becoming aware of the discriminating potential of glass analysis by ICP-MS. This has created a demand for increased collaboration among the more and less equipped forensic labs: forensic research groups often consult for local crime labs, while larger crime labs (such as the FBI and some state crime labs) will similarly consult for less well-funded labs.

Since a variety of techniques are available for the forensic analysis of glass by ICP-MS, it is important to provide a direct comparison of the figures of merit achievable

using each technique. One report exists describing the application of both SN-ICP-MS and LA-ICP-MS (30) to forensic casework samples; a multitude of publications exist describing some aspects of the analytical performance of SN and LA (8, 21, 24, 27, 30, 31, 42-46, 48-51). However, none were dedicated to the comparison between traditional flow SN, micro-flow SN and LA sampling in terms of classical figures of merit. Here, the relative figures of merit for SN using a traditional concentric nebulizer (CN), a microflow concentric nebulizer (or microconcentric nebulizer, MCN), and LA using a 213-nm Nd:YAG laser ablation unit are compared. These are among the most common methods of SN and LA introduction available; it is likely that members of the forensic community will encounter these sample introduction techniques before others.

The Forensic Significance of Elemental Variation in Glass

The face of forensic glass examination has changed dramatically with the advent of trace elemental analysis by ICP-MS. Classical methods of forensic glass analysis, such as color comparison, density measurement and RI comparison, do not offer the individualizing potential that quantitative trace elemental analysis promises. While the discriminating potential of trace elemental analysis has been demonstrated, the individualizing power of this technique has not been well characterized.

Technically, glass is an amorphous, super cooled liquid formed by fusion (52). Glass is manufactured from inorganic oxides, which when melted together chemically react to form the final glassy product. The primary component of glass is silica sand (SiO_2). Because the fusion temperature of pure silica is too high for most commercial furnaces, sodium oxide (Na_2O) is added to reduce the fusion temperature. Such an

additive is a “fluxing agent.” Glass is classified by the chemical “modifiers” added to produce the glass end product having certain performance characteristics. Common classes of glass are soda-lime-silicates, alumino-silicates, and borosilicates. Respectively, these are silicate glasses with limestone (CaO), alumina (Al₂O₃) and boric oxide (B₂O₃) modifiers. The major inorganic constituents of common consumer glasses are described in Table 1.

Table 1. Major constituents of common consumer glasses (52).

Glass type	Use	Major constituents (0.02 – 80 % by weight)
Container		
<i>White</i>	Bottles, jars	SiO ₂ , Al ₂ O ₃ , Fe ₂ O ₃ , CaO, MgO (except Amber), Na ₂ O, K ₂ O (except Green) and Cr ₂ O ₃ (Green only)
<i>Amber</i>		
<i>Green</i>		
Float	Windows, windshields	SiO ₂ , Al ₂ O ₃ , Fe ₂ O ₃ , CaO, MgO, Na ₂ O, K ₂ O
Borosilicate	Kitchenware, labware	SiO ₂ , Al ₂ O ₃ , Fe ₂ O ₃ , CaO, Na ₂ O, K ₂ O, B ₂ O ₃
Lead crystal	Decorative	SiO ₂ , Al ₂ O ₃ , Fe ₂ O ₃ , Na ₂ O, K ₂ O, PbO, B ₂ O ₃ , As ₂ O ₅

The process of glass manufacture can be summarized by the following steps: (1) weighing and mixing of raw materials, (2) glass melting, (3) glass forming, (4) annealing, and (5) secondary processing (52, 53). The process of weighing and mixing of raw materials for the manufacture of consumer glass is highly automated, making use of conveyer belts and computer-operated chutes that dispense specified amounts of raw

materials. The glass is melted in brick furnaces, wherein temperatures rise to approximately 2000°C. During this process, the glass is mixed to ensure adequate homogenization. Mixing during melting also facilitates the release of gaseous carbon dioxide created during chemical reactions of inorganic constituents. Glass formation is progressive; as melted material moves forward in the furnace (which is continuously fed with raw materials), the temperature is manipulated such that fusion occurs at the rate appropriate for the glass forming method used. The annealing process involves slow cooling of the glass, so that stress points are minimized. Finally, depending on the glass end product desired, the glass may require secondary treatments such as tempering, coating or decorating.

The most common type of glass encountered in the forensic context is “float glass,” so named for the bed of molten tin on which glass is floated during forming. After exiting the melting furnace, glass is floated in melted tin in a controlled environment. The glass forms a sheet, called a “ribbon,” that exits the tin chamber and is progressively cooled on lehrs. This method was first introduced by the Pilkingtons of Great Britain in the late 1950s. The float process produces glass of exceptional quality over other methods of glass manufacture (52). Over the years, glass produced by the float process has begun to vary less and less in physical properties, including RI (8). As a result, RI measurement alone has limited utility for discriminating float glass, especially modern float glass. The success of trace element analysis in discriminating float glass products of different origin, yet having similar physical properties, is related to the detection of trace constituents. These constituents are unintentional components of the batch, and their amounts are uncontrolled at the manufacturing stage.

The amounts and sources of major batch constituents, such as silica sand (SiO_2), soda ash (Na_2O) and limestone (CaO), are never modified (Personal communication, Chris Miller of Pilkington-Libbey Owens Ford). However, the amounts of colorants and recycled glass, or cullet, are varied depending on the desired characteristics of the glass end product (52, 53). Colorants are added in predictable amounts; like the major constituents, these chemicals are of little forensic utility since their amounts are consistent among manufacturers producing similar glass products. Cullet introduces the greatest potential for individualizing otherwise similar glass, since the amount of cullet that is incorporated in the batch can change daily. Further, there is no federal or state-mandated minimum for cullet consumption in the manufacture of float glass. The amount of cullet that is incorporated is left to the judgment of the manufacturer alone. An additional source of compositional variation is the potential for micro-impurities in the batch constituents. Such low-level impurities are not likely to be made manifest in color changes and probably vary by source of the raw material in question.

While trace elemental analysis is currently the most distinguishing technique available for the forensic analysis of glass, it is difficult to assign the significance of trace elemental data because the potential for natural variation in glass composition has not been adequately addressed. Little has been published regarding the potential for compositional variation within a single glass product, or within a class of glass products.

Trejos and Almirall conducted a study aimed at evaluating the potential for micro-heterogeneity in glasses pertinent to forensic casework, targeting compositional variations at the micro-scale. It was shown that the typical ablation parameters used for bulk analysis by LA-ICP-MS did not result in misrepresentative sampling (22). A similar

conclusion was reached by Kempanaers, *et al* in a study describing the micro-heterogeneities found in glass standard reference materials (54). Duckworth, *et al* published a report describing significant elemental variation in a population of 72 automotive side windows produced by 19 separate manufacturers (55); the large variations observed within this class of glass facilitated a high degree of individualization, especially when RI data was included with elemental data. Duckworth, *et al*, however, failed to report whether within-sample variation was observed in these automotive side windows.

It is reasonable to hypothesize that some compositional variation exists in glass, since it is continuously manufactured with the addition of new raw materials and cullet in variable amounts. This is particularly true of automotive windshields, which are composed of two relatively large discrete panes of glass joined by a layer of lamination (53). If compositional heterogeneity in glass exists at the trace level, it is reasonable to postulate that such heterogeneity would become apparent in larger glass products. Further heterogeneity is possible in automotive windshields, since they are not always composed of panes that are manufactured sequentially. In fact, certain manufacturers assemble windshields from panes of glass produced from completely separate batches, which differ in thickness and color.

While potential micro-heterogeneities in glass have been shown to have no effect on the quality of forensic glass analysis by LA-ICP-MS, the potential impact of macro-heterogeneity has not been assessed, especially with respect to automotive windshield glass. The potential for elemental variation between the two panes of glass comprising automotive windshields has been shown (22), but this variation has not been determined

for a large population of windshields. Without confidence in the homogeneity of automotive windshields, it is difficult to establish the suitable number of reference samples to be collected for forensic comparisons by LA-ICP-MS. Further, it is difficult to assign the significance of similar or dissimilar elemental profiles when the potential for heterogeneity has not been excluded.

Trace elemental profiling has, thus far, been used exclusively as a comparative tool. That is, as a means to compare questioned and reference glass fragments to establish whether the questioned fragments could have originated from the reference glass. The potential for elemental profiling to provide investigative information has not been explored. Typically, individual glass manufacturing plants are dedicated facilities that specialize in the production of a single type of consumer glass product. Since the major batch constituents used to produce various glass products are rarely changed, the trace impurities present in the raw materials may serve as a unique fingerprint for a specific manufacturing facility. Such impurities would necessarily exhibit larger variation in a broad population of windshields from various manufacturers than the variation observed between windshields produced by the same manufacturer, to successfully fingerprint glass.

The elemental variation of automotive windshields was investigated in three ways: within-pane variation, within-sample variation and population variation. This was done to supplement the existing body of knowledge regarding the discriminatory potential of elemental analysis by LA-ICP-MS, since this potential has not been fully evaluated for automotive windshield glass exclusively.

Research Purpose

With the advent of forensic trace element detection by ICP-MS comes the unique opportunity to evaluate the variability in the elemental composition of automotive windshield glass. Of particular interest to the Sacramento County District Attorney's Laboratory of Forensic Services is the utility of trace elemental profiling for fingerprinting automotive windshields produced by a specific manufacturer. The impetus for this research is a long-standing case. Recently, we became involved in a homicide case wherein a vehicle was used as the murder weapon. Glass fragments were the only recovered evidence from the victim. Though a vehicle was seen running the victim down, a suspect was not immediately identified. After several months of investigation, a man who had argued with the victim became the primary suspect in the case. However, when investigators examined the suspect's car, there was no apparent damage. None of the windows were broken, and the vehicle's paint appeared flawless. Upon further examination, investigators were able to locate glass fragments inside the engine compartment of the vehicle. These were collected and compared to the glass fragments recovered from the victim. The techniques used to analyze these glass samples included RI measurement and elemental analysis by SEM-EDS and LA-ICP-MS. In terms of RI and major elemental composition, the questioned and reference fragments appeared similar. The results of trace elemental analysis by LA-ICP-MS corroborate this finding, however, it is difficult to assign significance to this finding as the uniqueness of a given trace elemental profile is unknown. Further, the homogeneity of automotive windshields is unknown.

The goal of this study was to provide forensic caseworkers with sufficient context regarding within-sample variation and population variation in the compositions of automotive windshields so that the appropriate significance can be assigned to trace elemental data. To do so, we collected and analyzed 50 automotive windshields representing 17 separate manufacturers and one unknown manufacturer. We examined the within-pane variation of the interior and exterior panes of automotive windshields using a subset of 10 windshields, the total variation in elemental composition exhibited by all 50 windshields (100 panes of glass all together), and the variation observed within groups of manufacturers. The elemental data for all 50 windshields was organized into a Microsoft Access database. Qualitatively, we examined the variation in glass production by analyzing quality control samples collected directly from float glass manufacturers' stocks. This was done to determine whether other types of float glass products could exhibit the patterns of variation observed in automotive windshields.

We observed that some, not all, windshield panes exhibited heterogeneity and found that about half the windshields we analyzed were composed of significantly different panes of glass. We also found that the compositional variation of windshields from individual manufacturers was much smaller than that observed in the total population of automotive windshields. This finding suggests the potential for fingerprinting glass produced by specific manufacturers; additional research is required to fully evaluate this potential. Should this prove to be a feasible means of correlating consumer glass products with their manufacturers, investigative information may be gained from analyzing questioned fragments in the absence of reference samples. Using elemental data to provide investigators with putative sources of evidentiary glass

fragments is an attractive possibility, since this is a common occurrence in hit-and-run offenses.

Prior to commencing the above research, we validated the use of SN- and LA-ICP-MS for forensic casework. As a public service forensic laboratory, it is our priority to make new techniques immediately available for casework analysis. Once we have tested the validity of new techniques, it is our mission to make these techniques available to other public service forensic laboratories that, for whatever reason, do not otherwise have access to them. We found that SN- and LA-ICP-MS can be confidently applied to casework analyses, as long as the relative shortcomings of each technique are acknowledged. However, we found that LA-ICP-MS emerges as the superior technique for forensic glass analysis when the performance characteristics of SN- and LA-ICP-MS are compared.

At the close of this research, we were able to establish the validity of trace elemental analysis for the forensic analysis of casework samples and determine what level of significance to apply to trace elemental data.

Materials and Methods

SN-ICP-MS: Figures of Merit

We characterized the figures of merit achievable using SN-ICP-MS and the ASTM method E 2330-04 (with some modifications) for two different nebulizers alternatively joined to the same quartz conical spray chamber. The common concentric nebulizer (CN) and the microconcentric nebulizer (MCN) were investigated. The MCN operates on the same principles as the CN, but is designed for low sample consumption.

The CN used in this study was operated at a nominal sample uptake rate of 1 mL min⁻¹ while the MCN was operated a nominal sample uptake rate of 0.1 mL min⁻¹.

The figures of merit established for each nebulizer included: method detection limits (MDLs), limits of quantitation (LOQs), analytical sensitivity, accuracy, precision, and bias as well as short- and long-term reproducibility.

Analyte Selection and Sample Preparation. The element menu used for this comparison was based on ASTM E 2330-04 (Table 2).

Table 2. Table of analytes.

Element, Symbol	<i>m/z</i>
Magnesium, Mg	25, 26
Titanium, Ti	47
Manganese, Mn	55
Gallium, Ga	69, 71
Rubidium, Rb	85
Strontium, Sr	86, 88
Zirconium, Zr	90, 91, 92, 94
Antimony, Sb	121
Barium, Ba	137, 138
Lanthanum, La	139
Cerium, Ce	140
Hafnium, Hf	178
Lead, Pb	206, 207, 208

Two Standard Reference Materials (SRMs) from the National Institute of Standards and Technology (NIST; Gaithersburg, MD, USA) were selected to examine the accuracy, precision and bias of SN-ICP-MS: NIST SRMs 610 (nominally 500 µg g⁻¹ in selected trace elements) and 612 (nominally 50 µg g⁻¹ in selected trace elements). These SRMs were selected over other available standard glasses because they are well characterized (56).

A single wafer of each SRM was broken from which ten fragments were sampled spanning a mass range of 0.1 to 0.5 mg (Table 3). These fragments were washed in methanol (VWR, West Chester, PA, USA), and soaked in 10% ultra pure nitric acid (HNO₃, OmniTrace *Ultra*; EM Sciences, Merck KgaA, Darmstadt, Germany) for no less than 30 minutes. Each was rinsed deionized water between washings (Resistivity = 18 MΩ • cm; Barnstead, Dubuque, IA, USA). Every sample was allowed to air-dry. Masses for each fragment were recorded (±0.002 mg) before each was transferred to a 15-mL metal free polyethylene sample tube (CPI International, Santa Rosa, CA, USA).

Table 3. Masses of selected NIST SRM fragments.

NIST SRM 610		NIST SRM 612	
<i>Designation</i>	<i>Mass, mg</i>	<i>Designation</i>	<i>Mass, mg</i>
1	0.306	1	0.279
2	0.180	2	0.273
3	0.195	3	0.194
4	0.422	4	0.230
5	0.189	5	0.307
6	0.409	6	0.269
7	0.095	7	0.309
8	0.182	8	0.235
9	0.374	9	0.191
10	0.549	10	0.504

Samples were digested using 600 µL of a 3:1:1 concentrated hydrofluoric acid (HF, from OmniTrace; EM Sciences, Merck KgaA, Darmstadt, Germany), concentrated HNO₃, and concentrated hydrochloric acid (HCl, from OmniTrace; EM Sciences, Merck KgaA, Darmstadt, Germany) mixture. The sample tubes were capped, vortex mixed and placed in a sonicating bath for at least two hours until completely dissolved. The samples

were then uncapped and placed on a heating block at 80°C for approximately 36 hours or until dry. Samples were stored dry, at room temperature.

Samples were reconstituted with 4 mL 10%-HNO₃ for at least 24 hours but not longer than 48 hours. Finally, each sample was internally standardized by adding 25 µL of a 10-µg mL⁻¹ rhodium (Rh) stock solution (CPI International, Santa Rosa, CA, USA) and diluted to a final volume of 5 mL using 18-MΩ H₂O. The final concentration of Rh in each of the samples was 50 ng mL⁻¹. NIST SRMs 610 and 612 prepared in this way yielded approximately 30 – 50 ng mL⁻¹ and 1 – 5 ng mL⁻¹ trace elements, respectively. Procedural blanks were prepared by adding the acid mixture to a clean, empty sample tube. These samples were digested, reconstituted and diluted as above.

For reproducibility testing, a single fragment of SRM 610 was selected (mass = 6.963 mg). This fragment was chosen to serve as a stock from which multiple dilutions could be made, to eliminate the digestion procedure as a potential source of variation. Following digestion (as described above), this solution was reconstituted in 5 mL 10%-HNO₃ for 24 hours. To prepare reproducibility solutions, a 500-µL aliquot of this stock solution (approximately 700 ng mL⁻¹ in concentration) was transferred to a metal free sample tube; the aliquot was diluted with 25 µL 10-µg mL⁻¹ Rh and 4.750 mL 18-MΩ H₂O to obtain solutions that were approximately 70 ng mL⁻¹ in concentration.

Instrumentation and Analytical Methods. A Perkin Elmer Elan DRC II ICP-QMS (Boston, MA, USA), equipped with a Cetac Autosampler/Autodilutor (Omaha, NE, USA), was used for this study. The instrument was operated in normal mode (i.e., without reaction gas), using default mathematical corrections for common isobaric interferences (corrected elements are shown in Table 4). Prior to analysis, instrument

optimization was performed using standard solutions. Table 5 summarizes the typical instrumental parameters used during this study.

Table 4. Default interferent correction.

Isotopes	Interferents	Correction
^{86}Sr	$^{86}\text{Kr}^+$	$- 1.505657 \times S(^{83}\text{Kr}^+)$
^{92}Zr	$^{92}\text{Mo}^+$	$- 0.932161 \times S(^{95}\text{Mo}^+)$
^{94}Zr	$^{94}\text{Mo}^+$	$- 0.581030 \times S(^{95}\text{Mo}^+)$
^{138}Ba	$^{138}\text{La}^+, ^{138}\text{Ce}^+$	$- 0.000901 \times S(^{138}\text{La}^+) - 0.002838 \times S(^{138}\text{Ce}^+)$

Key: $S(^{83}\text{Kr}^+)$ refers to the signal due to $^{83}\text{Kr}^+$

For all solution analyses, the same quartz cyclonic spray chamber (Perkin Elmer, Boston, MA, USA) was alternately joined to a quartz concentric nebulizer (CN; Perkin Elmer, Boston, MA, USA) or a MicroMist quartz microconcentric nebulizer (MCN; Glass Expansion, West Melbourne, Victoria, AU). The quartz CN had a typical sample uptake rate of approximately 1 mL min^{-1} ; the quartz MCN had a typical sample uptake rate of approximately 0.1 mL min^{-1} .

Table 5. Typical ICP-MS operating parameters.

Parameter	Value
Nebulizer Gas Flow	
<i>CN</i>	1.0 L min^{-1}
<i>MCN</i>	1.1 L min^{-1}
Auxiliary Gas Flow	1.2 L min^{-1}
Plasma Gas Flow	15 L min^{-1}
RF Power	1350 W
MS Analytical Settings	20 sweeps / reading 1 reading / replicate 3 replicates

External calibration was performed using a simple linear model with the multielement calibration standards described in Table 6. Each was internally standardized with 50 ng mL⁻¹ Rh. To prepare these standards, multielement standard stock solutions obtained from Spex CertiPrep (Metuchen, NJ, USA) were used. A quality control (QC) sample was prepared using the same standard stocks to monitor calibration drift. The QC sample was a multielement solution, containing all analytes of interest prepared at 60 ng mL⁻¹ with 50 ng mL⁻¹ Rh. A 10% tolerance was applied to the QC sample.

Table 6. Calibration and QC standard concentrations.

Calibration Level	Final Concentration, ng mL ⁻¹
Blank, S(0)	0
Level 1, S(1)	1
Level 2, S(2)	10
Level 3, S(3)	50
Level 4, S(4)	75
Level 5, S(5)	150
Quality Control	60

To determine method detection limits, three procedural blanks were analyzed on two nonconsecutive days. To fairly compare the CN and MCN, these were analyzed on the same days to eliminate potential interday variation in instrument performance. Sensitivity was determined by averaging calibration data for two nonconsecutive days. For accuracy and precision testing, ten fragments of NIST SRMs 610 and 612 were digested, reconstituted and prepared as above. Single replicates were performed on these samples using both the CN and MCN. Bias determinations were made from these results. Within-run reproducibility could be established for MCN introduction only; this was accomplished by analyzing the first five digests of NIST SRMs 610 and 612 in quadruplicate. Within-day reproducibility was determined by single replicates of three

reproducibility samples (dilutions from a single stock, as described above) separated by no less than 90 minutes using the CN. Triplicate analyses were run on the same solutions at similar time intervals using the MCN. Long-term reproducibility was determined by analyzing freshly prepared reproducibility samples using CN and MCN for four nonconsecutive days. Each day, the same solution was analyzed using the CN and MCN. Single replicates were performed using the CN; triplicate analyses were performed using the MCN.

Data Analysis and Calculations. Method detection limits (MDLs) and limits of quantitation (LOQs) were then calculated using the method described by Miller and Miller (57), modified to account for internal standardization:

$$MDL = \frac{3s_b}{(Rh_s)(m)}$$

$$LOQ = \frac{10s_b}{(Rh_s)(m)}$$

Where s_b is the standard deviation in the blank measurement in counts per second (CPS), Rh_s refers to the internal standard signal in CPS and m refers to the slope of the calibration curve with units of:

$$m = \frac{[A, ng mL^{-1}] \cdot CPS_A (background\ subtracted)}{CPS_{IS}}$$

Where $[A, \text{ng mL}^{-1}]$ is the concentration of analyte A in units of ng mL^{-1} ; CPS_A refers to the background-subtracted analyte signal in CPS; and CPS_{IS} refers to the internal standard signal in CPS.

Absolute detection limits (ADLs) were calculated by multiplying MDLs, in units of ng mL^{-1} , by the average sample volume consumed per analysis (approximately 1.2 mL using a CN and 0.12 mL using a MCN).

To establish the accuracy of SN-ICP-MS, experimental results for NIST SRMs 610 and 612 were compared to previously published values (56) using the Student's t -test (57). When:

$$\|\bar{x}_{Exp} - \bar{x}_P\| > t \cdot S_D$$

The difference in the experimental (\bar{x}_{Exp}) and published (\bar{x}_P) values were considered significant, given $t =$ Student's t at 95% confidence and S_D , the standard deviation in the difference between the two means, equals:

$$S_D = S_{pooled} \cdot \sqrt{\frac{N_1 + N_2}{N_1 N_2}}$$

Where N_1 and N_2 respectively refer to the number of replicate measurements in the experimental and published data sets. S_{pooled} is expressed as:

$$S_{pooled} = \sqrt{\frac{s_1^2(N_1 - 1) + s_2^2(N_2 - 1)}{N_1 + N_2 - 2}}$$

Where s_1^2 and s_2^2 refer to the variance in the experimental and published data sets, respectively. These calculations were performed for results obtained using each nebulizer.

The precision of the method was established by determining the percent relative standard deviations (%-RSDs) in replicate measurements of each SRM using both nebulizers (N = 10, for both). The bias of SN-ICP-MS using either a CN or MCN was calculated using the following relationship:

$$Bias = \mu - x_t$$

Where μ is the experimentally determined population mean and x_t is the true value for a particular element. In this case, the NIST certified values were used as the true value. It was determined that ten replicates were good estimates of the true population means, given the difficulty in sample preparation.

Within-day and long-term reproducibility results using the CN were compared using an arbitrary 3%-tolerance of the result. This value was used because it is the maximum %-RSD tolerated during instrument optimization. Mean isotopic concentrations and standard deviations were calculated for results obtained using the MCN. Confidence intervals at 95% confidence ($p = 0.05$) were used as a measure of analysis error.

LA-ICP-MS: Figures of Merit

Sample Selection and Preparation. NIST SRMs 610, 612 and 614 (Table 7) were chosen to evaluate the linearity of LA-ICP-MS. NIST SRMs 610 and 612 were then used to evaluate the accuracy and precision of this technique. Bias was calculated using accuracy results. Finally, NIST SRM 610 was used to evaluate the short- and long-term reproducibility of this method.

Standard glass wafers were washed in methanol (VWR, West Chester, PA, USA) and soaked in 10 % by volume trace metal grade nitric acid for approximately 30 minutes. Each wafer was rinsed with 18-M Ω H₂O following the methanol and acid washes. They were allowed to air dry prior to ablation.

Table 7. Nominal composition of NIST SRMs.

Designation	Nominal concentration of trace metals
610	500 mg kg ⁻¹
612	50 mg kg ⁻¹
614	1 mg kg ⁻¹

Instrumentation and Analytical Methods. A 213-nm neodymium-yttrium aluminum garnet (Nd:YAG) laser ablation unit (New Wave Research; Fremont, CA USA) was connected to the same Perkin Elmer ELAN DRC II ICP-MS described above. Helium was used as the ablation gas (flow = 1 L min⁻¹). The sample line exiting the ablation cell was connected to the nebulizer argon flow with a t-connector approximately one foot in front of the ICP torch entrance. The ICP-MS was optimized and tuned for the best possible performance using solution standards, introduced to the instrument by way

of the traditional quartz CN used above and quartz cyclonic spray chamber. Following solution optimization, the helium carrier gas flow rate was optimized using an external mass flow controller with NIST SRM 612. Refer to Table 4 for instrumental interference corrections.

Elements of interest included those described in Table 2, with one exception: ^{49}Ti was used to quantify titanium. Calibration for accuracy, precision, bias and reproducibility testing was accomplished using a single point calibrant, primarily SRM 612. SRM 610 was used as a calibrant when obtaining quantitative data for NIST SRM 612. A quality control sample, NIST SRM 1831 (soda lime sheet glass), was analyzed following calibration to ensure accurate quantitation and monitor instrument drift. Ablation of samples was accomplished using a 60- μm spot at 100% laser power (providing ~ 0.4 mJ output energy), 10-Hz repetition rate and 50-sec dwell time. Approximately 300 ng sample was introduced to the plasma during a single ablation.

Glitter Time Resolved Software (marketed by New Wave Research; Fremont, CA USA) was used to convert raw instrumental signal in counts per second (CPS) to quantitative data. Compositional information for each calibrant was taken from Pearce, *et al* (56); ^{29}Si was used as the internal standard for all elements.

Because the signal generated during a laser ablation experiment is transient (Figure 1), background and signal were manually selected for integration. The ablation burst (Figure 1), where apparent, was not included for signal integration. This signal characteristic corresponds to the initial burst of material ejected during the ablation event (called an “eruption”). It is routinely excluded from the signal to ensure sample

equilibration in the sample transfer line and as an added measure to avoid potential signal contributions from surface contaminants.

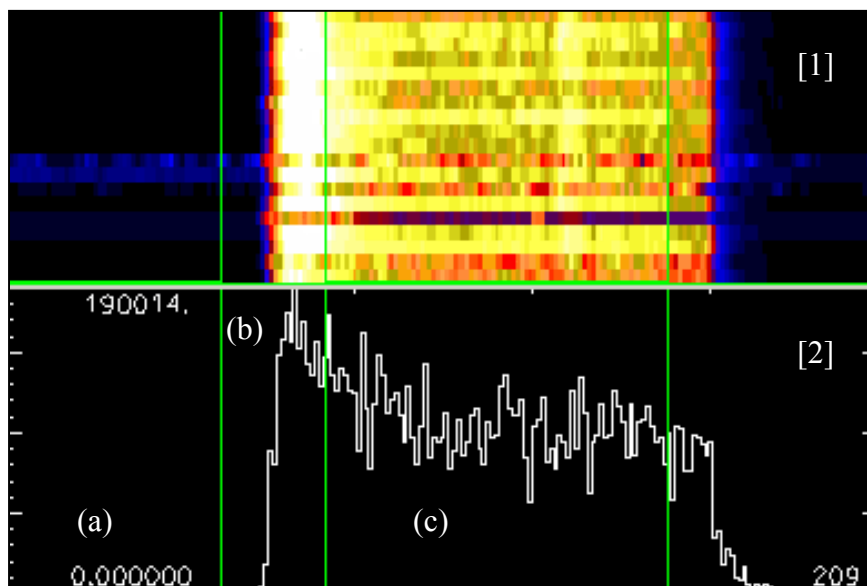


Figure 1. Screen shot of *Signal Selection Window: Glitter Time Resolved Software*. [1]: Three-dimensional representation of time-dependent signal intensity data. Time is represented by the x -plane, the isotope examined is represented by the y -axis, and signal intensity is represented by the z -plane. [2]: ${}^7\text{Li}$ signal intensity as a function of time, NIST SRM 612). *Key:* (a) Selected background signal, (b) ablation “burst,” and (c) selected steady state signal.

Two ablations were performed for calibration, once before QC analysis and again following sample analysis. Instrumental drift was corrected by bracketing samples with calibrants. For linearity testing, SRMs 614, 612 and 610 were each ablated four times, without calibration. Twenty consecutive ablations were performed for accuracy, precision and bias testing using SRMs 610 and 612. For reproducibility testing, four to five ablations were performed on SRM 610 at three time points, which were separated by no

less than 90 minutes on four nonconsecutive days. No more than 25 ablations were performed between calibration standard analyses.

Data Analysis and Calculations. To verify that a linear response in analyte: internal standard is obtained over the analytical mass range used during LA sample introduction, the raw signals of ^{49}Ti , ^{85}Rb , and $^{206,207,208}\text{Pb}$ in NIST SRMs 610, 612 and 614 were divided by the raw signal due to ^{29}Si during each run. Average analyte: internal standard signal values for four ablations were plotted as a function of NIST reported concentrations. Linear regression using Microsoft Excel was applied to determine the slope, y-intercept, and correlation coefficient (R^2) as well as the errors in the slope and y-intercept. ^{49}Ti , ^{85}Rb and $^{206, 207, 208}\text{Pb}$ were selected as representatives of the relevant isotopic mass range and because NIST reported values¹ for these isotopes in all three glasses.

Method detection limits were reported by Glitter Time Resolved Software (58) on the basis of the following relationship:

$$MDL = 2.3\sqrt{2 \cdot B}$$

Where B refers to the mean background signal of a particular isotope, obtained during a given ablation experiment. Absolute detection limits (ADLs) were calculated by multiplying MDLs (in units of $\mu\text{g g}^{-1}$) by the approximate mass of ablated material during a single run (300 ng or 3.0×10^{-7} g).

¹ Concentration values of rubidium and lead are NIST-certified. Titanium concentrations are provided for “information-only.”

As before, the accuracy of this technique was determined by comparing quantitative results for NIST SRMs 610 and 612 ($N = 20$, each) to previously published data using a Student's t test (57) for each element. Precision was determined by calculating percent %-RSDs for replicate analyses. Bias was calculated as before. Since numerous data points could be collected ($N = 20$), it was assumed that the experimental data collected for both NIST SRMs 610 and 612 were good estimates of true population means.

For reproducibility testing, mean isotopic concentrations and standard deviations were calculated and compared using confidence intervals at 95% confidence ($p = 0.05$) as a measure of analytical error.

Evaluation of SN and LA for Forensic Casework

To determine what effects the relative figures of merit of SN and LA might have on casework analyses, a blind test was designed to simulate a case. The sample amounts used for this study were such that enough sample would be available for chemical analysis by three methods and refractive index (RI) measurement. Thus, in terms of sample size this study did not accurately mimic a case.

An individual having knowledge of the glass sources chose three samples of several fragments each. Each was submitted in a plastic dish respectively labeled, "Reference Glass #1," "Questioned Glass #1," "Questioned Glass #2," and "Questioned Glass #3." Hereafter to be referred to as "K-1," "Q-1," "Q-2," and "Q-3."

K-1, Q-1, and Q-2 were transparent and green in color; Q-3 was transparent and clear. At first observation, it was noted that Q-3 could be excluded from sharing a

common origin as K-1 on the basis of color. K-1, Q-1, and Q-2 could not be distinguished on the basis of color; these samples were then subjected to RI measurement and chemical analysis.

For RI measurement, one fragment of each glass sample was selected and scraped with a diamond-tipped scribe. Glass particles were transferred to Standard B oil (Locke Scientific Limited; Tadley, Hampshire, UK) on a glass slide and covered with a standard glass cover slip. A Glass Refractive Index Measurement System II (Foster and Freeman; Evesham, Worcestershire, UK) was used for RI measurement. Five measurements of RI were taken for the reference glass, while four were taken for each questioned fragment.

Additional samples were taken for chemical analysis by SN-ICP-MS and LA-ICP-MS. Both the CN and MCN were used during SN introduction. Fragment masses selected for digestion are described in Table 8. Multiple fragments of the reference were digested and analyzed via single and quadruplicate analyses with a CN and MCN respectively. Questioned fragments were analyzed similarly, with the exception that single fragments were removed for acid digestion. This was done to simulate a case. Fragments subjected to LA were not weighed; four ablations were performed on the reference glass fragment while three were performed on questioned glass fragments. Sample preparation, analysis and data analysis was conducted as before.

Table 8. Sample masses dissolved for SN-ICP-MS analysis.

Sample name	Mass, mg (± 0.002)
Reference Glass (K)	
<i>Subsample 1</i>	0.594
<i>Subsample 2</i>	0.313
<i>Subsample 3</i>	0.324
<i>Subsample 4</i>	0.235
<i>Subsample 5</i>	0.817
<i>Subsample 6</i>	0.242
Questioned Glass #1 (Q-1)	0.423
Questioned Glass #2 (Q-2)	0.515

Elemental Variation in Automotive Windshield Glass

Analyte Selection and Sample Preparation. The analytes chosen for this portion of the study included $^{25,26}\text{Mg}$, ^{47}Ti or ^{49}Ti , ^{55}Mn , ^{57}Fe , ^{85}Rb , ^{88}Sr , ^{71}Ga , ^{90}Zr , ^{121}Sb , ^{137}Ba , ^{139}La , ^{140}Ce , ^{178}Hf , and ^{208}Pb . For comparison purposes, elemental ratios from these analytes were determined for each sample with the exception of $^{25,26}\text{Mg}$ and ^{121}Sb (Table 9). $^{25,26}\text{Mg}$ was not used for comparison purposes because magnesium is a major batch constituent; as a result, the amounts of magnesium were the same in every sample. ^{121}Sb was not used for comparison purposes because the antimony concentration in every windshield sample was at or below the detection limit of LA-ICP-MS. Elemental ratios were used to correct for instrumental drift typical of LA-ICP-MS (30, 59).

Table 9. Table of analytes and element ratios.

Elemental Ratio
Titanium (^{49}Ti) : Iron (^{57}Fe)
Manganese (^{55}Mn) : Strontium (^{88}Sr)
Rubidium (^{85}Rb) : ^{88}Sr
Gallium (^{71}Ga) : ^{85}Rb
Zirconium (^{90}Zr) : Barium (^{137}Ba)
Lanthanum (^{139}La) : Cerium (^{140}Ce)
Hafnium (^{178}Hf) : Lead (^{206}Pb)

Fifty automotive windshields and windshield samples were donated by Mygrant Glass Company (Sacramento, CA USA), Central Valley Tow (Sacramento, CA USA) and Pilkington/ Libbey Owens Ford Company (Lathrop, CA USA; Table 10). These windshields represented 17 separate manufacturers and one unknown manufacturer (60) and approximately one decade of glass manufacture (ca 1995 – 2005). Mygrant Glass Company and Pilkington/ Libbey Owens Ford Company donated whole windshields that were not suitable for retail sale because they were broken in stock or during shipping. Central Valley Tow allowed collection of windshield samples directly from totaled vehicles.

Where possible, the logo of each windshield was photographed for later identification. Windshields having identical markings were grouped together as multiple samples representing the same manufacturing lot. For example, Lamisafe windshields 1a and 1b had identical bugs as did Lamisafe windshields 2a and 2b; Lamisafe windshield 3 had a distinct bug (Table 10).

Ten of these automotive windshields were selected to evaluate the homogeneity of trace elements in automotive float glass: Lamishield 1, PLOF 1a, PLOF 1b, Sekurit 1a, Sekurit 1b, Vitro Flex/ Carlite 1a, Vitro Flex/ Carlite 1b, Vitro Flex/ Carlite 2 and Xyg 1. Core subsamples of each windshield were taken from six locations: top left, top right, top

center, bottom left, bottom center, and bottom right. Core samples were removed by chiseling or drilling; in the latter case, a 1-inch diameter diamond tipped coring drill bit (Advantage Drills Incorporated; Winter Park, FL USA) was used.

Core subsamples from the remaining 40 windshields were similarly collected. As some windshield samples were taken directly from vehicles, only one location in the windshield could be subsampled; whole windshields were subsampled in three places: left, right and center. The exterior pane of each subsample was marked so that the origin of each glass sample could be known. Hereafter, "Pane 1" refers to the outer pane of a windshield; "Pane 2" refers to the inner pane of a windshield.

Subsamples that were removed by chiseling were too large to fit into the LA sample cell chamber. Thus, fragments from each pane of each subsample were picked off using a diamond tipped scribe. These fragments were washed in methanol, soaked in 10% ultra pure nitric acid for no less than 30 minutes, and rinsed with 18-M Ω H₂O. Each was then allowed to air-dry. Subsamples that were removed by drilling were cut in half using wire cutters; they were cleaned as described above and allowed to air dry.

Table 10. Windshield sample set.

Manufacturer, Brand	Manufacturer, Brand
<i>AP Technoglass Corporation</i> Bellefontaine, OH USA	<i>L-N Safety Glass SA de CV of Mexicali</i> Toledo, OH USA
<p><i>Lamisafe Brand</i></p> <ul style="list-style-type: none"> • Lamisafe 1a, 1b • Lamisafe 2a, 2b • Lamisafe 3 • Lamisafe 4 	<p><i>Pilkington Brand</i></p> <ul style="list-style-type: none"> • L-N 1
<p><i>Lamisafe for Honda Brand</i></p> <ul style="list-style-type: none"> • Lamisafe 5 	<p><i>Pittsburgh Plate Glass (PPG) Industries</i> Pittsburgh, PA USA</p>
<p><i>Carlex Glass Company</i> Vonore, TN USA</p>	<p><i>PPG for Toyota Brand</i></p> <ul style="list-style-type: none"> • PPG 1
<p><i>Carlex Brand</i></p> <ul style="list-style-type: none"> • Carlex 1 • Carlex 2 	<p><i>PPG Brand</i></p> <ul style="list-style-type: none"> • PPG 2 • PPG 3
<p><i>Cristales Inastillables de Mexico</i> Xalostoc EDO, Mexico</p>	<p><i>Sekurit Saint-Gobain Cuautla</i> Ciudad de Ayala, Estado de Morelos Mexico</p>
<p><i>Crinamex Brand</i></p> <ul style="list-style-type: none"> • Crinamex 1 • Crinamex 2a, 2b, 2c 	<p><i>Sekurit Brand</i></p> <ul style="list-style-type: none"> • Sekurit 1a, 1b
<p><i>Ford Motor Company</i> Dearborn, MI USA</p>	<p><i>Shenzhen Benxun Auto-Glass Co., Ltd.</i> Shekou, Shenzhen China</p>
<p><i>Carlite Brand</i></p> <ul style="list-style-type: none"> • Ford 1 	<p><i>Lamishield Brand</i></p> <ul style="list-style-type: none"> • Lamishield 1
<p><i>Not branded</i></p> <ul style="list-style-type: none"> • Ford 2 	<p><i>Societa Italiana Vetro</i> San Salvo (Chieto) Italy</p>
<p><i>Fox Fire Incorporated</i> Pontiac, MI USA</p>	<p><i>Sicursiv Brand</i></p> <ul style="list-style-type: none"> • Sicursiv 1
<p><i>Not branded</i></p> <ul style="list-style-type: none"> • Fox 1 	<p><i>United L-N Glass Incorporated</i> Versailles, KY USA</p>
	<p><i>Toyota Brand (from Pilkington)</i></p> <ul style="list-style-type: none"> • Toyota 1a, 1b, 1c, 1d, 1e

Table 10, continued: Windshield sample set.

Manufacturer, Brand	Manufacturer, Brand
<p><i>Fujian Yanhua Glass Industry, Co., Ltd.</i> Honglu Town, Fujian Province China</p> <p><i>Not branded</i></p> <ul style="list-style-type: none"> • Fy 1 • Fy 2 <p><i>Industrias Venezolanas Automotrices</i> Caracas, Venezuela</p> <p><i>Not branded</i></p> <ul style="list-style-type: none"> • Iva 1 <p><i>Pilkington, Libbey Owens Ford (LOF) Company</i> USA</p> <p><i>LOF Brand</i></p> <ul style="list-style-type: none"> • LOF 1 • LOF 2 • LOF 3 <p><i>Pilkington/ Pilkington-LOF Brand</i></p> <ul style="list-style-type: none"> • PLOF 1a, 1b • PLOF 2a, 2b • PLOF 3 <p><i>PPG Brand</i></p> <ul style="list-style-type: none"> • PLOF/ PPG 1 	<p><i>Viracon Incorporated</i> Owatonna ME USA</p> <p><i>PPG Brand</i></p> <ul style="list-style-type: none"> • Viracon/ PPG 1a, 1b <p><i>Vitro Flex SA</i> Monterrey, Mexico</p> <p><i>Carlite Brand</i></p> <ul style="list-style-type: none"> • Vitro Flex/ Carlite 1a, 1b • Vitro Flex/ Carlite 2 <p><i>Ford Brand</i></p> <ul style="list-style-type: none"> • Vitro Flex/ Ford 1 • Vitro Flex/ Ford 2 <p><i>Xinyi Automobile Glass Company</i> Shenzhen City, Guangdong Province China</p> <p><i>Not branded</i></p> <ul style="list-style-type: none"> • Xyg 1 <p><i>Unknown Manufacturer</i></p> <p><i>Carlite Brand</i></p> <ul style="list-style-type: none"> • Unknown/ Carlite 1

Instrumentation and Analytical Methods. LA-ICP-MS was used to analyze these fifty windshields. The instrument parameters used are described in Tables 4 and 5, with helium flow set to 1 L min⁻¹ as before. Each sample was analyzed in quadruplicate. NIST SRM 612 was analyzed before and after sample analysis, and converted to calibration data using Glitter Time Resolved Software. The calibrant was analyzed before and after sample analysis to correct for instrumental drift. The quality of the calibration was tested

by analyzing NIST SRM 1831 prior to sample analysis. A 10%-tolerance was used for QC values.

Data Analysis and Calculations. Elemental variation in automotive windshield glass was evaluated by examining the variation in composition within a single pane, within a single windshield and within a population of 50 windshields. Elemental variation within a single pane and within a single windshield was determined using the 10-windshield subset described above. The analytical results for each of the six subsamples were compared to establish the variation within a single pane. The results for each of the six subsamples were then compiled so that the overall composition of each pane within a windshield could be compared. Finally, the variation within a population of 50 windshields was determined by compiling and comparing all analytical results for a given windshield pane ($N = 3$ to 24 for each of 100 panes).

Within-pane variation was characterized in three ways. Firstly, the percent relative standard deviations (%-RSDs) associated with quantifying a given elemental ratio was calculated for each of the 20 panes analyzed in the 10-windshield subset.

Secondly, the analytical results of each elemental ratio from each of the six subsamples were compared using a univariate Student's *t*-test (57, 61). This was done to determine whether significantly different amounts of each elemental ratio were present in each of the subsamples. The results of each subsample from each pane were systematically compared; in total, there were fifteen possible comparisons per pane (top left to top center, top left to top right, etc.). Every elemental ratio was treated as an independent variable; the Student's *t*-test used here was a two-tailed test assuming unequal variance. Unequal variance was assumed because the LA sampling technique is

very sensitive to laser focusing, sample placement within the sample cell, and small changes in the flow of helium (as when the sample cell is opened and shut between analyses). Because these conditions cannot be exactly reproduced from sample to sample, subsequent datasets do not have the same variance. When:

$$t_{\text{Calculated}} > t_{\text{Critical}}$$

The difference between two means was considered significant at 95% confidence. Since the two datasets had unequal variances, $t_{\text{Calculated}}$ was determined by the following:

$$t_{\text{Calculated}} = \frac{\bar{x} - \bar{y}}{\sqrt{(s_x^2/n) + (s_y^2/m)}}$$

Where \bar{x} was the mean value of the first dataset to be compared, \bar{y} was the mean value of the second dataset to be compared, s_x and s_y refer to the standard deviations of the first and second datasets respectively; n and m refer to the number of trials in the first and second datasets, respectively. The degrees of freedom, df , for this comparison was determined by:

$$df = \left\{ \frac{\left[\frac{(s_1^2/n_1) + (s_2^2/n_2)}{\frac{(s_1^2/n_1)^2}{n_1 + 1} + \frac{(s_2^2/n_2)^2}{n_2 + 1}} \right]^2}{\frac{(s_1^2/n_1)^2}{n_1 + 1} + \frac{(s_2^2/n_2)^2}{n_2 + 1}} \right\} - 2$$

The resultant was nonintegral. To use traditional charts of $t_{Critical}$, the value was rounded up to the next integer and the decimal portion was truncated. The final value, $int(df + 1)$, was then used as the degrees of freedom so that the appropriate $t_{Critical}$ at 95% confidence could be found using a table. All univariate t-tests were conducted with a user-defined macro in Microsoft Excel.

Thirdly, each subsample of one windshield (Vidro Flex/ Carlite 2) was compared using a multivariate t -test to determine whether small differences in individual elemental ratios were significant within a single pane of glass if the total variation of all elemental ratios was simultaneously considered. A multivariate analog to the Student's t -test was used, called Hotelling's T^2 (61). This test statistic facilitates the comparison of two samples in terms of all available variables, which may or may not be covariant. As before, each subsample was systematically compared to the remaining subsamples for a total of 15 comparisons. Vidro Flex/ Carlite 2 was chosen as a model to represent the remaining windshields.

When x and y represent the following multivariate datasets:

$$x = \begin{bmatrix} x_{11} & x_{21} & x_{31} & \cdots & x_{n1} \\ x_{12} & x_{22} & x_{32} & \cdots & x_{n2} \\ \vdots & \vdots & \vdots & & \vdots \\ x_{1p} & x_{2p} & x_{3p} & \cdots & x_{np} \end{bmatrix} \quad y = \begin{bmatrix} y_{11} & y_{21} & y_{31} & \cdots & y_{m1} \\ y_{12} & y_{22} & y_{32} & \cdots & y_{m2} \\ \vdots & \vdots & \vdots & & \vdots \\ y_{1p} & y_{2p} & y_{3p} & \cdots & y_{mp} \end{bmatrix}$$

Where x_{11} refers to the first analysis of the first variable, when p variables are considered, the test statistic, $T^2_{Calculated}$, was determined by the following:

$$T^2_{\text{Calculated}} = (\bar{x} - \bar{y})^T \left[\left(\frac{1}{n} + \frac{1}{m} \right) S_{\text{Pooled}} \right]^{-1} (\bar{x} - \bar{y})$$

Where \bar{x} and \bar{y} are vectors describing the average values for two multivariate datasets, x and y , and S_{Pooled} is the covariance matrix of the two multivariate data sets. The quantity $(\bar{x} - \bar{y})^T$ is simply the transpose of column vector $(\bar{x} - \bar{y})$. The mean vectors, \bar{x} and \bar{y} , are described by:

$$\bar{x} = \begin{bmatrix} \bar{x}_{n1} \\ \bar{x}_{n2} \\ \bar{x}_{n3} \\ \vdots \\ \bar{x}_{np} \end{bmatrix} \quad \bar{y} = \begin{bmatrix} \bar{y}_{m1} \\ \bar{y}_{m2} \\ \bar{y}_{m3} \\ \vdots \\ \bar{y}_{mp} \end{bmatrix}$$

The pooled variance matrix, S_{Pooled} was then estimated by:

$$S_{\text{Pooled}} = \frac{(n-1)S_x + (m-1)S_y}{n+m-2}$$

Where the variance matrices, S_x and S_y , are:

$$S_x = \frac{1}{n} \sum_{j=1}^n (x_j - \bar{x})(x_j - \bar{x})^T \quad \text{and} \quad S_y = \frac{1}{m} \sum_{j=1}^m (y_j - \bar{y})(y_j - \bar{y})^T$$

Hotelling's T^2 distribution has the same general shape as the F-distribution. Therefore, the critical value, $T^2_{Critical}$, was calculated by the following:

$$T^2_{Critical} = \frac{(n + m - 2)p}{(n + m - p - 1)} F_{p, n+m-p-1}$$

Where $F_{p, n+m-p-1}$ is the value of the F distribution for p variables, and $n+m-p-1$ degrees of freedom. Hotelling's T^2 test has the condition that $n + m > p + 1$; thus, there must be at least two more data points than there are variables. The null hypothesis was rejected when $T^2_{Calculated}$ was greater than $T^2_{Critical}$. Because there must be two more data points than there are variables, only four elemental ratios could be considered when comparing subsamples due to the limited number of replicate analyses performed on each. To make the most conservative statistical comparisons, then, the four most variable elemental ratios from Vitro Flex/ Carlite 2 Pane 1 and Pane 2 were selected. For the comparisons made between subsamples of Pane 1, the elemental ratios $^{49}\text{Ti}/^{57}\text{Fe}$, $^{85}\text{Rb}/^{88}\text{Sr}$, $^{139}\text{La}/^{140}\text{Ce}$, and $^{178}\text{Hf}/^{208}\text{Pb}$ were used. For Pane 2, $^{55}\text{Mn}/^{88}\text{Sr}$, $^{85}\text{Rb}/^{88}\text{Sr}$, $^{90}\text{Zr}/^{137}\text{Ba}$, and $^{178}\text{Hf}/^{208}\text{Pb}$ were used. All multivariate T^2 tests were conducted using MatLab 6.5 (The MathWorks Incorporated; Natick, MA USA).

To establish the variation within a single windshield, the analytical results of each subsample that represented a single pane were compiled ($N = 18 - 24$). The overall results for each pane within a given windshield were compared at 95% confidence.

Within the 10-windshield subset selected for sample homogeneity testing, there were three sets of windshields produced within the same lot: PLOF 1a and 1b; Sekurit 1a and 1b; and Vitro Flex/ Carlite 1a and 1b. The panes of each set were compared using

Hotelling's T^2 test at 95% confidence to determine whether each pane within a set could be distinguished from the others manufactured at or around the same time.

To test the "fingerprinting" capability of trace elemental profiling, the population variation of all 50 windshields was compared to the variation observed within single groups of manufacturers. The concentration ranges of trace elements in the population of all 50 windshields was inter-compared to the concentration ranges observed in Lamisafe windshields, Pilkington-LOF windshields, and Vitro Flex windshields at 95% confidence. The average trace elemental profile of each of these manufacturers' windshields was also inter-compared at 95% confidence. Lamisafe, Pilkington-LOF and Vitro Flex windshields were selected for these comparisons because these groups contained five or more windshields.

Finally, the discrimination of trace elemental profiling for automotive windshield glass was examined by comparing compiled results from all panes of windshield glass at 95% confidence. Due to the number of samples (100 panes), a preliminary grouping method was employed. The samples were first grouped according to $^{85}\text{Rb}/^{88}\text{Sr}$ values, because this elemental ratio exhibited the greatest variation within the total population. Each windshield pane was placed into one of four groups. Windshield panes with $^{85}\text{Rb}/^{88}\text{Sr}$ of 0.01 or less were placed into Group 1; those with $^{85}\text{Rb}/^{88}\text{Sr}$ of 0.01 – 0.1 were placed into Group 2. Windshield panes having $^{85}\text{Rb}/^{88}\text{Sr}$ of 0.1 – 1 were placed into Group 3 and those with $^{85}\text{Rb}/^{88}\text{Sr}$ greater than 1 were placed into Group 4. Each group was then further divided into subgroups by comparing the remaining elemental ratios of each pane within a group at 95% confidence. Each division was made on the basis of the next most variable elemental ratio. For these 100 panes, the order of elemental ratios used

to subdivide groups after $^{85}\text{Rb}/^{88}\text{Sr}$ was $^{55}\text{Mn}/^{88}\text{Sr}$, $^{90}\text{Zr}/^{137}\text{Ba}$, $^{71}\text{Ga}/^{85}\text{Rb}$, $^{49}\text{Ti}/^{57}\text{Fe}$, $^{178}\text{Hf}/^{208}\text{Pb}$, and $^{139}\text{La}/^{140}\text{Ce}$.

Elemental Variation in Float Glass

Quality control (QC) samples donated by Pittsburgh Plate Glass Company (PPG; Fresno, CA USA), Libbey Owens Ford (LOF; Lathrop CA USA) and Pilkington-Libbey Owens Ford (Lathrop, CA USA)² were used for this study. These QC samples were collected by staff at predetermined locations in the ribbon and specified times in order to monitor the batch color and thickness over time. PPG donated QC samples collected between May and June 2004. These were collected from three different locations in the ribbon (left, right and center) at three times (0700 h, 1500 h and 2300 h). The batch samples donated by LOF were originally given to the Sacramento California Department of Justice Crime Lab in 1997; the Department of Justice laboratory then donated these samples for this study. This set contained QC samples manufactured by LOF in November and December of 1997. These QC samples were collected from a single location in the ribbon at 0500 h of each day. The Pilkington-LOF batch samples were manufactured in May of 2005; these were also collected from a single location in the ribbon at 0500 h of each day. Only a subset of each group was analyzed to establish the short- and long-term variation typical of these manufacturing plants.

Spatial variations in float glass composition were determined by analyzing the left, center and right batch samples each collected at 0700 h, 1500h and 2300 h from the PPG float glass ribbon for three consecutive days. Daily variations were examined using

² Pilkington acquired LOF in the late 1990s, after the LOF batch samples were donated.

the center QC samples collected at each time point for these three days, as well. The short-term variation in this manufacturer's batch was examined by comparing the analytical results for the center QC samples each collected 1500 h. The long-term variation in this manufacturer's product was determined by analyzing center samples collected weekly at 1500 h, for four weeks.

The short-term variation in float glass manufactured by LOF was determined by analyzing QC samples collected at 0500 h for three consecutive days; long-term variation was determined by analyzing QC samples collected at 0500 h on the fifth day, the 17th day, and the 24th days of November as well as the sixth day of December in 1997.

The short-term variation in float glass manufactured by Pilkington LOF was determined by analyzing QC samples collected at 0500 h for three consecutive days; the long-term variation was determined by analyzing QC samples collected at 0500 h weekly for three weeks.

Each QC sample was approximately four inches long and two inches wide with variable thickness. Each was broken into smaller fragments using a chisel and hammer. Smaller fragments of each QC sample were washed in methanol, soaked in 10% ultra pure nitric acid, and rinsed with deionized water. Each was then allowed to air-dry. Samples were mounted on glass slides with blue putty.

Analysis was conducted as described above (p. 38). The elemental composition of each QC sample (represented by elemental ratios described in Table 9) was compared using 95% confidence limits.

Findings

SN-ICP-MS: Figures of Merit

Detection Limits and Sensitivity. MDLs ranged from 0.005 – 0.2 ng mL⁻¹ using either a CN or MCN (Table 11). In general, MDLs determined using the MCN were greater than that determined by using a CN. In some cases, this difference was as large as an order of magnitude. It is of interest that MDLs for ²⁵Mg and ⁴⁷Ti were similar using either nebulizer, suggesting that the variation in signal due to ²⁵Mg and ⁴⁷Ti is independent of the total amount of sample delivered to the instrument. Both have relatively low isotopic abundances (10% and 7.3%, respectively), which may explain the variations observed since lower abundance ions are less effectively transferred to the mass spectrometer than higher abundance ions. ADLs ranged from 0.001 – 0.1 picograms, the MCN providing lower ADLs by as great as a factor of 10 for certain isotopes. Sub-ng mL⁻¹ LOQs were achievable using either a CN or MCN.

Table 11. Summary of MDLs, ADLs, and LOQs.

Analyte	MDLs, ng mL⁻¹		ADLs, ng		LOQs, ng mL⁻¹	
	CN	MCN	CN	MCN	CN	MCN
²⁵ Mg	0.11	0.18	0.13	0.022	0.37	0.59
²⁶ Mg	0.053	0.20	0.064	0.024	0.18	0.65
⁴⁷ Ti	0.028	0.026	0.034	0.0031	0.096	0.085
⁵⁵ Mn	0.0099	0.070	0.012	0.0084	0.033	0.23
⁶⁹ Ga	0.0047	0.065	0.0056	0.0078	0.016	0.22
⁷¹ Ga	0.0074	0.060	0.0089	0.0072	0.025	0.20
⁸⁵ Rb	0.0061	0.051	0.0073	0.0061	0.020	0.17
⁸⁶ Sr	0.014	0.057	0.017	0.0068	0.047	0.19
⁸⁸ Sr	0.0073	0.044	0.0088	0.0053	0.024	0.15
⁹⁰ Zr	0.017	0.091	0.020	0.011	0.057	0.30
⁹¹ Zr	0.017	0.073	0.020	0.0088	0.058	0.24
⁹² Zr	0.017	0.083	0.020	0.0010	0.056	0.28
⁹⁴ Zr	0.015	0.092	0.018	0.011	0.049	0.31
¹²¹ Sb	0.0076	0.058	0.0091	0.0070	0.025	0.19
¹³⁷ Ba	0.011	0.050	0.013	0.0060	0.037	0.17
¹³⁸ Ba	0.0054	0.052	0.0065	0.0062	0.018	0.17
¹³⁹ La	0.0055	0.046	0.0066	0.0055	0.018	0.15
¹⁴⁰ Ce	0.0051	0.046	0.0061	0.0055	0.017	0.15
¹⁴⁷ Sm	0.0063	0.045	0.0076	0.0054	0.021	0.15
¹⁷⁸ Hf	0.013	0.097	0.016	0.012	0.044	0.32
²⁰⁶ Pb	0.019	0.15	0.023	0.018	0.064	0.77
²⁰⁷ Pb	0.034	0.12	0.041	0.014	0.11	0.75
²⁰⁸ Pb	0.024	0.11	0.029	0.013	0.080	0.78

Analytical sensitivity was calculated by averaging the slopes of two calibrations performed on nonconsecutive days using either a CN or MCN (Table 12). The average error in the slope determination made by linear regression was no greater than $\pm 1 \times 10^{-6}$ for any particular isotope.

Generally speaking, there was a decrease in sensitivity using MCN over CN with the exception of ^{55}Mn and $^{25,26}\text{Mg}$. No difference was observed in the sensitivity for ^{55}Mn ; there was a 4 – 6 % increase in sensitivity for $^{25,26}\text{Mg}$. All other isotopes showed 0.3 – 9% decreases in sensitivity. This effect seemed to be mass dependent. Mid-mass isotopes (m/z 85 – 94) showed only 2 – 3% reductions in sensitivity, whereas the higher mass isotopes showed decreases of $> 5\%$. The magnitude of this sensitivity reduction increased with mass, which may be due to mass-related differences in response of analyte: internal standard.

Internal standardization is a common practice in plasma spectrometry due to well-known occurrence of instrumental drift inherent to plasma spectrometry, as well as certain types of noise and various matrix effects. Matrix effects are minimized by internal standardization if the sample matrix equally affects the internal standard and analyte. In many cases, matrix effects are mass dependent. For example, space charge effects are known to bias ion sampling in favor of larger ions (higher mass analytes). Matrix effects can also predictably alter instrument response as a function of ionization potential. For example, if solvent loading cools the plasma, elements with higher first ionization potentials are not as easily ionized. This situation creates a sampling bias in favor of analytes with lower first ionization potentials. It should be noted that instrument optimization could have an impact on internal standardization, as well. Modern ICP-MS

instruments make use of an “autolens” to selectively focus ions within a certain m/z range prior to mass selection and detection. The autolens increases voltage to select for higher m/z analytes; the voltage increase is calibrated for maximum sensitivity using a mixture of low, middle and high mass elements. Over time, the optimum voltage that provides the greatest sensitivity for each of the low, middle and high mass elements changes. Low and high mass elements are selected against when this occurs. It is difficult to assign the apparent mass-dependent decrease in sensitivity to a result of matrix or instrumental effects. However, these known effects make mass-dependent differences in instrumental response not unexpected.

Finally, it was observed that isotopic differences in sensitivity for each nebulizer type correlated well with isotopic abundance. This is a strong indication that a negligible amount of isobaric interference is occurring.

Table 12. Analytical sensitivity.

Analyte	Sensitivity (Slope, m^3)	
	CN	MCN
²⁵ Mg	6.58×10^{-4}	6.82×10^{-4}
²⁶ Mg	7.51×10^{-4}	7.93×10^{-4}
⁴⁷ Ti	5.88×10^{-4}	5.63×10^{-4}
⁵⁵ Mn	1.19×10^{-2}	1.18×10^{-2}
⁶⁹ Ga	9.12×10^{-3}	9.10×10^{-3}
⁷¹ Ga	6.60×10^{-3}	6.50×10^{-3}
⁸⁵ Rb	1.63×10^{-2}	1.58×10^{-2}
⁸⁶ Sr	2.48×10^{-3}	2.42×10^{-3}
⁸⁸ Sr	1.98×10^{-2}	1.92×10^{-2}
⁹⁰ Zr	1.01×10^{-2}	9.75×10^{-3}
⁹¹ Zr	2.38×10^{-3}	2.30×10^{-3}
⁹² Zr	3.59×10^{-3}	3.50×10^{-3}
⁹⁴ Zr	3.81×10^{-3}	3.71×10^{-3}
¹²¹ Sb	5.91×10^{-3}	5.65×10^{-3}
¹³⁷ Ba	2.87×10^{-3}	2.74×10^{-3}
¹³⁸ Ba	1.73×10^{-2}	1.62×10^{-2}
¹³⁹ La	2.38×10^{-2}	2.21×10^{-2}
¹⁴⁰ Ce	2.22×10^{-2}	2.07×10^{-2}
¹⁴⁷ Sm	4.36×10^{-3}	4.18×10^{-3}
¹⁷⁸ Hf	7.35×10^{-3}	6.93×10^{-3}
²⁰⁶ Pb	4.97×10^{-3}	4.71×10^{-3}
²⁰⁷ Pb	4.19×10^{-3}	3.94×10^{-3}
²⁰⁸ Pb	9.96×10^{-3}	9.09×10^{-3}

Accuracy, precision and bias. Pearce, *et al* (56) compiled existing elemental data and experimental data gathered for NIST SRMs 610 and 612; results were found by numerous techniques including SN-ICP-MS, SN-ICP atomic emission spectrometry (-AES), atomic absorption spectrometry (AAS), electron probe microanalysis (EMPA) and instrumental neutron activation analysis (INAA). Elemental data for each SRM was provided in two ways: as “overall” and “preferred” values. Overall values represented

³ The slope of a calibration where analyte: internal standard ratio in counts per second is plotted as a function of analyte concentration. See page 26.

every compiled and new result, whereas preferred values were those that fell within one standard deviation (1σ) of the overall averages for each element.

Experimental determinations made for NIST SRM 610 using a CN resulted in seven isotopes having concentrations similar to preferred results (Table 13). There were insignificant differences for magnesium (m/z 25 and 26), antimony, lanthanum, cerium and lead (m/z 207 and 208). Results gathered using the MCN for the same SRM 610 digests resulted in six isotopes having comparable concentrations (Table 15). Magnesium (m/z 25 and 26), lanthanum, cerium and hafnium were similar to preferred values.

Data gathered for NIST SRM 612 using a CN was insignificantly different in nine isotopes: magnesium (m/z 25 and 26), rubidium, strontium (m/z 86 and 88), zirconium (m/z 92, 94), lanthanum, and hafnium (Table 14). Data gathered using a MCN was similar to preferred values in seven isotopes: magnesium, (m/z 25 and 26), strontium (m/z 86 and 88) and zirconium (m/z 90, 92, 94; Table 16).

Table 13. NIST SRM 610: Accuracy of SN-ICP-MS using a CN (95% CL).

Overall values	Preferred values
$\ \bar{x}_{Exp} - \bar{x}_P\ < t \cdot S_D$ $^{25,26}\text{Mg}, ^{71}\text{Ga}, ^{121}\text{Sb}, ^{137,138}\text{Ba},$ $^{139}\text{La}, ^{140}\text{Ce}, ^{207,208}\text{Pb}$	$\ \bar{x}_{Exp} - \bar{x}_P\ < t \cdot S_D$ $^{25,26}\text{Mg}, ^{121}\text{Sb}, ^{139}\text{La}, ^{140}\text{Ce},$ $^{207,208}\text{Pb}$
$\ \bar{x}_{Exp} - \bar{x}_P\ > t \cdot S_D$ $^{47}\text{Ti}, ^{55}\text{Mn}, ^{69}\text{Ga}, ^{85}\text{Rb}, ^{86}\text{Sr},$ $^{88}\text{Sr}, ^{90,91,92,94}\text{Zr}, ^{178}\text{Hf}, ^{206}\text{Pb}$	$\ \bar{x}_{Exp} - \bar{x}_P\ > t \cdot S_D$ $^{47}\text{Ti}, ^{55}\text{Mn}, ^{69}\text{Ga}, ^{71}\text{Ga}, ^{85}\text{Rb}, ^{86}\text{Sr},$ $^{88}\text{Sr}, ^{90,91,92,94}\text{Zr}, ^{137,138}\text{Ba}, ^{178}\text{Hf},$ ^{206}Pb

Table 14. NIST SRM 610: Accuracy of SN-ICP-MS using a MCN (95% CL).

Overall values	Preferred values
$\ \bar{x}_{Exp} - \bar{x}_P\ < t \cdot S_D$ $^{25,26}\text{Mg}, ^{121}\text{Sb}, ^{137,138}\text{Ba}, ^{139}\text{La},$ $^{140}\text{Ce}, ^{178}\text{Hf}$	$\ \bar{x}_{Exp} - \bar{x}_P\ < t \cdot S_D$ $^{25,26}\text{Mg}, ^{139}\text{La}, ^{140}\text{Ce}, ^{178}\text{Hf}$
$\ \bar{x}_{Exp} - \bar{x}_P\ > t \cdot S_D$ $^{47}\text{Ti}, ^{55}\text{Mn}, ^{69,71}\text{Ga}, ^{85}\text{Rb}, ^{86,88}\text{Sr},$ $^{90,91,92,94}\text{Zr}, ^{206, 207, 208}\text{Pb}$	$\ \bar{x}_{Exp} - \bar{x}_P\ > t \cdot S_D$ $^{47}\text{Ti}, ^{55}\text{Mn}, ^{69,71}\text{Ga}, ^{85}\text{Rb}, ^{86,88}\text{Sr},$ $^{90,91,92,94}\text{Zr}, ^{121}\text{Sb}, ^{137,138}\text{Ba},$ $^{206, 207, 208}\text{Pb}$

Table 15. NIST SRM 612: Accuracy of SN-ICP-MS using a CN (95% CL).

Overall values	Preferred values
$\ \bar{x}_{Exp} - \bar{x}_P\ < t \cdot S_D$ $^{25,26}\text{Mg}, ^{85}\text{Rb}, ^{86}\text{Sr}, ^{92,94}\text{Zr}, ^{139}\text{La},$ $^{140}\text{Ce}, ^{178}\text{Hf}$	$\ \bar{x}_{Exp} - \bar{x}_P\ < t \cdot S_D$ $^{25,26}\text{Mg}, ^{85}\text{Rb}, ^{86}\text{Sr}, ^{92,94}\text{Zr}, ^{139}\text{La},$ ^{178}Hf
$\ \bar{x}_{Exp} - \bar{x}_P\ > t \cdot S_D$ $^{47}\text{Ti}, ^{55}\text{Mn}, ^{69,71}\text{Ga}, ^{88}\text{Sr}, ^{90,91}\text{Zr},$ $^{121}\text{Sb}, ^{137,138}\text{Ba}, ^{206,207,208}\text{Pb}$	$\ \bar{x}_{Exp} - \bar{x}_P\ > t \cdot S_D$ $^{47}\text{Ti}, ^{55}\text{Mn}, ^{69,71}\text{Ga}, ^{88}\text{Sr}, ^{90,91}\text{Zr},$ $^{121}\text{Sb}, ^{137,138}\text{Ba}, ^{140}\text{Ce},$ $^{206,207,208}\text{Pb}$

Table 16. NIST SRM 612: Accuracy of SN-ICP-MS using a MCN (95% CL).

Overall values	Preferred values
$\ \bar{x}_{Exp} - \bar{x}_P\ < t \cdot S_D$ $^{25,26}\text{Mg}, ^{86,88}\text{Sr}, ^{90,92,94}\text{Zr}$	$\ \bar{x}_{Exp} - \bar{x}_P\ < t \cdot S_D$ $^{25,26}\text{Mg}, ^{86,88}\text{Sr}, ^{90,92,94}\text{Zr}$
$\ \bar{x}_{Exp} - \bar{x}_P\ > t \cdot S_D$ $^{47}\text{Ti}, ^{55}\text{Mn}, ^{69,71}\text{Ga}, ^{85}\text{Rb}, ^{91}\text{Zr},$ $^{121}\text{Sb}, ^{137,138}\text{Ba}, ^{139}\text{La}, ^{140}\text{Ce},$ $^{178}\text{Hf}, ^{206,207,208}\text{Pb}$	$\ \bar{x}_{Exp} - \bar{x}_P\ > t \cdot S_D$ $^{47}\text{Ti}, ^{55}\text{Mn}, ^{69,71}\text{Ga}, ^{85}\text{Rb}, ^{91}\text{Zr},$ $^{121}\text{Sb}, ^{137,138}\text{Ba}, ^{139}\text{La}, ^{140}\text{Ce},$ $^{178}\text{Hf}, ^{206,207,208}\text{Pb}$

The general trend observed was that the MCN provided less accurate results when using the data provided by Pearce, *et al* for comparison. The difference in accuracy by SN type may be a result of the general decrease in sensitivity observed when using MCN over CN. For some elements, there appears to be no difference in accuracy if a particular isotope is selected for quantitation over another. ^{25}Mg provided equally accurate results as ^{26}Mg for either isotope determined using a CN or MCN. By contrast, $^{90,92,94}\text{Zr}$ provided more accurate quantitation of Zr than did ^{91}Zr in NIST SRM 612, depending on the nebulizer used.

Neither CN nor MCN provided experimental data that was comparable to published data in every element pertinent to forensic glass analysis. Since either technique is accurate for only a subset of the element menu, care must be taken when comparing quantitative data gathered by different laboratories. This is especially true of casework-related data, where false associations between questioned and reference glass fragments can have staggering consequences. These results emphasize a need to fully characterize the analytical performance typical of each instrument used in casework. When such performance data is on-hand, collaboration and communication are made possible among criminalists using elemental data.

The precision of these SN techniques, expressed as percent relative standard deviation (%-RSD), is presented in Figures 2 and 3. Digests of NIST SRM 610 were approximately 50 ng mL^{-1} in trace elements and had %-RSDs between 4 – 10% (Figure 2). There was little difference in precision between CN and MCN for these solutions. This variance was similar to that reported by Catterick and Hickman (9) in 1981, who used ICP-AES for the quantification of major elements in the high $\mu\text{g g}^{-1}$ (> 70) to low

weight percent (< 1% by mass) in concentration. They used a similar digestion protocol of 1:2 HF: HCl.

Digests of SRM 612 were $\leq 1 \text{ ng mL}^{-1}$ in concentration and had %-RSDs as great as 35 – 40% depending on the nebulizer used (Figure 3). There were significant differences in precision between these techniques for ^{55}Mn , $^{69,71}\text{Ga}$, ^{85}Rb , ^{90}Zr , ^{139}La , ^{140}Ce , and ^{178}Hf where CN yielded %-RSDs that were at least half as large as those obtained for MCN. For most of these isotopes, %-RSDs using a CN were less than 8% while those using MCN were as great as 20%. ^{90}Zr is the exception, having %-RSDs of 25 and 41% using a CN or MCN, respectively.

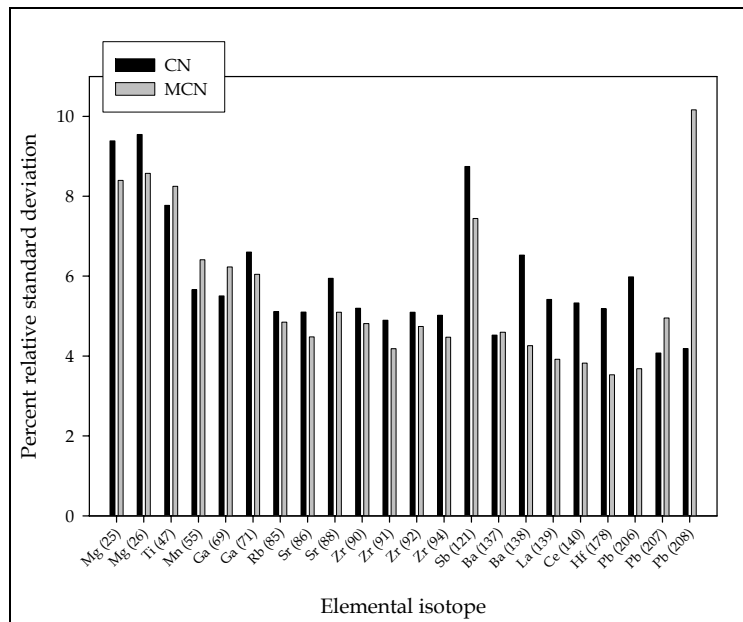


Figure 2. Relative standard deviations by elemental isotope: SRM 610, N = 10.

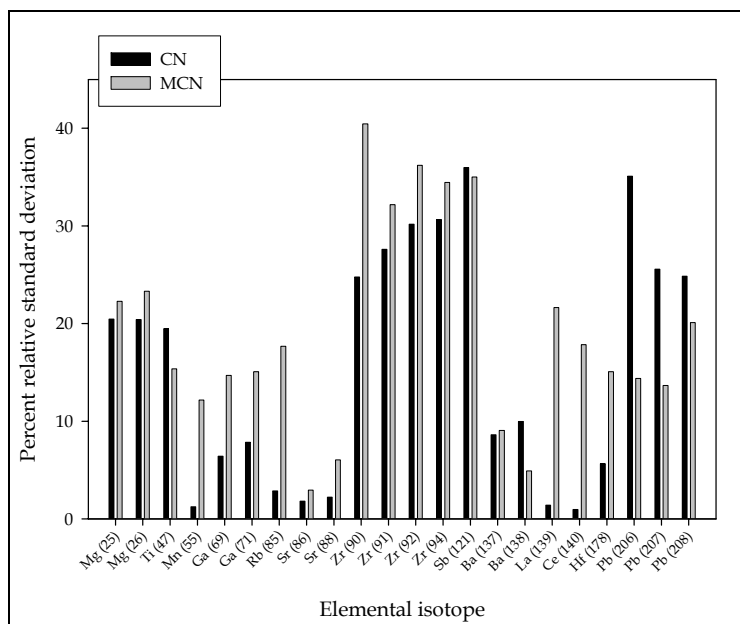


Figure 3. Relative standard deviations by elemental isotope: SRM 612, N = 10.

The large %-RSDs obtained for NIST SRM 612 digests appears to be the combined effects of low-level quantitation and acid digestion (Figure 4). Five SRM 612 digests were analyzed in quadruplicate. The %-RSDs obtained for each digest were compared to the %-RSD obtained by averaging all 20 results. Percent relative deviations obtained for quadruplicate analyses of a single 612 digest were < 5% for most elements, but the majority of overall %-RSDs (N = 20) were 10 – 20% for the same set of replicate analyses. Strontium is the only element that appeared to be unaffected by digestion. A similar pattern was observed when quadruplicate analyses were performed on five SRM 610 digests, though the differences in %-RSDs of quadruplicate analyses and overall results were not as disparate as those obtained for SRM 612. On average, %-RSDs for quadruplicate analyses of SRM 610 were < 2% while overall %-RSDs (N = 20) were between 4 and 8%.

Duckworth, *et al* (55) examined acid digestion as a source of potential variation for elemental quantitation. Using analysis of variance, they determined that boron, copper, silver and nickel were the most susceptible to dissolution-based variation in detection because of weighing or dilution errors; they further proposed that these elements were particularly vulnerable due to their potentials to form volatile complexes or precipitates during the digestion process. Other sources of variation governing the quantitative precision of other elements were determined, including day-to-day variation, calibration variation and variation due to other instrumental parameters.

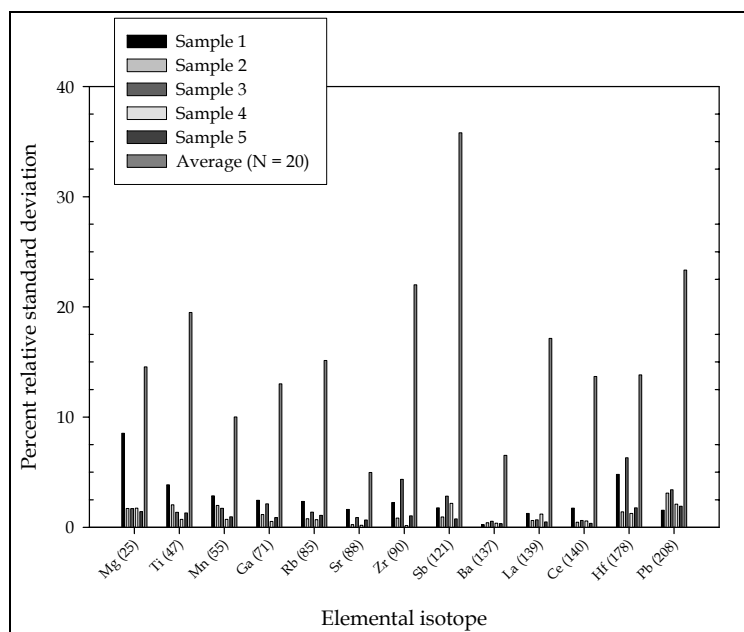


Figure 4. Precision of replicate analyses vs. overall precision: Samples 1 – 5, N = 4 Average, N = 20 (Selected isotopes, NIST SRM 612).

While Duckworth, *et al* did not associate dissolution error as the primary source of variation in detecting the elements shown here, the experimental results shown in

Figure 5 would indicate that the acid digestion process has a large impact on the analytical precision available for a wide range of elements. Further, dissolution error appears to have a greater impact on low-level determinations.

Bias, or the directional error inherent to a technique for a particular analyte, was evaluated by experimentally determining population values for ^{85}Rb , $^{86,88}\text{Sr}$, and $^{206,207,208}\text{Pb}$ in NIST SRMs 610 and 612 as well as ^{55}Mn in SRM 610. These results were then compared to NIST-certified values (Table 17).

Table 17. Bias results, where x_i = NIST certified value.

<i>Analyte</i>	Bias, NIST SRM 610 ($\mu\text{g mL}^{-1}$)		Bias, NIST SRM 612 ($\mu\text{g mL}^{-1}$)	
	<i>CN</i>	<i>MCN</i>	<i>CN</i>	<i>MCN</i>
^{55}Mn	40.048	76.986		
^{85}Rb	34.390	44.775	0.123	-9.123
^{86}Sr	17.381	41.311	-1.028	-0.252
^{88}Sr	51.626	71.362	2.926	-2.466
^{206}Pb	-52.187	-101.532	-16.809	9.705
^{207}Pb	-14.988	-84.619	-11.119	13.241
^{208}Pb	-12.260	-105.706	-9.423	-9.441

There was a positive bias in elemental determinations for lower mass elements and a negative bias for higher mass elements in SRM 610 irrespective of the nebulizer used. Bias results found by CN and MCN did not similarly correlate for elements quantified in NIST SRM 612. Strontium (m/z 88) and lead (m/z 208) were the only isotopes for which a negative bias was observed using both nebulizers. The magnitude of bias observed in SRM 610 was as high as 25% of the true value using the MCN, whereas the magnitude in bias using the CN did not exceed 12%. Both the CN and MCN yielded

bias that was between 0.3 and 40% of the true value for SRM 612. Using the CN, the magnitude of bias determined using SRM 612 increased with mass. Using the MCN, only strontium quantitation had an associated bias of less than 5% of the true value.

It is difficult to assign significance to bias calculations made using SRM 612, given the population variation observed (Figures 3 and 4). However, there does appear to be a mass-dependent effect in bias for the SRM 610 results using CN and MCN as well as the 612 bias determinations using a CN. The positive bias in the 610 results for lower mass elements would suggest mass bias in favor of lighter elements as would the negative bias results for higher mass elements. The fact that the magnitude of bias increases for 612 results also suggests a mass bias for lighter elements; however, it is important to assert that these results are merely corroborative.

Reproducibility. The reproducibility of SN-ICP-MS was evaluated by analyzing diluted samples of a single NIST 610 digest. Three aspects of the analytical reproducibility available by SN-ICP-MS were evaluated: (a) within-run reproducibility, or repeatability, (b) within-day reproducibility, and (c) long-term reproducibility. Within-run reproducibility was established for only the MCN, due to the limited sample volume. For reproducibility testing, instrument calibration was performed only once prior to sample analysis.

The within-run reproducibility of SN using a MCN varied over time, becoming increasingly less precise (Figures 5 and 6). Day 1 yielded the most precise results, having within-run precision of ≤ 1 % RSD. Day 4 yielded the least precise results, having within-run precision of < 5 % RSD. The decrease in reproducibility was mass dependent, indicating poor performance of either the internal standard or autolens. Quantitation of

isotopes having m/z 25, 26 and 178 – 208 resulted in %-RSDs of 4 – 5% while all other isotopes resulted in %-RSDs of 0.2 – 2%.

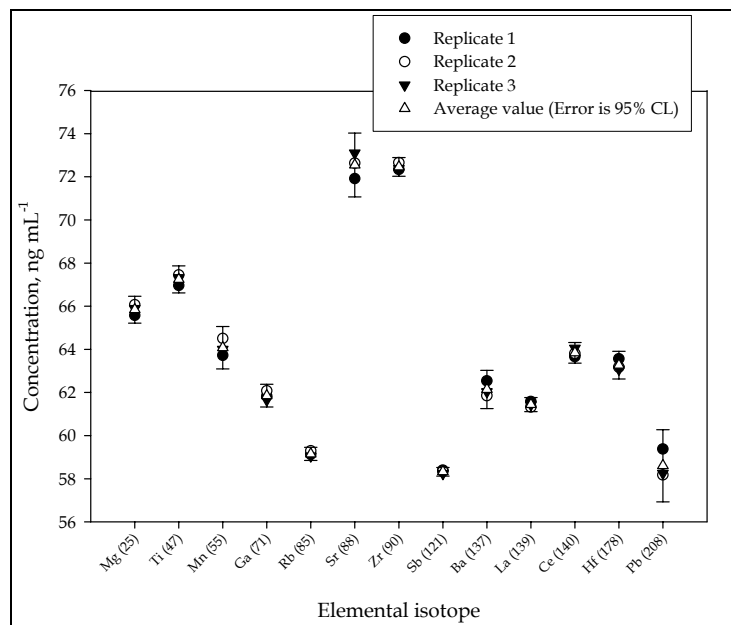


Figure 5. Within-run reproducibility, Day 1 (Selected isotopes).

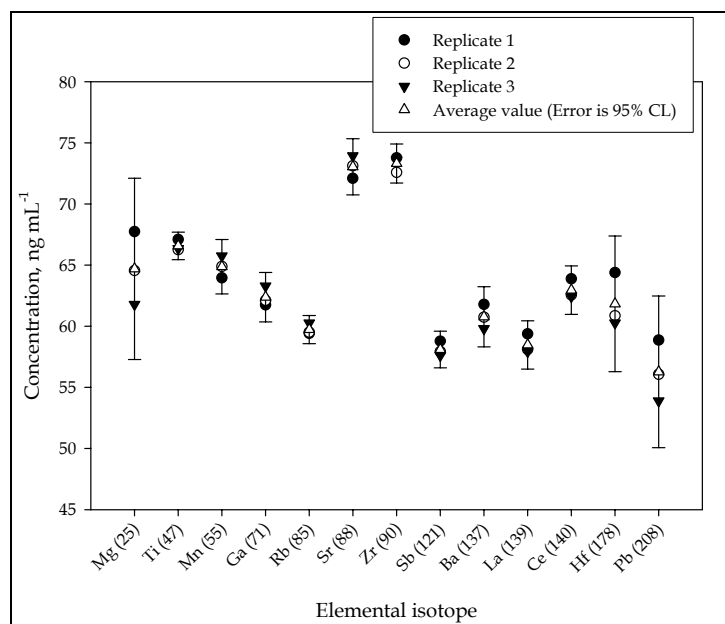


Figure 6. Within-run reproducibility, Day 4 (Selected isotopes).

The daily reproducibility results obtained using a CN were compared nominally at 3% of each value. This standard was chosen because it is the maximum RSD tolerated during instrument tuning. Using this nominal measure of error, there was no difference in the results obtained from one time point to the next (Figure 7). The daily reproducibility available from the MCN, determined using the same solutions analyzed in triplicate, were also indistinguishable at a nominal 3% about each average value. When 95% confidence intervals were calculated, however, there was a difference in the ^{25}Mg average value obtained at time point three with respect to the first two time points (Figure 8).

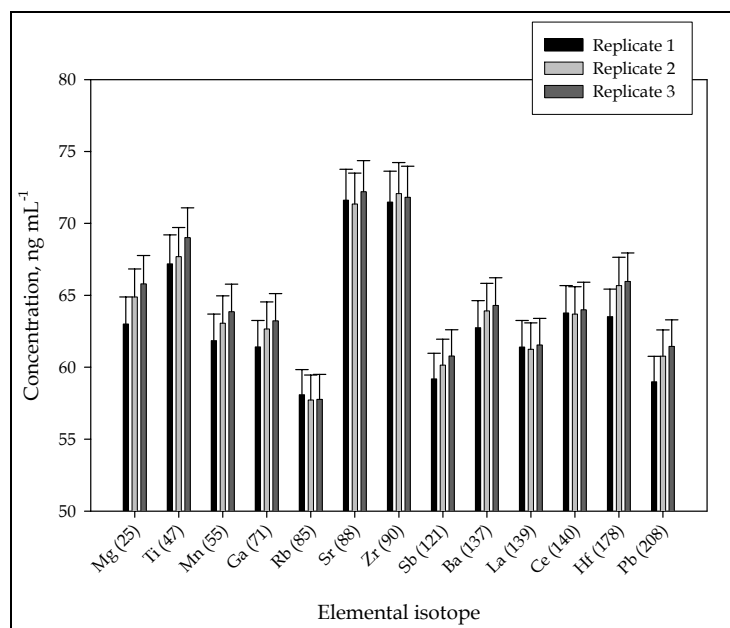


Figure 7. Within-day reproducibility using a CN (N = 1). Error shown is 3%.

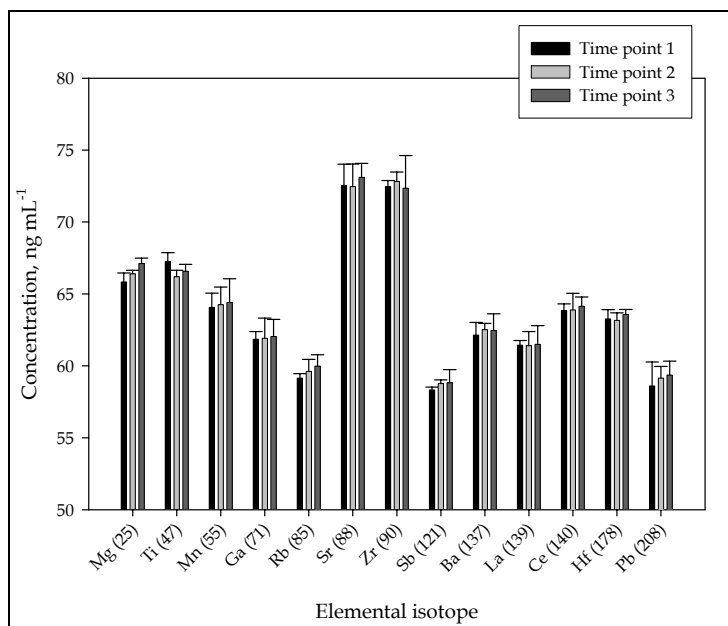
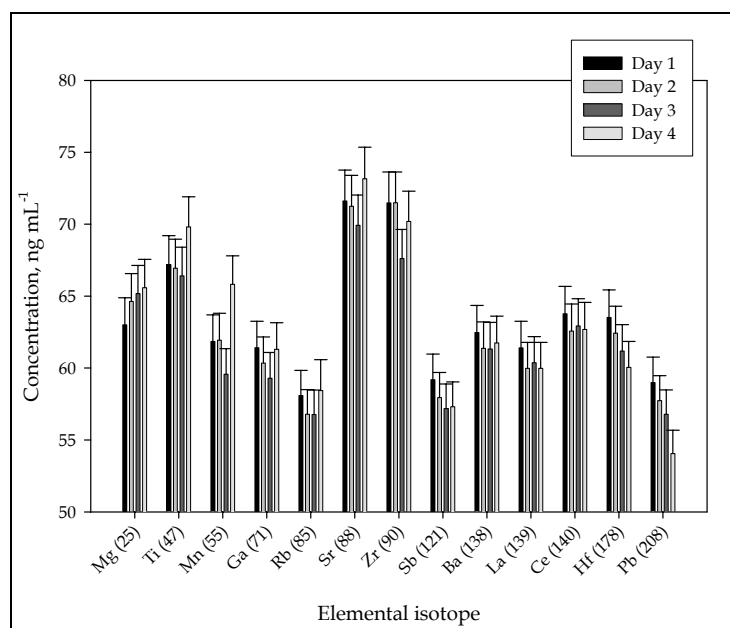


Figure 8. Within-day reproducibility using a MCN (N = 3). Error shown is 95% CL.

There were differences in the long-term data for ^{206,207,208}Pb using a 3%-tolerance for long-term data collected using a CN (Figure 9). Results obtained for all other isotopes were not significantly different using a 3%-tolerance. Only ²⁵Mg showed significant long-term differences in quantitation using a MCN when a 3% tolerance was applied. However, when 95% confidence intervals were calculated significant variation was observed for many isotopes (Figure 10). Only ^{25,26}Mg, ⁴⁷Ti, ^{86,88}Sr, ¹²¹Sb, ¹³⁷Ba and ^{206,207,208}Pb quantitation yielded statistically consistent results day-to-day. Of note is that the magnitude of the error was greatest for ^{25,26}Mg, ¹⁷⁸Hf, and ^{206,207,208}Pb. Because confidence intervals take into account the standard deviation of the mean value, these results are statistically indistinguishable because the error in individual means was higher. This echoes the mass-dependent variations seen run-to-run. The fact that ⁴⁷Ti, ^{86,88}Sr, ¹²¹Sb, and ¹³⁷Ba were statistically similar day-to-day over a longer period of time,

with relatively small errors compared to the low and high mass results, would suggest that the internal standard has a very similar instrumental response to these elements. Finally, there is evidence of autolens calibration deterioration because Day 4 has the greatest error over the entire mass range observed. The autolens and detector were not optimized over the course of reproducibility testing; typically, these settings are optimized bimonthly by recommendation of the manufacturer.



**Figure 9. Long-term reproducibility using a CN (N = 1).
Error shown is 3%.**

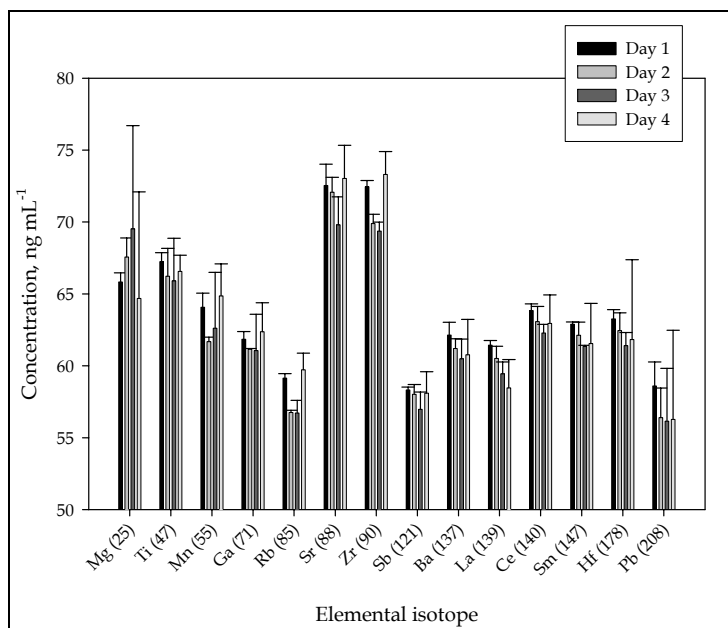


**Figure 10. Long-term reproducibility using a MCN (N = 3).
Errors shown are 95% CL.**

Summary. The difficulty in sample preparation makes the use of SN-ICP-MS seem an unlikely choice for forensic glass analysis, given that more convenient sample introduction techniques are now available. However, this technique remains widely used in the criminalistics community and warrants attention. Surprisingly, no report dedicated to the analytical figures of merit achievable using various nebulizer/spray chamber combinations for forensic glass analysis by SN-ICP-MS exists.

This study showed that sub-ng mL⁻¹ method detection limits and limits of quantitation were achievable using either a CN or MCN. The MCN provided comparably lower absolute detection limits, due to the reduced sample introduced. For both nebulizers, absolute detection limits were < 100 femtograms. The analytical sensitivity using a MCN was as much 10% less than the analytical sensitivity achievable using a CN. There was limited accuracy of results obtained for standard reference materials using

either nebulizer. Precision testing showed that variation in quantification using either nebulizer was concentration-dependent and greatly affected by the variation in acid digestion. At concentrations of 50 ng mL^{-1} , %-RSDs using either nebulizer were 10% or less. Percent relative standard deviation approached 40% at sample concentrations of 1 ng mL^{-1} or less. Bias calculations showed that the MCN provided analytical bias that was greater in magnitude than that provided by the CN. Both nebulizers are suitably reproducible using a 3% tolerance. However, when confidence intervals are calculated for replicate analyses using a MCN intraday and interday variations become apparent. Some of these effects are mass dependent.

A few mass-dependent differences in analytical performance between the MCN and CN were observed. Among these, there was a general decrease in sensitivity using MCN that increased in magnitude as a function of increasing isotopic mass. Bias determinations appeared to show mass bias in favor of lighter elements; the degree to which this bias affected the result was greater if the MCN was used. Mass effects were also seen in reproducibility testing using the MCN. Whether the apparent mass bias is strictly associated with instrument performance or matrix effects remains to be determined. Neither of these potential effects can be eliminated – very likely, one or both of these effects have a greater impact on the analysis depending on the nebulizer used. The results presented here do not conclusively support one source of mass bias over another.

While these issues remain to be resolved, it seems both the MCN and CN techniques provide adequate analytical performance for application to casework samples. The MCN is preferred over the CN, so that data can be interpreted statistically. One

important limitation to be recognized in using either nebulizer is that %-RSDs increase dramatically with low-level detection, and that the variation due to acid dissolution can be two to ten times greater than inherent instrumental variability.

LA-ICP-MS: Figures of Merit

Linearity of LA-ICP-MS and validation of ²⁹Si as internal standard. Suitable linearity was obtained for the five isotopes examined (Table 18). The linearity of the response in analyte: internal standard as a function of concentration showed high correlation following linear regression ($R^2 > 0.999$).

Table 18. Linear regression data for titanium, rubidium and lead.

Isotope	Slope, m^4	y-intercept (CPS)	Correlation (R^2)
⁴⁹ Ti	$1.591 \times 10^{-5} \pm 2.4 \times 10^{-7}$	$-7.1 \times 10^{-5} \pm 6.1 \times 10^{-5}$	0.99976
⁸⁵ Rb	$5.6295 \times 10^{-4} \pm 4.6 \times 10^{-7}$	$-1.1 \times 10^{-4} \pm 1.1 \times 10^{-4}$	0.99999
²⁰⁶ Pb	$1.5539 \times 10^{-4} \pm 8.6 \times 10^{-7}$	$-1.9 \times 10^{-4} \pm 2.1 \times 10^{-4}$	0.99997
²⁰⁷ Pb	$1.4348 \times 10^{-4} \pm 8.6 \times 10^{-7}$	$-2.3 \times 10^{-4} \pm 2.1 \times 10^{-4}$	0.99996
²⁰⁸ Pb	$3.417 \times 10^{-4} \pm 2.1 \times 10^{-6}$	$-5.1 \times 10^{-4} \pm 5.3 \times 10^{-4}$	0.99996

Because NIST reported values are not available for all the elements of interest in these three SRMs, it was not possible to validate the linearity in analyte: internal standard response for all the analytes used. It is very possible that nonlinear effects exist for certain elements (47), but these results would indicate that a linear response exists for at least three orders of magnitude in concentration for these elements.

⁴ See page 26 for units.

The data further indicate the relative sensitivity of LA-ICP-MS for each isotope. Sensitivity values for the $^{206,207,208}\text{Pb}$ isotopes of lead appear to correlate well with their relative isotopic abundances (24.1, 22.1, and 52.4%). This is a strong indication that no isobaric interferences exist at these m/z values. Further, the differences in sensitivity between titanium, rubidium and lead might indicate a sampling bias in favor of higher mass elements as reported elsewhere, or may be a sampling error resulting from differences in isotopic abundances. ^{85}Rb (72.2% abundant) and $^{206,207,208}\text{Pb}$ have isotopic abundances at least twice that of ^{49}Ti (5.5% abundant).

Method detection limits. Typical MDLs and ADLs obtained during the analysis of NIST SRM 612 are provided in Table 18. The background signal for each isotope was averaged over twenty ablations of SRM 612, representing background levels in the carrier gas, sample cell chamber, and sample transport tubing.

MDLs ranged from approximately $0.20 - 5 \mu\text{g g}^{-1}$ while absolute detection limits ranged from $0.01 - 1.5$ picograms (pg). Several differences in MDLs were observed for isotopes of the same element, which appears to be inversely related to isotopic abundance. This relationship is not unexpected, since less abundant isotopes suffer from greater measurement uncertainty. One difference stands out: two orders of magnitude separate the MDLs for ^{86}Sr ($1.2 \mu\text{g g}^{-1}$) and ^{88}Sr ($0.022 \mu\text{g g}^{-1}$). There are three isobaric overlaps at m/z 86: strontium ($^{86}\text{Sr}^+$), krypton ($^{86}\text{Kr}^+$), and ytterbium ($^{172}\text{Yb}^{2+}$). The mathematical corrections for elemental isobaric overlaps corrected the signal at m/z for $^{86}\text{Kr}^+$ but not $^{172}\text{Yb}^{2+}$ (Table 4). There is approximately $40 \mu\text{g g}^{-1}$ Yb in NIST SRM 612. The increased background of $^{86}\text{Sr}^+$ might be solely due to low abundance, but the

contribution of $^{172}\text{Yb}^{2+}$ cannot be ruled out if this element is susceptible to memory effects.

Table 19. Average MDLs and ADLs obtained during background data acquisition of NIST SRM 612 (N = 20).

Isotope	MDL, $\mu\text{g g}^{-1}$	ADL, pg
^{25}Mg	0.55	0.16
^{26}Mg	4.3	1.3
^{49}Ti	5.2	1.5
^{55}Mn	0.33	0.10
^{69}Ga	0.08	0.03
^{71}Ga	0.05	0.07
^{85}Rb	0.03	0.01
^{86}Sr	1.2	0.36
^{88}Sr	0.02	0.01
^{90}Zr	0.04	0.01
^{91}Zr	0.24	0.07
^{92}Zr	0.08	0.03
^{94}Zr	0.08	0.03
^{121}Sb	0.14	0.04
^{137}Ba	0.12	0.04
^{138}Ba	0.02	0.01
^{139}La	0.02	0.01
^{140}Ce	0.02	0.01
^{178}Hf	0.06	0.02
^{206}Pb	0.09	0.03
^{207}Pb	0.08	0.03
^{208}Pb	0.05	0.01

There is a general inconsistency among users of LA-ICP-MS regarding the calculation and reporting of MDLs¹⁻⁶, which makes comparison of experimental and published results difficult. Further, no mention of a standard limit of quantitation has been mentioned in the literature. For casework purposes, some criminalists use all values

at or above the detection limit. This presents a problem when determining the reliability of a quantitative result. This can be circumvented by recognizing that as detection limits are approached, %-RSDs increase. For example, quantitative data for antimony (Sb) in NIST SRM 1831 was typically on the order of $0.1 \mu\text{g g}^{-1}$, with relative standard deviation as great as 30%. In contrast, the average quantitative result for Sb in NIST SRM 612 was $31 \mu\text{g g}^{-1}$ with relative standard deviation of 2%. The precision of a concentration result may then serve as an index of its reliability.

Accuracy, precision and bias. The accuracy of this method was evaluated by comparing experimental and published compositional data for NIST 610 and 612. By comparison to NIST-certified values, quantitative results fell within ten percent of the reported value for both NIST 610 and 612. Confidence intervals could not be calculated for NIST reported values because certificates of analysis do not report the number of data points acquired. Thus, a statistical interpretation of quantitative differences could not be performed.

The accuracy of this method was further evaluated by comparing experimental concentration results to those published by Pearce, *et al* (Tables 20 and 21). Experimental values for each isotope were compared at 95% confidence using the Student's *t* test.

Experimental values for NIST SRM 610 agreed better with Pearce *et al* than did experimental results for NIST SRM 612. Of the 22 isotopes examined, 12 isotopes quantified in SRM 610 were statistically indistinguishable from the overall values reported by Pearce *et al* while nine were indistinguishable from the preferred values (Table 19). Nine of the isotopes quantified in NIST SRM 612 agreed with the overall values published by Pearce, *et al*. Four of these agreed with the preferred values (Table

21). The fact that NIST SRM 610 shows greater agreement than SRM 612 may be related to the resulting concentrations of sample digests. SRM 610 digests had final elemental concentrations in the range of 10 – 50 ng g⁻¹ (depending on the mass of glass digested) whereas final elemental concentrations of SRM 612 digests were typically < 5 ng g⁻¹. It is possible that the sample handling processes cited in Pearce *et al* resulted in sample digests that approached the lower quantitation limits of the analytical methods used. Analysis using LA-ICP-MS does not require sample dilution and the concentrations in both SRMs are well above detection limits (at least one order of magnitude). One explanation for the discrepancy in agreement with published values between SRMs 610 and 612 may be that the relative precision of LA-ICP-MS is greater than the precision of SN-ICP-MS techniques. Only Ga, Rb and one isotope of Zr seemed to agree well with preferred published data for both SRMs.

Table 20. Comparison of experimental and published values, NIST SRM 610.

Overall values	Preferred values
$\ \bar{x}_{Exp} - \bar{x}_P\ < t \cdot S_D$ <p> ⁶⁹Ga, ⁷¹Ga, ⁸⁵Rb, ⁹⁰Zr, ⁹¹Zr, ⁹²Zr, ⁹⁴Zr, ¹³⁷Ba, ¹³⁸Ba, ¹³⁹La, ¹⁴⁰Ce, ¹⁷⁸Hf </p>	$\ \bar{x}_{Exp} - \bar{x}_P\ < t \cdot S_D$ <p> ⁶⁹Ga, ⁷¹Ga, ⁸⁵Rb, ⁹⁰Zr, ⁹¹Zr, ⁹²Zr, ⁹⁴Zr, ¹³⁹La, ¹⁷⁸Hf </p>
$\ \bar{x}_{Exp} - \bar{x}_P\ > t \cdot S_D$ <p> ²⁵Mg, ²⁶Mg, ⁴⁹Ti, ⁵⁵Mn, ⁸⁶Sr, ⁸⁸Sr, ¹²¹Sb, ²⁰⁶Pb, ²⁰⁷Pb, ²⁰⁸Pb </p>	$\ \bar{x}_{Exp} - \bar{x}_P\ > t \cdot S_D$ <p> ²⁵Mg, ²⁶Mg, ⁴⁹Ti, ⁵⁵Mn, ⁸⁶Sr, ⁸⁸Sr, ¹²¹Sb, ¹³⁷Ba, ¹³⁸Ba, ¹⁴⁰Ce, ²⁰⁶Pb, ²⁰⁷Pb, ²⁰⁸Pb </p>

Table 21. Comparison of experimental and published values, NIST SRM 612.

Overall values	Preferred values
$\ \bar{x}_{Exp} - \bar{x}_P\ < t \cdot S_D$ <p> ²⁵Mg, ⁶⁹Ga, ⁷¹Ga, ⁸⁵Rb, ¹⁴⁰Ce, ¹⁷⁸Hf, ²⁰⁶Pb, ²⁰⁷Pb, ²⁰⁸Pb </p>	$\ \bar{x}_{Exp} - \bar{x}_P\ < t \cdot S_D$ <p> ⁶⁹Ga, ⁷¹Ga, ⁸⁵Rb, ⁹²Zr </p>
$\ \bar{x}_{Exp} - \bar{x}_P\ > t \cdot S_D$ <p> ²⁶Mg, ⁴⁹Ti, ⁵⁵Mn, ⁸⁶Sr, ⁸⁸Sr, ⁹⁰Zr, ⁹¹Zr, ⁹²Zr, ⁹⁴Zr, ¹²¹Sb, ¹³⁷Ba, ¹³⁸Ba, ¹³⁹La </p>	$\ \bar{x}_{Exp} - \bar{x}_P\ > t \cdot S_D$ <p> ²⁵Mg, ²⁶Mg, ⁴⁹Ti, ⁵⁵Mn, ⁸⁶Sr, ⁸⁸Sr, ⁹⁰Zr, ⁹¹Zr, ⁹⁴Zr, ¹²¹Sb, ¹³⁷Ba, ¹³⁸Ba, ¹³⁹La, ¹⁴⁰Ce, ¹⁷⁸Hf, ²⁰⁶Pb, ²⁰⁷Pb, ²⁰⁸Pb </p>

The precision of this method appears to be better than that reported in the literature (Figure 11), with approximately 2% RSD for most elements. The highest RSDs were observed in replicate measures of ²⁵Mg, ²⁶Mg, ⁵⁵Mn, and ⁹¹Zr in NIST SRM 612 (3.9, 6.2, 5.9 and 3.7% respectively). The precision of these same elements was improved for NIST SRM 610 (approximately 2% for each).

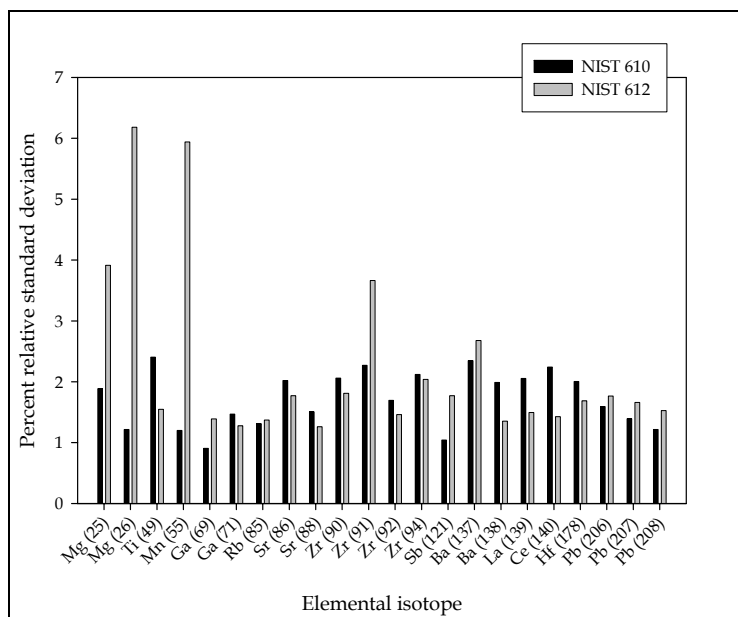


Figure 11. %-RSDs achieved by LA-ICP-MS.

Table 22 describes the bias found by LA-ICP-MS as compared to NIST reported values. On average, there was a positive bias in NIST SRM 610 concentrations and a negative bias in SRM 612 concentrations. The magnitude of these bias values does not exceed 10% of the NIST reported values.

Table 22. Bias results for SRMs 610 and 612 (N = 20).

NIST SRM 610 ($\mu\text{g g}^{-1}$)		NIST SRM 612 NIST SRM 610 ($\mu\text{g g}^{-1}$)	
<i>Isotope</i>	<i>Bias</i>	<i>Isotope</i>	<i>Bias</i>
⁵⁵ Mn	-29.891	⁸⁵ Rb	0.208
⁸⁵ Rb	7.213	⁸⁶ Sr	-8.321
⁸⁶ Sr	12.751	⁸⁸ Sr	-7.838
⁸⁸ Sr	5.812	²⁰⁶ Pb	-1.752
²⁰⁶ Pb	27.047	²⁰⁷ Pb	-1.718
²⁰⁷ Pb	31.433	²⁰⁸ Pb	-1.483
²⁰⁸ Pb	30.979		

Reproducibility. The within-run, within-day (short-term) and long-term reproducibility of LA-ICP-MS was determined by analyzing NIST SRM 610 for a total

of four nonconsecutive days. Typically, analyses by LA-ICP-MS are averages of three to four ablation events. The within-run reproducibility of this method was such that individual results fell within five percent of the average value (Figure 12). For most days, there was 1 – 3% RSD from run-to-run.

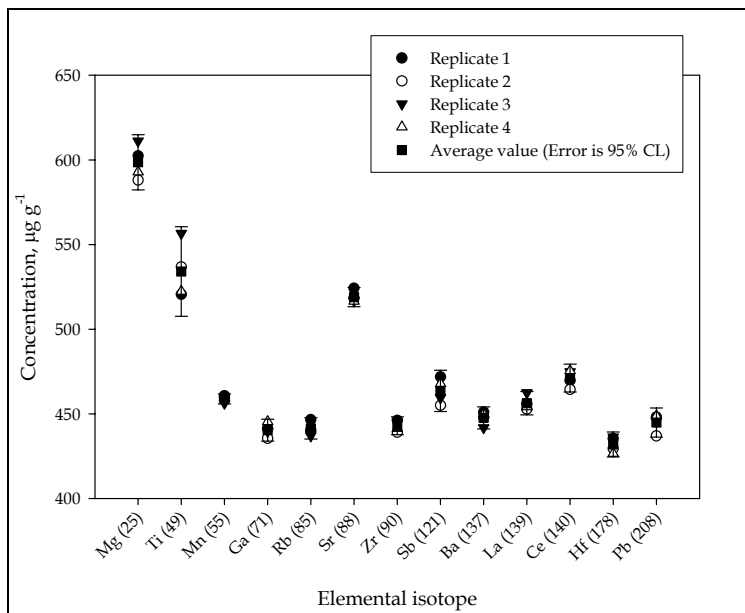


Figure 12. NIST SRM 610: Within-run reproducibility.

The short-term reproducibility of this method varied by day. On Day 1, the second analysis was distinguishable from the first and third analyses at 95% CL for ⁴⁹Ti; all other isotopes were indistinguishable within that day. Day 2 showed the worst agreement between analyses (Figure 13). In this case, the second analysis was distinguishable from the first and third in all but four isotopes. On Day 3, the first analysis was distinguishable from the second and third only in ^{90,91}Zr. On Day 4, the second analysis was distinguishable from the first and third in ^{206,207,208}Pb. These variations did not appear to depend on time, or isotopic mass; nor were these variations

specific to a particular element. These patterns would suggest instrumental drift, typical of plasma spectrometry.

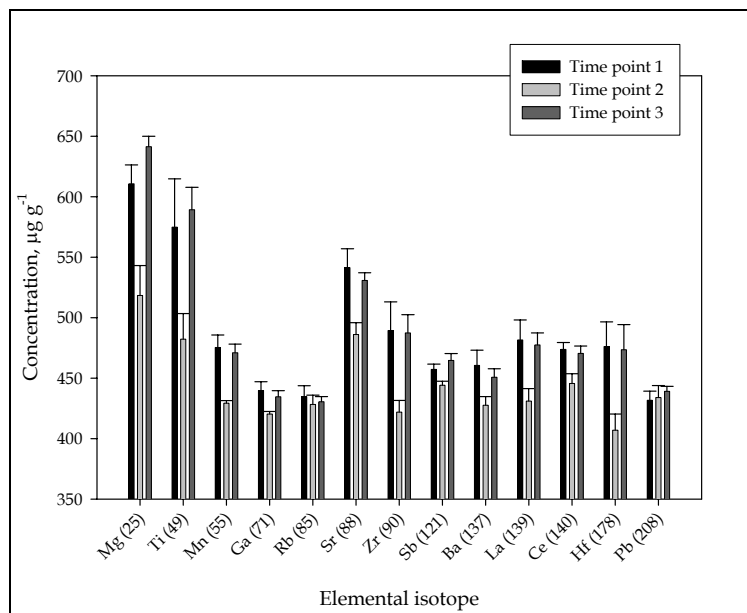


Figure 13. NIST SRM 610: Within-day reproducibility of LA-ICP-MS (N = 4).

Errors shown are 95% confidence limits.

The long-term variation, averages of all 12 – 15 ablations performed in a day, echoed the results obtained during short-term reproducibility testing (Figure 14). There were significant differences in ^{25,26}Mg, ⁴⁹Ti, ^{86,88}Sr, ^{90,91,92,94}Zr, ¹³⁹La, ¹⁷⁸Hf, and ^{206,207,208}Pb from day-to-day. As before, these differences did not appear to be related to mass or a specific element with the exception that groups of similar-mass isotopes showed comparable variations (Mg and Ti, Sr and Zr, etc), another strong indication of instrumental drift.

Trejos, *et al* (30) observed similar variations and corrected for these using elemental ratios. The isotopes they selected to ratio were similar in mass and detection variability. To determine the potential utility of isotopic ratios to correct for the apparent instrumental drift observed here, data shown in Figure 13 (within-day variation in NIST SRM 610) was modified by calculating: ($^{25}\text{Mg} / ^{49}\text{Ti}$), ($^{71}\text{Ga} / ^{85}\text{Rb}$), ($^{88}\text{Sr} / ^{92}\text{Zr}$), ($^{137}\text{Ba} / ^{140}\text{Ce}$), and ($^{139}\text{La} / ^{208}\text{Pb}$). Improvement in intraday variation was marked (Figure 15). This method of drift correction may serve users of LA-ICP-MS well.

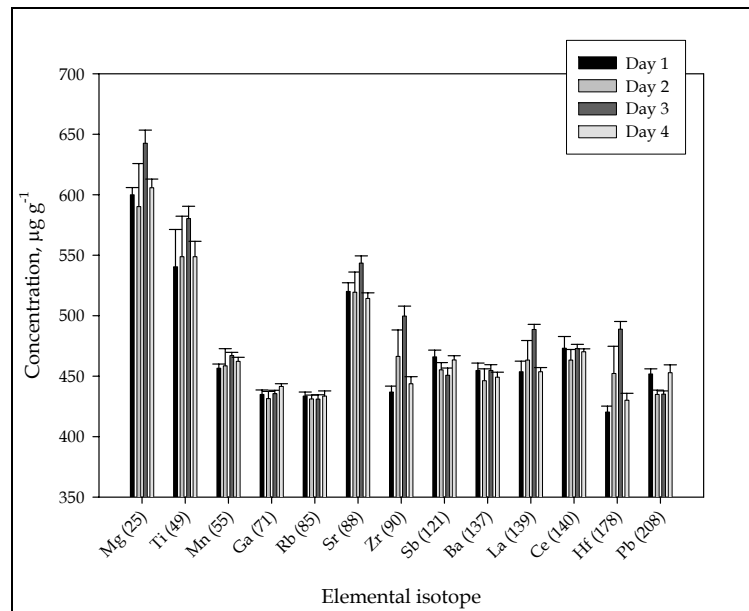


Figure 14. NIST SRM 610: Long-term reproducibility (N = 4).

Errors shown are 95% confidence limits.

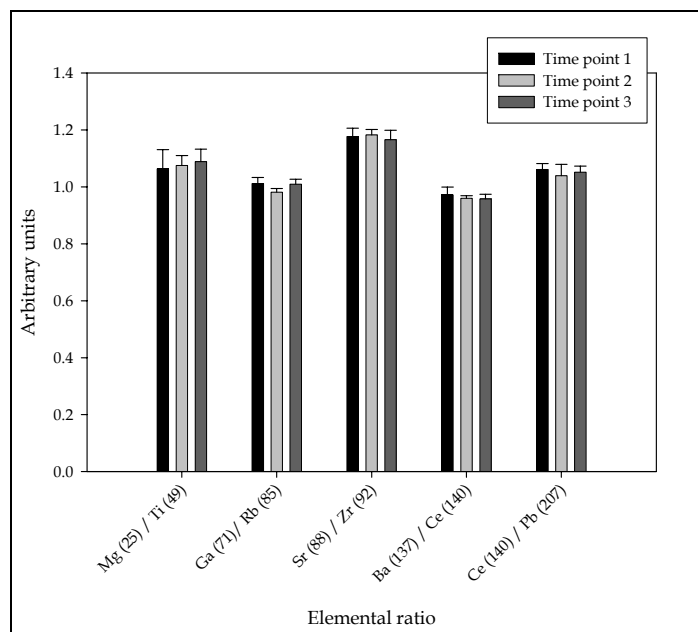


Figure 15. NIST SRM 610: Selected isotopic ratios.

Errors shown are 95% confidence limits.

Summary. LA-ICP-MS is a powerful technique for the elemental analysis of a wide variety of materials encountered in forensic casework. Among these, forensic glass analysis stands out as an application for which this technique has great utility to provide highly discriminating information while maintaining minimal sample consumption.

LA-ICP-MS exhibits linearity in analyte: internal standard response over the mass range of interest for forensic glass analysis, with excellent linear correlation. The sensitivity of this technique ranges from $1 \times 10^{-5} - 1 \times 10^{-4} \text{ CPS}_A \cdot (\mu\text{g g}^{-1})_A \cdot \text{CPS}_{IS}^{-1}$ analyte: internal standard response and offers sub- $\mu\text{g g}^{-1}$ method detection limits. Absolute detection limits are as low as 10 femtograms (fg) for certain elements. The accuracy achievable with this technique would indicate a certain amount of bias present. However, this bias is not greater than 10% of the true value for any particular element.

LA-ICP-MS offers excellent repeatability, with run-to-run RSDs of less than 5%. There is significant drift in analyte: internal standard response over time, the effects of which are observed within a single day of analysis. Elemental ratios correct for that drift, given that the behavior of the isotopes used for internal correction are similar during ablation and sampling in the plasma. The primary factors that influence such behavior are mass and isotopic abundance. All in all, these figures of merit indicate that LA-ICP-MS may be confidently applied to forensic casework, given that caution is used when assigning significance to low-level quantitative results and data gathered over time.

Glass composition as a means for increased discriminatory potential has been extensively explored. In particular, ICP-MS has been touted as the most discriminating technique currently available for the chemical analysis of glass, especially when combined with other methods of discrimination. The incorporation of LA sampling for routine forensic analysis facilitates the use of elemental data for forensic comparisons by making such analyses more convenient and cost-effective overall. With reference to solution sampling, sample preparation for solid sampling is reduced in time and cost; time-intensive and potentially hazardous digestion protocols that require special safety precautions are eliminated. Sample consumption is markedly decreased over other techniques; however, analysis time is increased somewhat as automated sampling has not yet been developed for LA. Overall, however, the time and cost savings in sample preparation for LA over other sample introduction techniques is larger than the time deficit required for analysis. Finally, LA allows for *in situ* analysis. This is a great advantage for forensic analysis, as there is less opportunity for sample mishandling.

Figures of Merit Compared

A primary criticism of LA is the practice of single point calibration. While linearity for LA could only be examined using three elements, excellent linear correlation obtained indicated a suitably linear response in analyte: internal standard over two orders of magnitude in concentration (Table 18). The linear correlation observed with LA was typical of CN, where five calibration standards were used also spanning two orders of magnitude in concentration. Further evidence that suitable linearity in analyte: internal standard is observed using a single point calibration for LA is the general agreement in quantitative results obtained by SN and LA using the same ICP-MS (Figure 16).

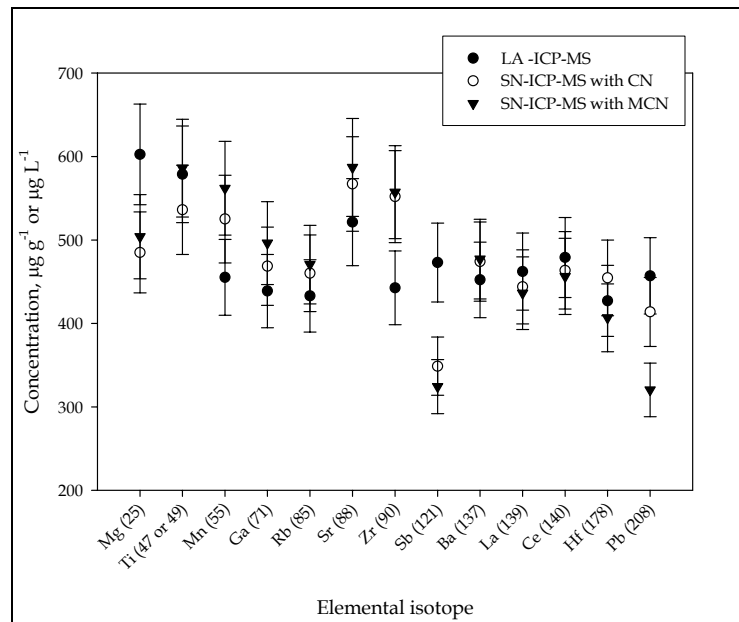


Figure 16. NIST SRM 610: Comparison of SN and LA at 10% tolerance.

Method detection limits (MDLs) for SN and LA were different by several orders of magnitude in concentration; however, this is not a fair comparison of detection limits between the two systems since varying amounts of sample were introduced to the plasma

depending on the technique. Over 1-mL sample volume was introduced to the plasma using a CN, while approximately 0.12-mL sample volume was introduced using a MCN. In terms of sample volume, $1.3 \times 10^{-7} \text{ cm}^3$ is introduced to the plasma during ablation. Thus, it is more appropriate to compare absolute detection limits (ADLs). Using LA, the majority of ADLs ranged from 0.01 – 0.1 picograms (pg). For certain isotopes, ^{26}Mg , ^{47}Ti , and ^{86}Sr , ADLs were higher (0.3 – 2 pg). Using a CN for liquid introduction, ADLs ranged between 6 and 130 pg while ADLs ranged between 5 and 20 pg using a MCN. LA proved to provide the lowest absolute detection limits.

The accuracy afforded by each SN technique and LA introduction was comparable in the number of isotopes that agreed with the results published by Pearce, *et al*¹⁶ for NIST SRMs 610 and 612. However, the isotopes that agreed did not correlate by introduction method (Tables 13 – 16; Tables 20 and 21). LA and SN with both nebulizers fell within 10% of the NIST certified concentrations for Rb and Sr; only the results obtained by LA and SN using a CN fell within 10% of the NIST certified concentration for Pb (Figure 17). Only LA provided results that were within 10% of the NIST reported values for every certified element in NIST SRM 612 (Figure 18).

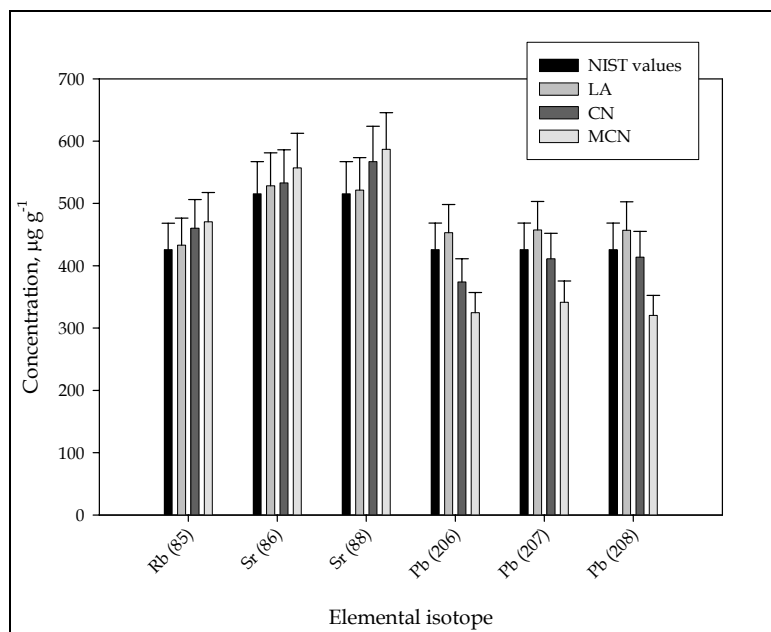


Figure 17. Comparison of LA and SN results for certified elements in NIST SRM

610. Errors shown are 10%.

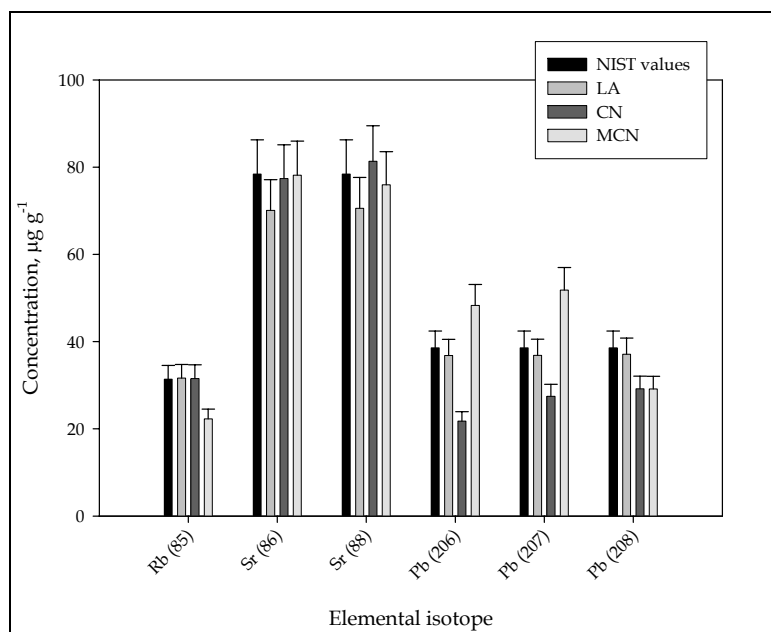


Figure 18. Comparison of LA and SN results for certified elements in NIST SRM

612. Errors shown are 10%.

The overall precision of LA is better than or equal to that achievable using SN (Figures 2, 3 and 11). Twenty replicate analyses of NIST SRMs 610 and 612 resulted in overall percent relative standard deviations (%-RSDs) $< 6\%$. For most isotopes, these %-RSDs were less than 3%. Ten analyses of NIST SRM 610 by SN using either nebulizer were comparable, whereas ten analyses of NIST 612 using a CN resulted in %-RSDs of 20 – 35%. For the same analyses conducted using a MCN for liquid introduction, %-RSDs were as great as 40%. As previously discussed, the poor precision associated with the SN results is due to the variation associated with sample dissolution (Figure 4). Thus, there is marked improvement in analytical precision of LA over SN techniques; the elimination of sample dissolution greatly improves the reliability of the analytical result. Sample dissolution may have contributed to the greater bias associated with SN over LA (Tables 17 and 22). Bias in concentration results obtained by LA for NIST 610 and 612 were generally less than those obtained by either SN technique. The absence of mass-dependent differences in bias results obtained by LA suggests that the observed mass bias during SN data collection was not a function of the internal standard chosen. These results support the second hypothesis that the mass dependent effects were likely associated with autolens calibration, rather than internal standardization.

It was observed that sufficient within-day variation exists using LA for elemental quantitation of the same sample to be statistically different in selected isotopes (Figure 13). It is difficult to compare this result to the within-day reproducibility observed using a CN for liquid digests since replicate analyses could not be performed with the higher flow nebulizer. While statistical differentiation of reproducibility samples could not be performed for within-day reproducibility testing by CN, quantitative results did not vary

by more than 3% (Figure 7). Replicate ablations over one day, however, did vary by more than 10% for some isotopes. Only one isotope was statistically distinguishable within a day using a MCN (Figure 8). With regard to within-day reproducibility, then, it seems SN offers improved performance.

The long-term reproducibility of LA echoed the within-day variation previously observed (Figure 14) while the long-term reproducibility of SN using a CN was greatly diminished by comparison (Figure 9). There was an apparent mass bias in the reproducibility observed using the CN, only high mass elements show significant variation using a 3% tolerance. This pattern is also consistent with drifting autolens calibration. There was some long-term variation in results obtained using the MCN (Figure 10); however, they were not as drastic as the variation observed with liquid introduction using CN or solid sampling by LA.

Researchers at the International Forensic Science Research Institute have proposed the use of elemental ratios to correct for the intra- and interday variation observed when using LA sample introduction (26). This idea was successfully applied to data collected that varied over several hours (Figure 15). From these results, it is apparent that ^{29}Si is an effective internal standard for analyses conducted within single runs, but fails to correct instrumental drift for analyses conducted over time. Elemental ratios are a successful remedy to this situation.

While SN offers increased reproducibility over LA, LA offers equivalent or better sensitivity, accuracy, precision, and bias. Further, the variation using LA can be easily corrected. Given the minimal sample preparation required and the negligible sample

consumption of LA sampling over SN, it is surprising that those facilities making use of ICP-MS for the forensic analysis of glass use SN rather than LA.

Evaluation of SN and LA for Forensic Casework

There were no statistically significant differences in the RIs of K-1, Q-1 and Q-2 (Figure 19).

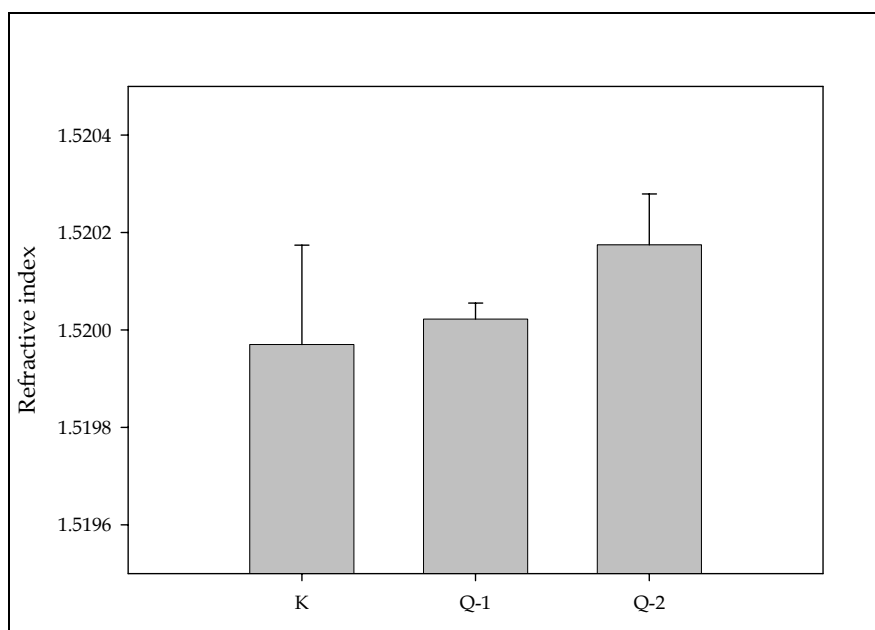


**Figure 19. Mock case samples - Refractive index (K, N = 5; Qs, N = 4).
Errors shown are 95% CL.**

The analysis of K-1, Q-2 and Q-3 by SN-ICP-MS using a CN presented some difficulties. First and foremost, statistical information could not be gathered for the questioned fragments since the sample volume limited the number of analyses that could be performed on each digest to one. The analysis of six separate digests could be performed on the reference sample, K-1, providing some statistical information as to the concentration ranges that could be expected from this glass source. Second, the limits of

quantitation excluded the possibility of comparing $^{69,71}\text{Ga}$, ^{121}Sb , and $^{206,207,208}\text{Pb}$ levels in the reference and some questioned glasses due to the dilution of low-level analytes ($< 1 \mu\text{g mL}^{-1}$).

Since confidence intervals could not be calculated for the quantitative results of Q-1 and Q-3, the reference and questioned glasses were compared using a 5% tolerance (Figure 20). This value was selected because it seemed to be the approximate %-RSD achievable when comparing concentrations determined by multiple digestions (Figure 3).

On the basis of this elemental data, Q-2 is excluded as potentially sharing a common origin as the reference glass, K. Q-1, likewise, could be excluded if a 5% tolerance is used. Notably, Q-1 and K share approximately the same composition in every isotope quantified. The significance of this finding is greatly diminished by the fact that only a nominal tolerance can be applied to the quantitative results for questioned fragments.

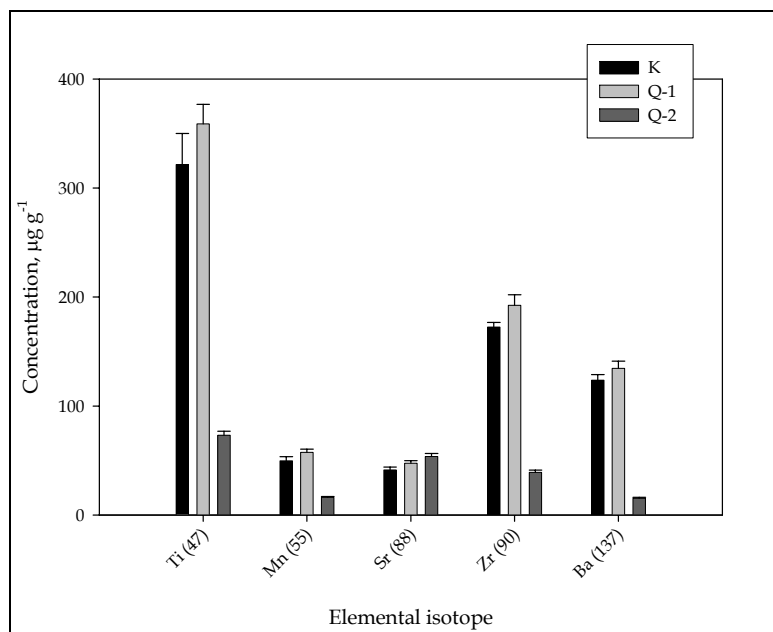


Figure 20. Trace elemental composition of K-1, Q-1 and Q-2 determined by SN-ICP-MS (CN). Errors shown are 95% CL for K-1; remaining errors are 5%.

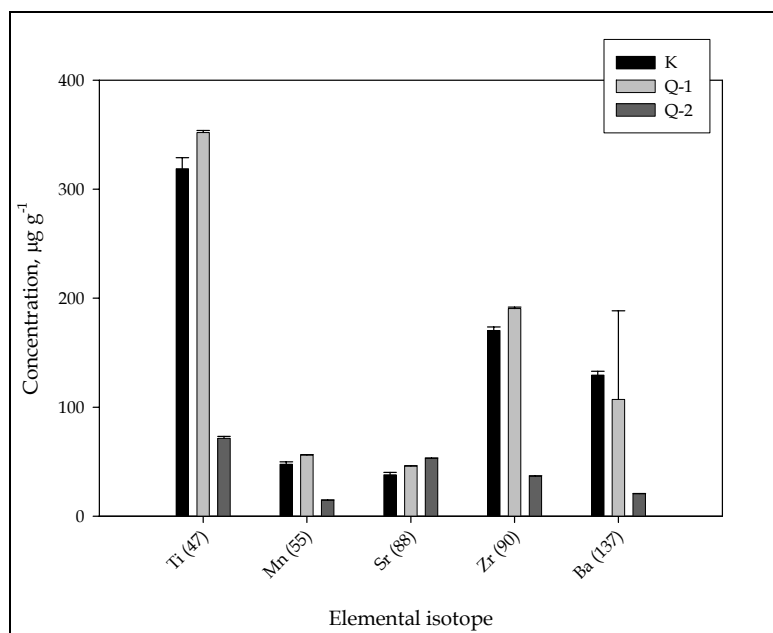


Figure 21. Trace elemental composition of K-1, Q-1, and Q-2 determined by SN-ICP-MS (MCN). Errors shown are 95% CL.

Elemental data gathered by SN-ICP-MS using a MCN facilitated quadruplicate analyses of each digest (24 total analyses for K; 4 total analyses for Q-1 and Q-2). On the basis of these results, it appears that both Q-1 and Q-2 can be excluded from sharing the same source as the reference glass. With this SN introduction technique, the element menu was also limited by the dilution of low-level elements.

The use of LA-ICP-MS allowed for a greater number of isotopes to be compared. The resulting quantitative results did not appear to suffer from drift affects, but this is not unexpected since analysis of K, Q-1 and Q-2 could be accomplished within a single run.

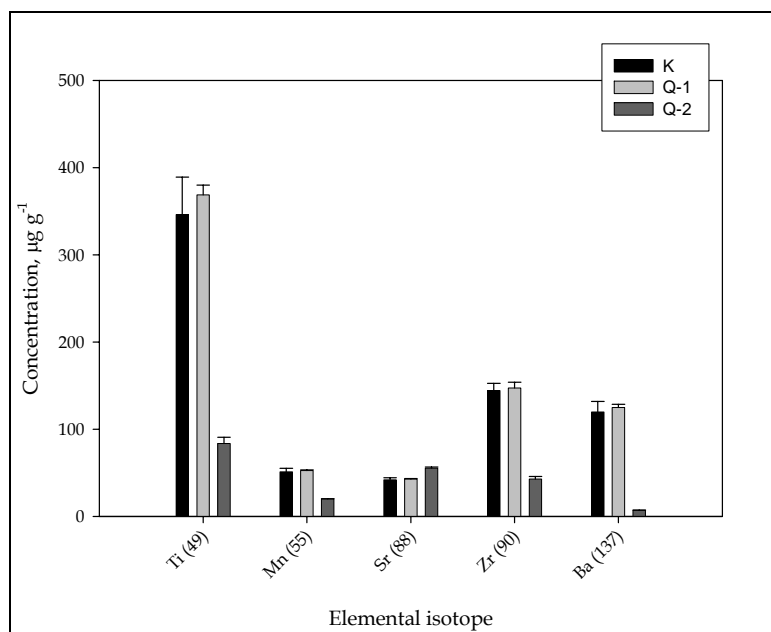


Figure 22. Trace elemental compositions of K-1, Q-1, and Q-2 determined by LA-ICP-MS. Errors shown are 95% CL.

Elemental compositions of K and Q-1 found by this method were such that Q-1 and K could *not* be excluded from sharing a common origin (Figure 22). These results are contrary to the results obtained using SN introduction.

The elemental data generated by each sample introduction technique, and the resulting associations/exclusions were submitted to the criminalist that selected the blind samples. It was revealed that the results obtained by LA facilitated the correct association: K and Q-1 were samples taken from the same automotive windshield. Q-2 and Q-3 were samples of differing automotive windshields (Table 23).

Table 23. Origin of blind samples.

Case reference	Sample origin
K, Q-1	Sicursiv Windshield
Q-2	Carlite Windshield
Q-3	XYG HK Windshield

While the correct association of K and Q-1 was made with LA-ICP-MS and not SN-ICP-MS using 95% confidence limits, it cannot be concluded that this outcome was solely due to the superiority of LA sampling, nor can it be concluded that SN-ICP-MS is unsuitable for casework. Rather, the different sources of variation associated with each technique must be considered. The sample preparation techniques for SN-ICP-MS and LA-ICP-MS are quite different; according to the results obtained here, acid dissolution has the potential to impact the outcome of SN-ICP-MS analyses greatly.

Certainly, when single fragments are submitted as evidence (as is almost always the case), a CN will not allow for repeated measurements of the same fragment. The lack of statistical information using a CN for liquid introduction greatly limits the significance

of any subsequent associations or exclusions. The MCN, however, will allow for multiple measurements when using SN sample introduction. One limitation of casework analysis by SN-ICP-MS – using either the CN or MCN – is the lengthy sample preparation that is required. Previous results show significant variation due to this method of sample preparation (Figure 4); it is not unreasonable to propose that such variations may have contributed to the incorrect exclusion of Q-1 from K at 95% confidence. Individual elemental concentrations in Q-1 and K as determined by SN-ICP-MS were similar at 10% RSD, but not at 95% confidence. Considering that the sample-to-sample variability in acid dissolution can be as great as 20% RSD, the differences in composition of the reference and questioned samples are not significant. When using SN-ICP-MS, therefore, the sample-to-sample variability due to acid dissolution must be accounted for.

LA-ICP-MS was proven to provide the greatest versatility in terms of the number of possible analytes and the greatest opportunity for replicate analyses with negligible sample consumption. While the cost of supplementing an existing ICP-MS with LA sampling is nominally greater than continuing to use SN introduction, the gains in terms of sample preservation, analyst convenience and greater opportunity to obtain statistical information are far greater.

Elemental Variation in Automotive Windshields

Elemental variation within a pane. The typical within-pane variation of the ten windshields examined was similar to that seen in Vitro Flex/ Carlite 2 (Figures 23 and 24). In this windshield, there were apparent differences at 95% confidence in $^{55}\text{Mn}/^{88}\text{Sr}$, $^{90}\text{Zr}/^{137}\text{Ba}$, and $^{178}\text{Hf}/^{208}\text{Pb}$ of subsamples collected from Pane 1 of Vitro Flex Carlite 2.

In contrast, several subsamples of Pane 2 were distinguishable in $^{55}\text{Mn}/^{88}\text{Sr}$, $^{85}\text{Rb}/^{88}\text{Sr}$, $^{90}\text{Zr}/^{137}\text{Ba}$, $^{139}\text{La}/^{140}\text{Ce}$, and $^{178}\text{Hf}/^{208}\text{Pb}$. Similarly, the majority of subsamples collected from the remaining windshields varied in multiple elemental ratios at 95% confidence. However, these differences were usually not greater than 10% of the elemental ratio value. Certain elemental ratios appeared to vary greater than others within a set of subsamples, regardless of the sample manufacturer or analyte concentration. $^{49}\text{Ti}/^{57}\text{Fe}$, $^{55}\text{Mn}/^{88}\text{Sr}$, $^{90}\text{Zr}/^{137}\text{Ba}$ and $^{178}\text{Hf}/^{208}\text{Pb}$ varied more within a set of subsamples than did $^{71}\text{Ga}/^{85}\text{Rb}$ and $^{139}\text{La}/^{140}\text{Ce}$.

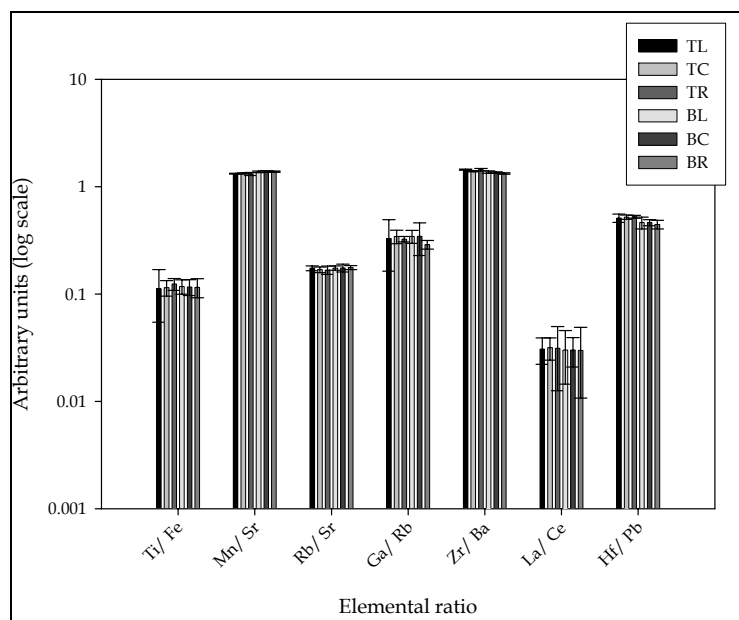


Figure 23. Within-pane variation in Pane 1 of Vitro Flex Carlite 2

Errors shown are 95% confidence limits, corrected for logarithmic scaling⁵.

⁵ The error in the logarithmic value is $\frac{1}{\ln 10} \cdot \frac{e}{x}$, where e is the error in the original value.

In general, the overall within-pane variation was less than or equal to 10% RSD when one or both of the elemental concentrations used to determine these ratios were $\geq 1 \mu\text{g g}^{-1}$. The range of observed %-RSDs in these twenty panes of glass was relatively large, from two to 20% RSD. Those elemental ratios exhibiting the greatest variation within a pane ($> 10\%$ RSD) were determined from low-level analytes. The variation in $^{71}\text{Ga}/^{85}\text{Rb}$ in Pane 1 of Sekurit 1a, for example, was 21% RSD while the variation in the same elemental ratio in Pane 2 of this windshield was 11%. The root of this discrepancy was the amounts of ^{71}Ga in these panes.

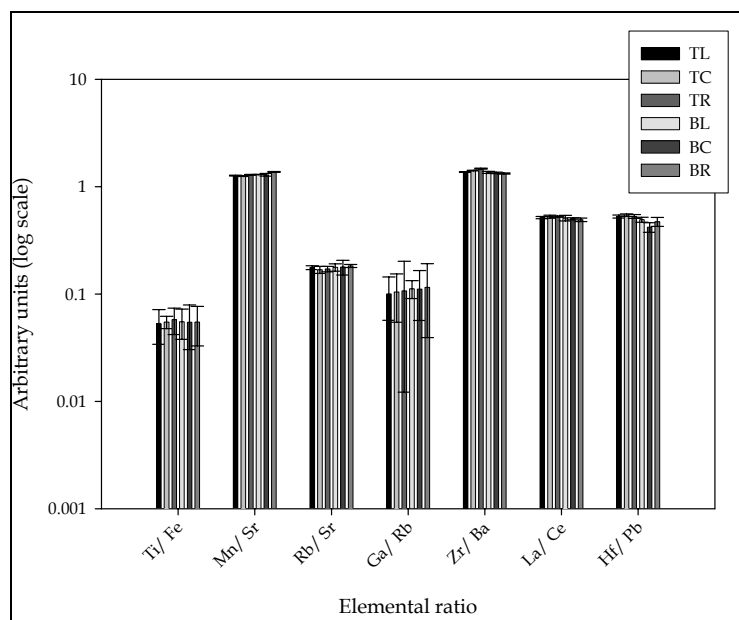


Figure 24. Within-pane variation in Pane 2 of Vitro Flex Carlite 2

Errors shown are 95% confidence limits, corrected for logarithmic scaling.

The concentration of ^{71}Ga in Pane 1 of this sample was $0.51_7 \pm 0.04_2 \mu\text{g g}^{-1}$; the concentration of ^{85}Rb was $3.1_7 \pm 0.4_1 \mu\text{g g}^{-1}$. The concentration of ^{71}Ga in Pane 2 was $0.85_6 \pm 0.04_6 \mu\text{g g}^{-1}$ while the concentration of ^{85}Rb was $2.4_3 \pm 0.3_6 \mu\text{g g}^{-1}$. The detection limits for most isotopes using LA-ICP-MS were between 0.05 and $0.1 \mu\text{g g}^{-1}$; limits of quantitation were between 0.5 and $1 \mu\text{g g}^{-1}$ concentration. The detection limit for ^{71}Ga was closer to $0.07 \mu\text{g g}^{-1}$, resulting in a limit of quantitation of approximately $0.7 \mu\text{g g}^{-1}$. The detection limit for ^{85}Rb was closer to $0.05 \mu\text{g g}^{-1}$; thus, the limit of quantitation for ^{85}Rb was approximately $0.5 \mu\text{g g}^{-1}$. The amounts of ^{85}Rb in both Panes 1 and Panes 2 of Sekurit 1a exceeded the limit of quantitation for this analyte, as did the amounts of ^{71}Ga in Pane 2 of this sample. The amount of ^{71}Ga in Pane 1 of Sekurit 1a, however, did not exceed the limit of quantitation for this technique – the outcome of which was an elevated %-RSD.

To determine whether the apparent differences in elemental ratios for groups of subsamples represented statistically distinguishable results, a Student's *t*-test was used to compare each elemental ratio in every subsample analyzed. In taking this approach, it was hoped to determine whether elemental ratios changed in value as a function of location in the glass. While most elemental ratios were found to be statistically distinguishable in most locations of the glass (Table 24), there was no clear correlation between differences and similarities in elemental ratios by location. When the values of one elemental ratio were compared in the top and bottom samples, for example, there was no clear indication that the elemental ratios found in the top subsamples were similar but different to those elemental ratios found in the bottom subsamples for any of the windshields examined. Similarly, no clear relationship existed between the elemental

ratios found in the right, center or left sides of any windshield. These results did, however, suggest a high degree of variability in the distribution of certain elemental ratios over others and that this distribution appears random at the level of subsampling pursued for this study. One interesting outcome of these univariate *t*-tests is that, out of the seven elemental ratios examined, $^{71}\text{Ga}/^{85}\text{Rb}$ was the most likely to be homogeneously distributed.

While the Student's *t*-test could be used to determine whether two results for a particular elemental ratio were significantly different, this test statistic had limited application for determining whether automotive windshields were homogenous in composition. To test this hypothesis, the similarity or dissimilarity of subsamples originating from a single pane of windshield glass must be demonstrated. Multivariate statistics were required for these comparisons, since each subsample was characterized by multiple variables.

Table 24. Summary of univariate Student's *t*-test results.

Elemental ratio	Number of comparisons where $t^2_{\text{Calculated}} > t^2_{\text{Critical}}$ (out of 15 possible comparisons)									
	Lam. 1	PLOF 1a	PLOF 1b	Sek. 1a	Sek. 1b	Sic. 1	VF/ Carl. 1a	VF/ Carl. 1b	VF/ Carl. 2	Xyg 1
<i>⁴⁹Ti/ ⁵⁷Fe</i>										
Pane 1	9	12	11	11	6	1	13	10	5	9
Pane 2	4	12	11	12	11	10	11	10	6	10
<i>⁵⁵Mn/ ⁸⁸Sr</i>										
Pane 1	2	9	5	9	1	10	2	8	1	9
Pane 2	5	6	4	9	6	13	8	12	7	13
<i>⁸⁵Rb/ ⁸⁸Sr</i>										
Pane 1	2	5	2	5	5	5	3	10	8	5
Pane 2	1	5	6	6	4	0	1	7	8	4
<i>⁷¹Ga/ ⁸⁵Rb</i>										
Pane 1	1	4	0	7	0	3	0	2	3	6
Pane 2	0	0	0	3	0	0	0	0	1	2
<i>⁹⁰Zr/ ¹³⁷Ba</i>										
Pane 1	9	8	5	11	10	2	8	11	4	4
Pane 2	6	9	5	9	9	8	6	11	9	8
<i>¹³⁹La/ ¹⁴⁰Ce</i>										
Pane 1	0	5	0	9	7	3	0	6	4	3
Pane 2	3	6	2	5	0	4	3	6	5	5
<i>¹⁷⁸Hf/ ²⁰⁸Pb</i>										
Pane 1	3	11	12	6	2	7	5	12	7	6
Pane 2	1	11	11	7	5	0	3	11	11	2

The results of Hotelling's T^2 test showed that Pane 1 of Vitro Flex/ Carlite 2 was homogeneous. Of all the possible comparisons between subsamples, there were no statistically significant differences at 95% confidence in the compositions of subsamples taken from Pane 1. Those differences in $^{49}\text{Ti}/^{57}\text{Fe}$, $^{85}\text{Rb}/^{88}\text{Sr}$, $^{139}\text{La}/^{140}\text{Ce}$ and $^{178}\text{Hf}/^{208}\text{Pb}$ that were graphically apparent were statistically insignificant.

Pane 2 of this windshield, however, was not homogeneous. There were significant differences between the top left and top right subsamples, the top left and bottom center subsamples, the top center and bottom center subsamples, the top right and bottom center subsamples and the bottom center and bottom right subsamples at 95% confidence. The differences in $^{55}\text{Mn}/^{88}\text{Sr}$, $^{85}\text{Rb}/^{88}\text{Sr}$, $^{90}\text{Zr}/^{137}\text{Ba}$ and $^{178}\text{Hf}/^{208}\text{Pb}$ were, in fact, significant.

As with any statistical test of differences between average values, Hotelling's T^2 takes into account the individual errors associated with each average value as well as the pooled error in these values. When the difference in the average values is small compared to the pooled error, the null hypothesis cannot be rejected. That is, the differences between the average values are considered insignificant because these differences fall within the natural variation of the sample. The individual errors associated with the average value of any variable used for comparing subsamples within a pane are described by the within-run precision for that variable; the pooled error is an estimate of the overall sample variation. Pane 1 of Vitro Flex/ Carlite 2 exhibited within-run precision that was comparably more similar to the overall sample variation than that exhibited by Pane 2 of this windshield (Figure 25). This is illustrated by the differences between the sample variation (V_s) and within-run precision (P), both expressed as %-RSD, for Panes 1 and 2.

These results suggest the analytical precision afforded by LA-ICP-MS may not adequately estimate the variation in elemental composition of automotive windshields. Since the analytical precision of LA-ICP-MS may be greater than the overall sample variation in a windshield, it is important to collect multiple reference samples from as many locations in the suspected original windshield as possible. Of course, the forensic scientist responsible for analyzing casework glass does not always have control over the collection of reference samples and crime scene investigators (CSIs) may not be aware of the potential for heterogeneity in automotive windshield glass. Thus, the collection of multiple references from the putative source should be integrated into the training programs of CSIs.

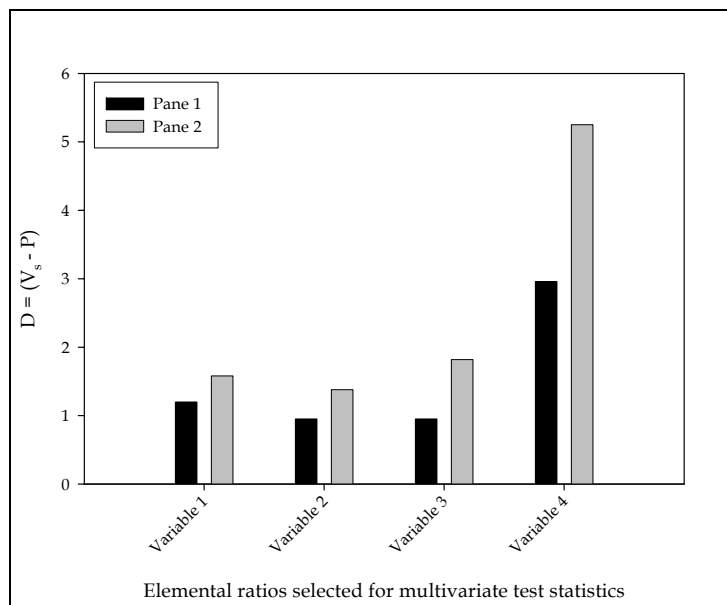


Figure 25. Differences in sample variation (V_s) and analytical precision (P) in Panes 1 and 2 of Vitro Flex/ Carlite 2.

An additional complication arises when only limited reference samples are available at the source – supposing only part of the putative original windshield was available for sampling. In these cases, statistical testing may not assist the criminalist in interpreting results. The criminalist will be required to form an opinion in the absence of statistically meaningful results. The fact that most elemental ratios did not vary by greater than 10% of their value when the concentrations used to determine the ratios were $> 1\mu\text{g g}^{-1}$ may assist the criminalist attempting to interpret apparent differences in questioned and reference fragments when adequate reference samples are not available.

Elemental variation within a windshield. Within the ten windshields examined, eight were composed of two distinct panes of glass while two were composed of similar panes of glass (Figures 26 and 27).

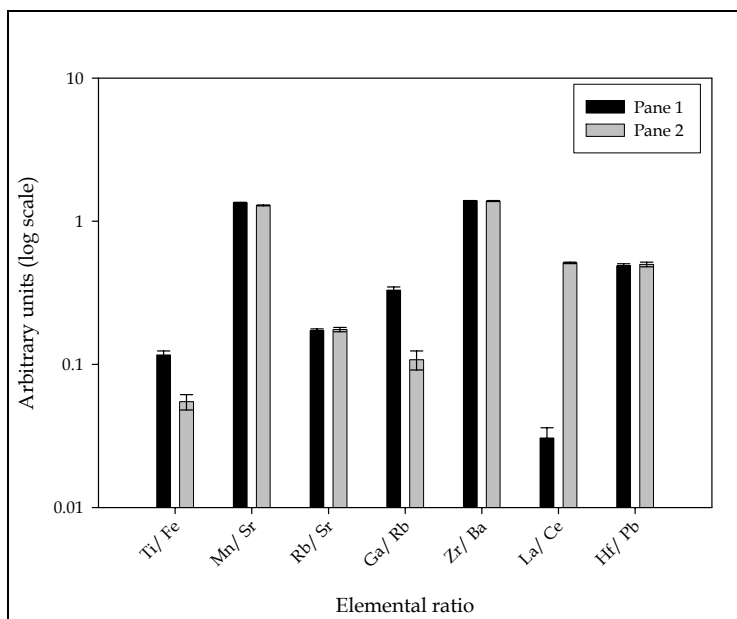


Figure 26. Within-sample variation: Panes 1 and 2 of Vitro Flex/ Carlite 2

Errors shown are 95% confidence limits, corrected for logarithmic scaling.

Like Vitro Flex/ Carlite 2, most windshields were composed of panes of glass having obvious differences in composition. PLOF 1a and 1b were composed of apparently similar profiles when compared graphically. According to hypothesis testing using Hotelling's T^2 at 95% confidence, there was not significant difference in the compositions of Panes 1 and 2 of PLOF 1a. There was, however, a significant difference between the two panes of PLOF 1b at 95% confidence.

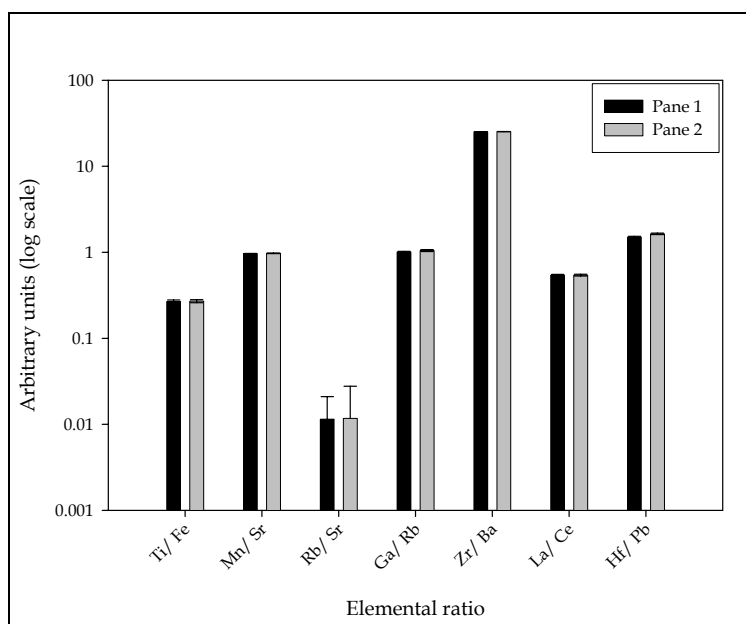


Figure 27. Within-sample variation: Panes 1 and 2 of PLOF 1a

Errors shown are 95% confidence limits, corrected for logarithmic scaling.

These results further emphasize a need to collect adequate reference samples when comparing questioned fragments to the putative source. Out of this sample subset, it was more likely to encounter a windshield composed of two different panes of glass than to encounter a windshield composed of two similar panes of glass. To adequately

describe the reference glass, fragments must be collected from each pane in as many locations as possible.

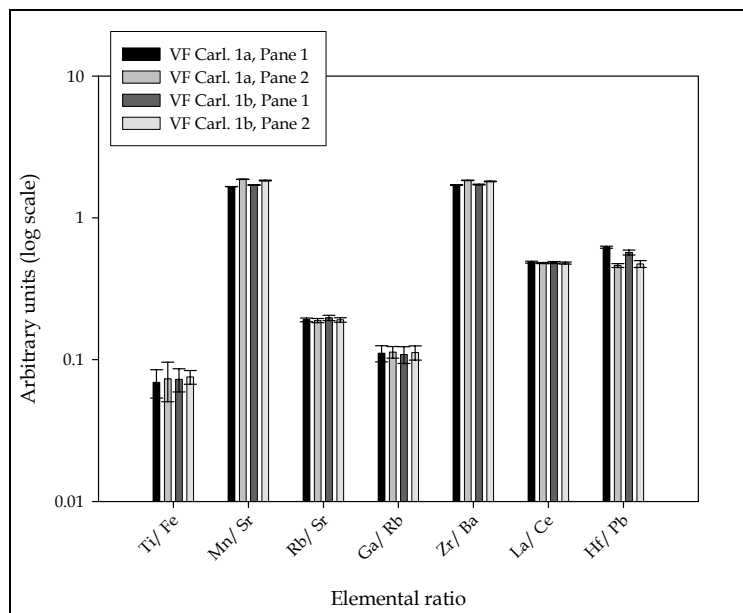


Figure 28. Correlation of Panes in Vitro Flex Carlite 1a and 1b

Errors shown are 95% confidence limits, corrected for logarithmic scaling.

In addition to PLOF 1a and 1b, there were two additional pairs of windshields manufactured in the same lot: Vitro Flex/ Carlite 1a, 1b and Sekurit 1a, 1b. An interesting pattern emerged when all four panes of Vitro Flex/ Carlite 1a and 1b were compared (Figure 28). By a simple graphical comparison, it appeared that Pane 1 of Vitro Flex/ Carlite 1a was similar to Pane 1 of Vitro Flex/ Carlite 1b. Similarly, Pane 2 of Vitro Flex/ Carlite 1a appeared to be similar to Pane 2 of Vitro Flex/ Carlite 1b. While these samples were apparently similar, they were statistically distinguishable using Hotelling's T^2 test at 95% confidence.

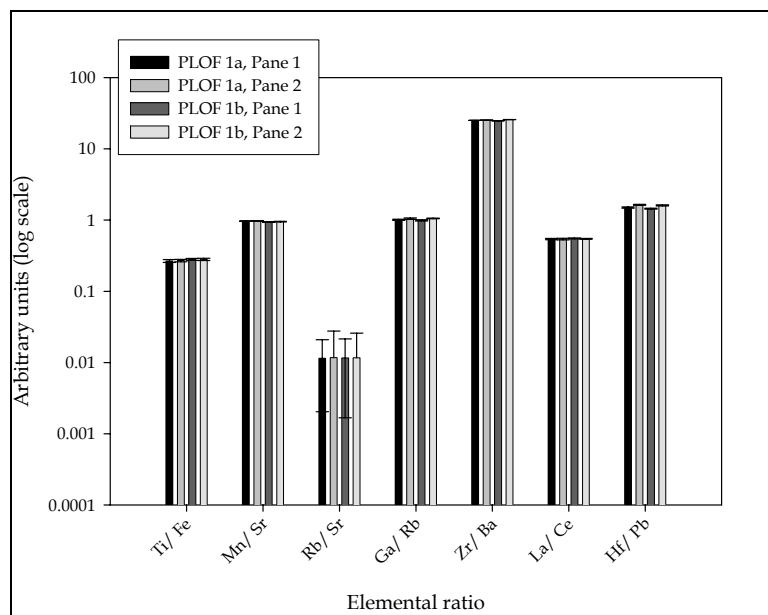


Figure 29. Correlation of Panes in PLOF 1a and 1b

Errors shown are 95% confidence limits, corrected for logarithmic scaling.

A similar pattern was observed among the panes of PLOF 1a and 1b. Graphically, it appeared that the inner and outer panes of PLOF 1a and 1b were correlated more so than the inner and outer panes of PLOF 1a or PLOF 1b (Figure 29). In this case, hypothesis testing using Hotelling's T^2 at 95% confidence resulted in significant differences between the two outer panes of PLOF 1a and 1b but insignificant differences between the two inner panes of these windshields.

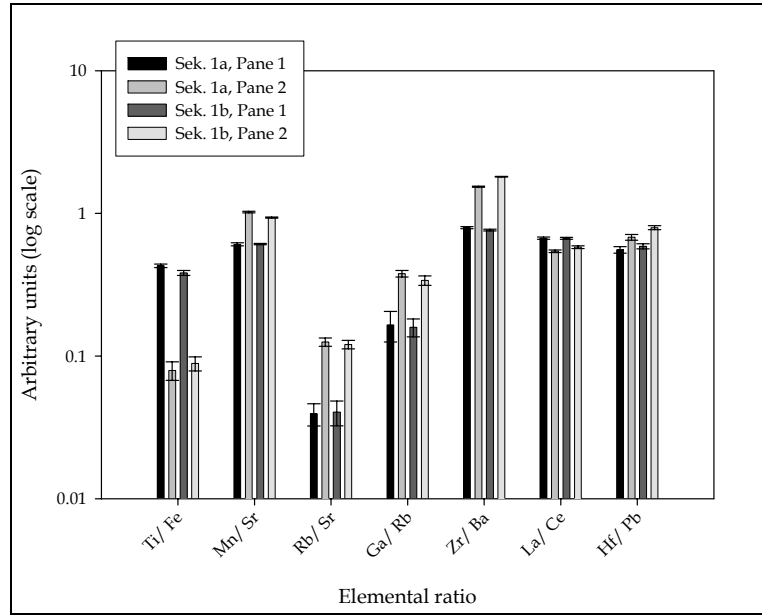


Figure 30. Correlation in Panes of Sekurit 1a and 1b

Errors shown are 95% confidence limits, corrected for logarithmic scaling.

There was no correlation between the inner and outer panes of Sekurit 1a and 1b, either graphically or through hypothesis testing. Each pane could be distinguished from the next (Figure 30).

Elemental variation within a population. The ranges of elemental concentrations observed in the total population varied by one to three orders of magnitude (Table 25). By comparison, the ranges observed within groups of manufacturers were significantly smaller for many elements (Table 26). The Vitro Flex windshields exhibited the greatest precision in elemental composition: the concentrations of rubidium, strontium, zirconium, lanthanum, and hafnium varied by only 2 – 10 % RSD. The Lamisafe windshields exhibited the greatest precision in lanthanum, cerium and lead concentrations (17, 19 and 11 % RSD, respectively) while the Pilkington-LOF windshields exhibited the greatest precision in iron, lanthanum and cerium concentrations (16, 8 and 10 % RSD, respectively).

Table 25. Population variation in 100 panes of automotive windshield glass.

Element	Concentration range observed, $\mu\text{g g}^{-1}$
⁴⁹ Ti	68.3 – 2510
⁵⁵ Mn	10.4 – 913
⁵⁷ Fe	541 – 7386
⁷¹ Ga	0.125 – 33.6
⁸⁵ Rb	0.265 – 60.4
⁸⁸ Sr	12.9 – 214
⁹⁰ Zr	20.7 – 318
¹³⁷ Ba	4.03 – 133
¹³⁹ La	1.34 – 57.0
¹⁴⁰ Ce	2.28 – 3790
¹⁷⁸ Hf	0.607 – 8.64
²⁰⁸ Pb	0.761 – 14.9

Table 26. Elemental variation within groups of manufacturers.

Element	<i>Lamisafe</i> Mean ± St dev, μg g⁻¹	<i>Pilkington-LOF</i> Mean ± St dev, μg g⁻¹	<i>Vitro Flex</i> Mean ± St dev, μg g⁻¹
⁴⁹ Ti	720 ± 840	1450 ± 790	403 ± 58
⁵⁵ Mn	14.1 ± 3.0	49 ± 18	71 ± 14
⁵⁷ Fe	4500 ± 990	5300 ± 850	5000 ± 870
⁷¹ Ga	0.218 ± 0.060	0.59 ± 0.27	0.90 ± 0.45
⁸⁵ Rb	0.94 ± 0.66	0.67 ± 0.16	6.95 ± 0.18
⁸⁸ Sr	46.0 ± 7.8	62 ± 13	37.7 ± 1.7
⁹⁰ Zr	62 ± 29	217 ± 68	183 ± 18
¹³⁷ Ba	11.9 ± 7.3	9.4 ± 2.4	107 ± 14
¹³⁹ La	1.80 ± 0.31	1.82 ± 0.14	3.96 ± 0.14
¹⁴⁰ Ce	3.39 ± 0.66	3.20 ± 0.33	23 ± 38
¹⁷⁸ Hf	1.61 ± 0.67	5.2 ± 1.7	4.55 ± 0.43
²⁰⁸ Pb	0.97 ± 0.11	2.3 ± 1.1	8.8 ± 1.8

These results suggest some utility in fingerprinting glass products by their trace elements. In no way are these results conclusive: there were not enough samples from different production lots of one particular manufacturer to characterize a predictable fingerprint for that glass product. However, the fact that multiple production lots from single manufacturers showed less variation than the population variation observed here warrants further research in this area. This requires the collection of additional windshields produced by the same manufacturer over longer periods of time.

Overall, the total elemental profiles of these fifty windshields was sufficiently variable so as to discriminate between samples produced by the same manufacturer, and sometimes, between samples produced in the same lot. Twenty-one groups of similar automotive windshield glass panes resulted from sequentially separating the entire population of windshields by elemental composition. Each group contained panes of glass made in the same manufacturing lot (Table 27).

Table 27. Groups of similar panes of glass.

<i>Group 1</i>	<i>Group 2</i>
Lamisafe 1a Pane 2 Lamisafe 1b Pane 2	Lamisafe 1a Pane 1 Lamisafe 1b Pane 1
<i>Group 3</i>	<i>Group 4</i>
Lamisafe 2a Pane 1 Lamisafe 2b Pane 1	Lamisafe 2a Pane 2 Lamisafe 2b Pane 2
<i>Group 5</i>	<i>Group 6</i>
Lamisafe 5 Pane 1 Lamisafe 5 Pane 2	Lamisafe 3 Pane 1 Lamisafe 3 Pane 2
<i>Group 7</i>	<i>Group 8</i>
PLOF 1a Pane 1 PLOF 1a Pane 2 PLOF 1b Pane 2	PLOF 2a Pane 2 PLOF 2b Pane 2
<i>Group 9</i>	<i>Group 10</i>
L-N 1 Pane 1 L-N 1 Pane 2	Toyota 1a Pane 1 Toyota 1a Pane 2
<i>Group 11</i>	<i>Group 12</i>
Toyota 1b Pane 1 Toyota 1b Pane 2	Toyota 1d Pane 1 Toyota 1d Pane 2
<i>Group 13</i>	<i>Group 14</i>
Toyota 1e Pane 1 Toyota 1e Pane 2	LOF 1 Pane 1 LOF 1 Pane 2
<i>Group 15</i>	<i>Group 16</i>
Iva 1 Pane 1 Iva 1 Pane 2	Viracon/ PPG 1a Pane 1 Viracon/ PPG 1b Pane 1 Viracon/ PPG 1b Pane 2
<i>Group 17</i>	<i>Group 18</i>
PPG 3 Pane 1 PPG 3 Pane 2	Vitro Flex/ Carlite 1a Pane 1 Vitro Flex/ Carlite 1b Pane 1
<i>Group 19</i>	<i>Group 20</i>
Vitro Flex/ Carlite 1a Pane 2 Vitro Flex/ Carlite 1b Pane 2	Crinamex 2b Pane 1 Crinamex 2c Pane 1
<i>Group 21</i>	
Ford 2 Pane 1 Ford 2 Pane 2	

The fact that only panes of glass manufactured within the same production lot were found to be similar is a significant finding. Out of 100 panes representing 17 manufacturers and approximately 10 years of manufacture, there were no “random” matches between glasses not sharing a common manufacture. Additionally, the majority

of automotive windshield panes were distinguishable from all other panes of glass – including those sharing a common manufacture. Sixty-six of 100 panes were distinguishable from all other panes of glass, while 44 of 100 panes were similar to panes of glass manufactured in the same production lot. These results illustrate the discriminatory power available from the chemical analysis of glass, especially the analysis of trace elements.

Summary. During the manufacturing process, there are many opportunities to introduce variability in the chemical composition of float glass. This is related to the source of the raw materials (and subsequently, the purity of the raw materials), and the unique mixtures of raw materials that each manufacturer makes use of. One important source of variation is the addition of cullet into the batch mixture, since manufacturers are not always required to use the same amount of recycled materials. To exploit this variability in chemical composition, elemental profiling has been used as a means to differentiate glass samples that fall into the same general class of glass but do not share a common manufacture.

One important consideration in the application of highly discriminating analytical techniques is the potential for sample heterogeneity, especially with respect to such a large sample type as an automotive windshield. It was found that most panes of automotive windshield glass varied in composition by location (top left, top center, ... etc.), but that these variations were usually less than 10% RSD. Further, it was found that these variations were random; there was no instance where all the top subsamples were similar but different to the bottom subsamples, for example. While there were variations within a pane of automotive windshield glass, these differences were insignificant when

the precision of analytical technique closely matched the overall variation in the sample. The potential to distinguish glass fragments originating from the same discrete glass sample is great, since the typical precision afforded by LA-ICP-MS is < 5% RSD while the typical variation in windshield composition is 10% RSD.

Not only does statistically significant variation in composition exist within discrete panes of automotive windshield glass, significant variation in composition exists between panes of a single windshield. In 9 out of 10 windshields examined for sample homogeneity, the inner and outer panes could be distinguished. This outcome was not surprising, since windshields are often manufactured from panes of glass produced in separate batches. The potential for significant variation between the panes comprising a single windshield necessitates the collection of multiple reference samples from both panes of a suspect's windshield. When suitable reference samples are not available, the potential for heterogeneity between the panes of a single windshield must be considered. Establishing a minimum number of reference samples requires further research; with further experimentation, it may be possible to model the expected outcomes of comparing evidentiary glass to increasingly fewer reference samples of the same origin.

The population variation observed in this study was such that 66 of 100 panes of glass could be distinguished from all other panes of glass. The 44 remaining panes of glass were similar to at least one other pane of glass produced in the same manufacturing lot, resulting in 21 groups of similar panes. Overall, the population variation observed in all 50 windshields was much greater than the variation observed within groups of manufacturers.

Hypothesis testing was applied to PLOF 1a and 1b (Group 7). Three of the four panes represented by this manufacturing lot were statistically indistinguishable. Thus, the composition of glass – when described by the seven elemental ratios used here – is not unique. However, the individualizing capability of these seven elemental ratios is such that individual manufacturing lots can be distinguished in the absence of hypothesis testing.

Elemental Variation in Float Glass

Quality control (QC) samples of float glass manufactured by two local glass furnaces were analyzed to determine whether the patterns of variation observed in windshields produced in the same manufacturing lot could be repeated in other float glass products. The two locations that we obtained samples from were Pittsburgh Plate Glass (PPG) Company in Fresno, CA and Pilkington-Libbey Owens Ford (previously, Libbey Owens Ford or LOF) in Lathrop, CA.

There were three instances where spatial variations in the PPG float glass ribbon became apparent, all involving the ratio of ^{90}Zr to ^{137}Ba . In the first set of QC samples, collected on the first day of the month collected at 1500 h, there were differences in $^{90}\text{Zr}/^{137}\text{Ba}$ between the QC sample collected from the left side of the ribbon and the QC samples collected from the center and right locations of the glass ribbon (Figure 31). The center QC sample collected on the second day at 1500 h differed from both the right and left sides of the float glass ribbon, while the right QC sample collected on the third day at 2300 h differed from the center and left locations. The remaining sets of QC samples collected from the left, right and center of the ribbon were similar in composition.

In addition to spatial variations, the PPG batch samples also exhibited compositional variations within a single day of manufacture (Figure 32). In each of the three days examined, there were differences in the compositions of the QC samples collected from the center of the float glass ribbon at different time points. The center samples collected on the first day, differed in amounts of $^{49}\text{Ti}/^{57}\text{Fe}$ at 1500 h and 2300 h; the center samples collected on the second day also differed in $^{49}\text{Ti}/^{57}\text{Fe}$ as well as $^{55}\text{Mn}/^{88}\text{Sr}$. On the third day (shown in Figure 32), the center QC samples differed in $^{85}\text{Rb}/^{88}\text{Sr}$ and $^{90}\text{Zr}/^{137}\text{Ba}$.

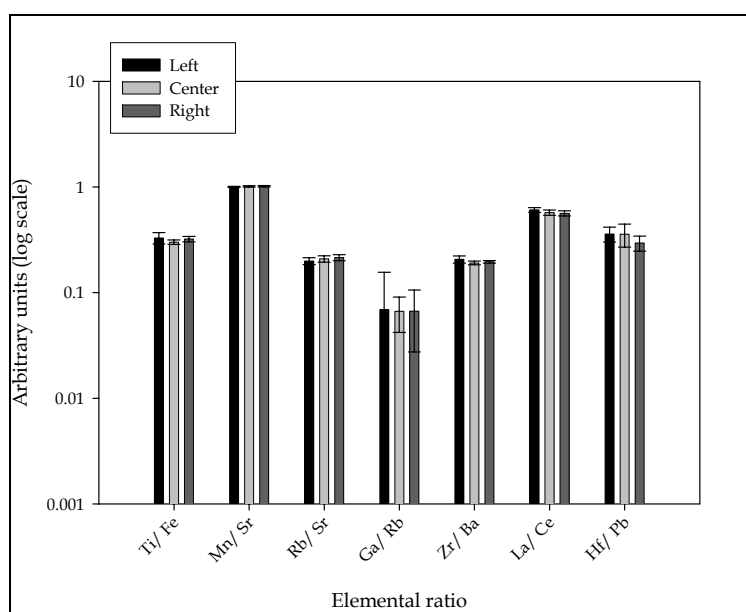


Figure 31. Spatial variation in float glass ribbon (PPG, 2004)

Errors shown are 95% confidence limits, corrected for logarithmic scaling.

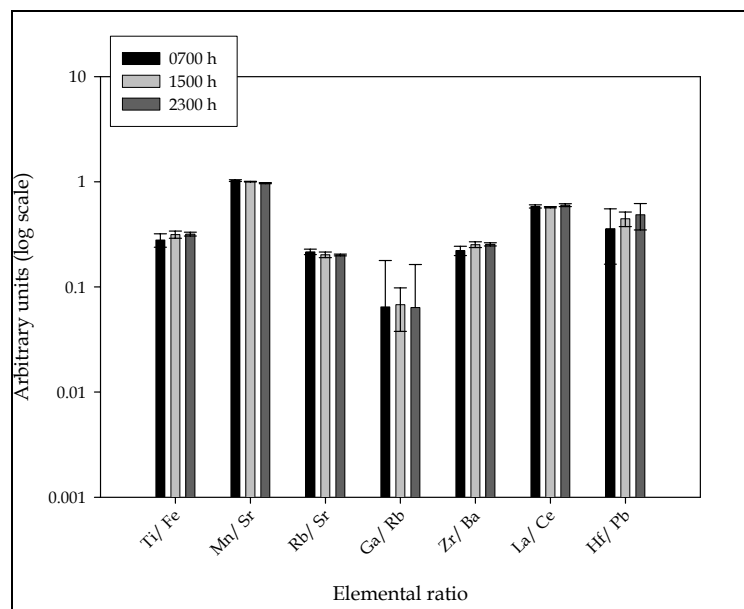


Figure 32. Daily variation in float glass ribbon (PPG, 2004)

Errors shown are 95% confidence limits, corrected for logarithmic scaling.

Short-term variation was observed in the QC samples collected from PPG (Figure 33), while LOF and Pilkington-LOF exhibited no compositional differences in the three consecutive days examined (Figure 34). The PPG QC samples collected the second day was distinguishable from the first and third days in $^{49}\text{Ti}/^{57}\text{Fe}$, $^{55}\text{Mn}/^{88}\text{Sr}$, and $^{139}\text{La}/^{140}\text{Ce}$, while it was the QC sample collected on the first day that differed from the second and third days in $^{90}\text{Zr}/^{137}\text{Ba}$. With the exception of $^{90}\text{Zr}/^{137}\text{Ba}$, the observed differences were less than 10% of the elemental ratio.

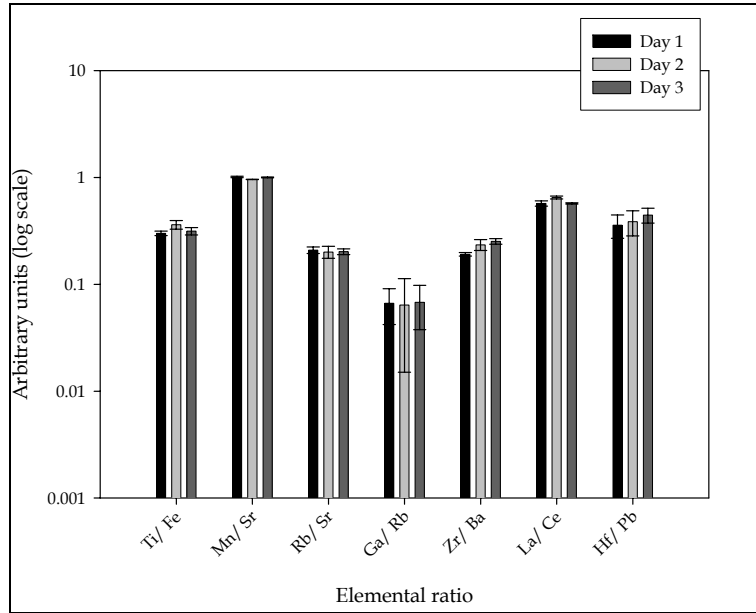


Figure 33. Short-term variation in PPG float glass

Errors shown are 95% confidence limits, corrected for logarithmic scaling.

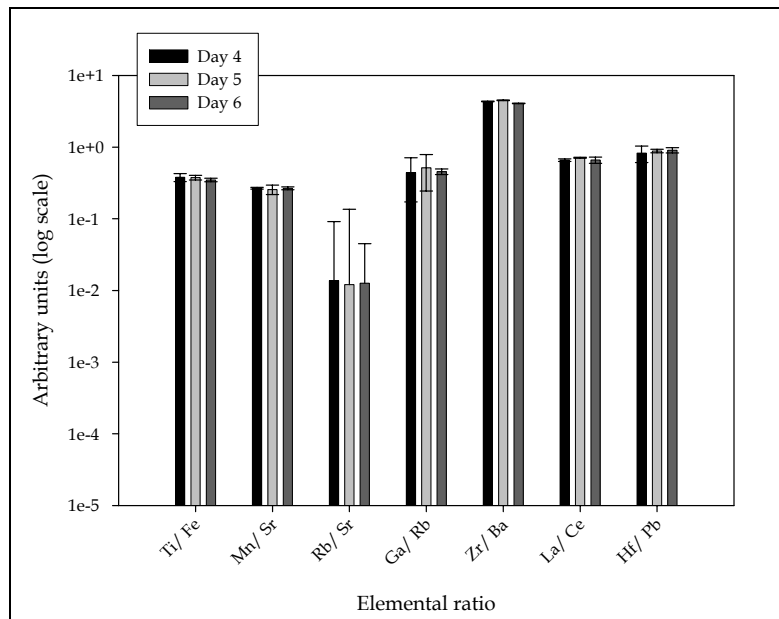


Figure 34. Short-term variation in Pilkington-LOF float glass

Errors shown are 95% confidence limits, corrected for logarithmic scaling.

Long-term variations in batch composition were most observed in $^{90}\text{Zr}/^{137}\text{Ba}$, as was observed in the June 2004 PPG QC samples (Figure 35). There were long-term variations apparent in $^{178}\text{Hf}/^{208}\text{Pb}$ as well as $^{90}\text{Zr}/^{137}\text{Ba}$ in the Pilkington-LOF QC samples collected in March and April of 2005 (Figure 36). The Pilkington-LOF QC samples collected in May of 2005 exhibited long-term variations in $^{49}\text{Ti}/^{57}\text{Fe}$. QC samples collected from LOF in November and December of 1997 exhibited differences in $^{90}\text{Zr}/^{137}\text{Ba}$ and $^{178}\text{Hf}/^{208}\text{Pb}$ (Figure 37).

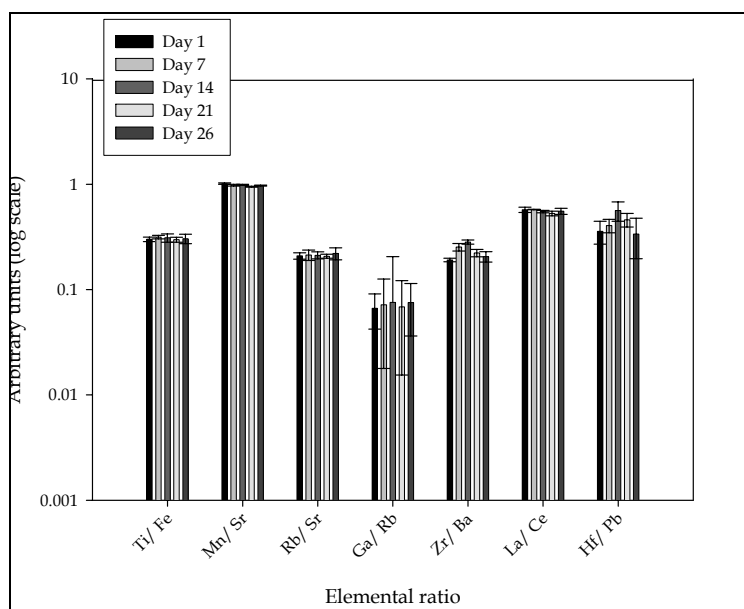


Figure 35. Long-term variation in PPG float glass

Errors shown are 95% confidence limits, corrected for logarithmic scaling.

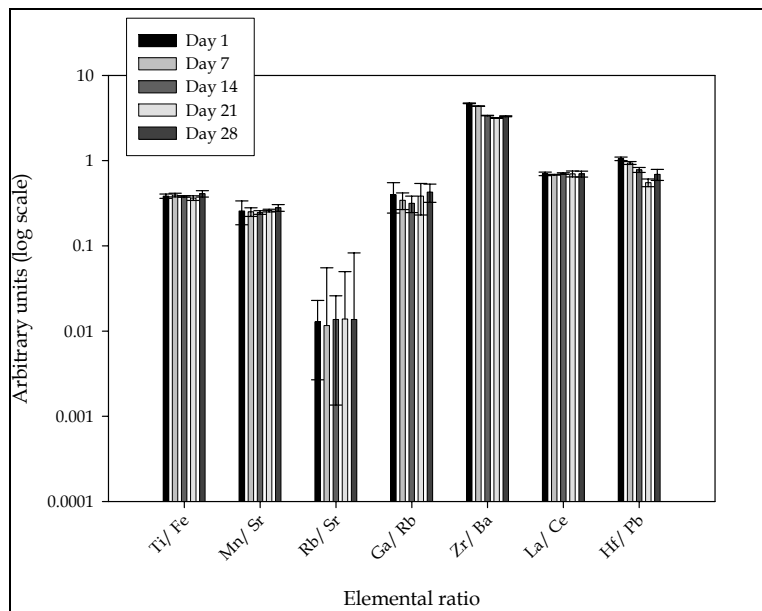


Figure 36. Long-term variation in Pilkington LOF float glass (March – April 2004)

Errors shown are 95% confidence limits, corrected for logarithmic scaling.

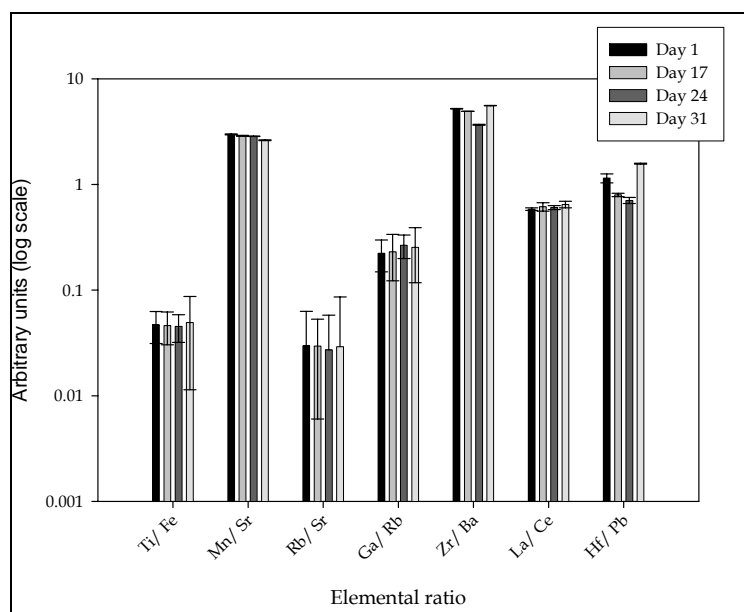


Figure 37. Long-term variation in LOF float glass

Errors shown are 95% confidence limits, corrected for logarithmic scaling.

With regard to short-term variability in glass composition, there was a significant discrepancy between manufacturers. Only one of the four float glass batches exhibited short-term variations in composition. The QC samples collected from PPG in June of 2004 differed in composition over as little as a 16-hour manufacturing period; comparable QC samples collected from LOF and Pilkington-LOF did not vary in composition over a 72-hour period. These results indicate that short-term variations in glass composition due to manufacture are greatly dependent on the specific manufacturer in question. Despite sharing a similar method of glass production, PPG, LOF and Pilkington-LOF do not share similar patterns of compositional variation.

There was not a significant discrepancy between manufacturers when the long-term variation in glass composition was considered; this suggests the possibility that the short-term variation observed in PPG glass was an isolated event. It is possible that the short-term variation observed in the PPG glass was the result of mechanical failure. Certainly, there is a particular rate of failure associated with the mechanics of raw material homogenization, mixing and delivery into the hopper. Such an event (or series of events) has a certain rate of occurrence, regardless of the manufacturer in question. It is also possible that the short-term variation in PPG glass production was the result of a purposeful modification of batch materials. The source of any raw material could have been changed, as well as the amounts of the raw materials. The incorporation of varying amounts of cullet is a frequent type of batch modification practiced by glass manufacturers. Because mechanical failures and batch modifications have a particular rate of occurrence (which may or may not be predictable) it cannot be concluded that PPG glass is more variable than LOF or Pilkington-LOF glass since the analysis of

additional LOF or Pilkington-LOF QC may have revealed comparable short-term variations. It can be concluded, however, that compositional variations in certain glass products may be observed even when these products are manufactured at or around the same time.

Of course, short-term variation in glass production is desirable to the forensic analyst since greater short-term variations in glass production increase the individualizing potential of elemental analysis. From these results, it is apparent that certain production lots will exhibit greater variations over other production lots; further, there is greater potential to discriminate between glass products manufactured at least several weeks apart. The forensic significance of these variations, however, depends on the sample type in question. More specifically, the forensic significance of these variations depends on the size of the sample type in question; sample size has a significant impact on the potential for within-sample heterogeneity.

Intuitively, it is reasonable to assume that larger float glass products are more likely to exhibit compositional variations than smaller float glass products since the float glass batch can vary in space and time. The likelihood for short-term variations in the elemental composition of the float glass ribbon translates to the potential for a high degree of discrimination for relatively small float glass products. Alternatively, the potential for short-term variations in the float glass ribbon may become manifest as within-sample variation in larger float glass products. Previously, it was observed that automotive windshield glass sometimes exhibits statistically significant within-sample variation in elemental composition. This finding has had a considerable impact on the interpretation of comparative analyses using LA-ICP-MS: in the event that a questioned

and reference fragment are found to be different, the potential for heterogeneity in the glass product of interest must be addressed. When the potential for sample heterogeneity has been eliminated, differences in the elemental compositions of questioned and reference fragments are obvious exclusions. Further, similarities in the elemental compositions of questioned and reference fragments are an excellent indication that the glass has a common origin.

Summary. The composition of float glass varies noticeably in time and space. Depending on the manufacturer, the float glass batch composition may change in as little as 16 hours of manufacture; further, the left, center and right portions of the batch may be distinguishable. The long-term variation in float glass composition is such that the potential for discriminating among glass products made at or around the same time is considerable.

The forensic significance of compositional variations in float glass due to manufacture depends greatly on the forensic sample type in question. Because larger float glass samples have a greater likelihood of incorporating compositional variations, sample heterogeneity may result in the false exclusion of a questioned fragment originating from the reference glass sample. The potential impact of sample heterogeneity in the forensic analysis of automotive windshield glass has been previously explored; it was found that multiple reference fragments from both panes of a windshield must be analyzed to obtain the best estimate of the natural compositional variation. These findings may be applied to other float glass products. For example, larger windows are expected to show greater within-sample heterogeneity than smaller windows. Original automotive side windows, likely to be manufactured at the same time, may exhibit significant compositional

differences. Thus, it is important to collect multiple reference fragments from each pane of reference glass to account for the within-sample variation of the suspected origin glass.

Conclusions

In summary, we have made several important findings:

- While solution nebulization and laser ablation are both effective sample introduction techniques for the casework analysis of glass by ICP-MS, laser ablation is the sample introduction technique of choice;
- The trace elemental profile used here for the forensic discrimination of glass is not unique to individual windshields;
- Automotive windshield glass can exhibit heterogeneity in two ways: (1) within-pane, and (2) between-panes;
- There is significantly greater variation in the elemental profiles of a population of 50 windshields than there is within a group representing a single manufacturer;
- Elemental profiling is highly distinguishing, enabling examiners to differentiate between and within manufacturing lots; and, finally,
- The short- and long-term variation in float glass batch composition indicates that other glass products such as containers, and windows can exhibit similar patterns of heterogeneity, population variability and within-manufacturer variability as automotive windshields.

These findings impact the collection of glass exemplars, the treatment of LA-ICP-MS data, and the interpretation of trace elemental data. The potential for heterogeneity in automotive windshields and other float glass products requires the collection of multiple exemplars from as many locations in the putative glass source as possible. Selecting the appropriate method of comparing reference and questioned samples depends on the sample introduction technique used: the use of laser ablation requires the use of elemental ratios to correct for instrumental drift; while the use of solution nebulization requires an accounting for the variability in acid dissolution contributes to the forensic analysis of glass. The interpretation of similar or dissimilar elemental profiles depends greatly upon a knowledge of the natural heterogeneity in float glass and the analytical limitations of the instrumental technique employed. Certainly, the finding that reference and questioned glass fragments are similar in trace elemental composition is significant – this finding would strongly support an association between these glass fragments. The finding that reference and questioned glass fragments are dissimilar in elemental composition would not immediately support an exclusion. In certain situations, an inconclusive result is certainly warranted. In the case where multiple reference samples could be collected from each pane of a windshield suspected to be the source of a questioned glass fragment, differing elemental profiles would support a firm exclusion. In the case where multiple reference samples are not available for comparison, the degree to which the reference and questioned glass fragments differ must be considered since minor differences can be examples of heterogeneity. In the latter situation, an inconclusive result may be offered with confidence given the within-sample variability observed in this study.

The goal of this project was to provide caseworkers with sufficient information regarding the elemental variation of float glass to assign the appropriate significance to forensic glass analysis by ICP-MS. In conducting this research, we evaluated the potential for correlating automotive windshield glass with the correct manufacturer. Preliminarily, these results support this potential. Further research into the use of trace elemental profiling to fingerprint float glass manufacturers will prove to be a worthwhile effort.

Acknowledgements

The authors wish to acknowledge the kind sample donations made by Craig Schoeneschafer of Mygrant Glass Company, Central Valley Tow; Dick Henricksen of Pilkington-Libbey Owens Ford; and Fred Tulleners of the UC Davis Forensic Science Graduate Group. We are also grateful for the efforts of Cheryl Sershen and Jerome Braun for their assistance with statistics, and Mark R. McCoy for sharing his programming knowledge.

Literature cited

1. Allen TJ, Scranage JK. The transfer of glass – part 1: Transfer of glass to individuals at different distances. *For Sci Intl* 1998 (93) 167 – 174.
2. Allen TJ, Hoefler K, Rose SJ. The transfer of glass – part 2: A study of the transfer of glass to a person by various methods. *For Sci Intl* 1998 (93) 175 – 193.
3. Allen TJ, Hoefler K, Rose SJ. The transfer of glass – part 3: The transfer of glass from a contaminated person to another uncontaminated person during a ride in a car. *For Sci Intl* 1998 (93) 195 – 200.
4. Allen TJ, Cox AR, Barton S, Messam P, Lambert JA. The transfer of glass – part 4: The transfer of glass fragments from the surface of an item to the person carrying it. *For Sci Intl* 1998 (93) 201 – 208.
5. Locke J, Underhill M. Automatic refractive index measurement of glass particles. *For Sci Intl* 1985 (27) 247 – 260.
6. Locke J, Underhill M, Rusell P, Cox P, Perryman AC. The evidential value of dispersion in the examination of glass. *For Sci Intl* 1986 (32) 219 – 227.
7. Hamer P. Microscopic techniques for glass examination, in *Forensic examination of paint and glass*. B Caddy (Ed). New York; Taylor & Francis: 2001.
8. Neufeld L. Application of laser ablation ICP-MS to the analysis of forensic glass samples. *Spectroscopy Magazine* July 2005.
9. Catterick T, Hickman DA. The quantitative analysis of glass by inductively coupled plasma –atomic-emission spectrometry: A five element survey. *For Sci Intl* 1981 (17) 253 – 263.
10. Hickman DA, Harbottle G, Sayre EV. The selection of the best elemental variables for the classification of glass samples. *For Sci Intl* 1983 (23) 189 – 212.
11. Ryland SG. Sheet or container?—Forensic glass comparisons with an emphasis on source classification. *J For Sci* 1986 (31) 1314 – 1329.
12. Blacklock EC, Rogers A, Wall CD, Wheals BB. Quantitative analysis of glass by emission spectrography: a six-element survey. *For Sci* 1976 (7) 121 – 130.
13. Hughes JC, Catterick T, Southeard G. The quantitative analysis of glass by atomic absorption spectroscopy. *For Sci* 1976 (8) 217 – 227.

14. German B, Morgans D, Butterworth A, Scaplehorn A. A survey of British container glass using spark source mass spectrometry with electrical detection. *J For Sci Soc* 1978 (18) 113 – 121.
15. Reeve V, Mathieson J, Fong, W. Elemental analysis by energy dispersive X-ray: A significant factor in the forensic analysis of glass. *J For Sci* 1976 (21) 291 – 306.
16. Pitts SJ, Kratochvil B. Statistical discrimination of flat glass fragments by instrumental neutron activation analysis, Methods for forensic science applications. *J For Sci* 1991 (36) 122 – 137.
17. Koons RD, Peters CA, Rebbert PS. Comparison of refractive index, energy dispersive X-ray fluorescence and inductively coupled plasma atomic emission spectrometry for forensic characterization of sheet glass fragments. *J Anal At Spectrom* 1991 (6) 451 – 456.
18. Buscaglia JA. Elemental analysis of small glass fragments in forensic science. *Anal Chim Acta* 1994 (288) 17 – 24.
19. Koons RD, Buscaglia JA. The forensic significance of glass composition and refractive index measurement. *J For Sci* 1999 (3) 496 – 503.
20. Koons RD, Fiedler C, Rawalt RC. Classification and discrimination of sheet and container glasses by inductively coupled plasma-atomic emission spectrometry and pattern recognition. *J For Sci* 1988 (33) 49 – 67.
21. Zurhaar A, Mullings L. Characterization of forensic glass samples using inductively coupled plasma mass spectrometry. *J Anal At Spectrom* 1990 (5) 611-617.
22. Trejos T, Almirall JR. Sampling strategies for the analysis of glass fragments by LA-ICP-MS part I. Microhomogeneity study of glass and its application to the interpretation of forensic evidence *Talanta* 2005 (67) 388 – 395.
23. Almirall JR. Elemental analysis of glass fragments, in *Forensic Examination of Glass and Paint*. B Caddy (Ed). New York; Taylor & Francis: 2001.
24. Parouchais T, Warner IM, Palmer LT, Kobus H. The analysis of small glass fragments using inductively coupled plasma mass spectrometry. *J For Sci* 1996 (41) 351 – 360.
25. Suzuki Y, Sugita R, Suzuki S, Marumo Y. Forensic discrimination of bottle glass by refractive index measurement and analysis of trace elements with ICP-MS. *Analyt Sci* 2000 (16) 1195 – 1198.

26. Montero S, Hobbs AL, French TA, Almirall JR. Elemental analysis of glass fragments by ICP-MS as evidence of association: Analysis of a case. *J For Sci* 2003 (48) 1101 – 1107.
27. ASTM E2330-04: Standard test method for determination of trace elements in glass samples using inductively coupled plasma mass spectrometry (ICP-MS).
28. Watling RJ, Lynch BF, Herring D. Use of laser ablation inductively coupled plasma mass spectrometry for fingerprinting scene of crime evidence. *J Anal At Spectrom* 1997 (12) 195 – 203.
29. Schmidt T. Identification of pharmaceutical glasses by laser ablation ICP-MS. *Pharmazie* 2001 (56) 852 – 856.
30. Trejos T, Montero S, Almirall JR. Analysis and comparison of glass fragments by laser ablation inductively coupled plasma mass spectrometry (LA-ICP-MS) and ICP-MS. *Anal Bioanal Chem* 2003 (376) 1255 – 1264.
31. Montaser A, Minnich MG, McLean JA, Liu H, Caruso JA, McLeod CW. Sample introduction in ICPMS, in *Inductively coupled plasma mass spectrometry*. A Montaser (Ed). New York; Wiley: 1998.
32. Sharp BL. Pneumatic nebulizers and spray chambers for inductively coupled plasma mass spectrometry, A review. Part 1 Nebulisers. *J Anal At Spectrom* 1988 (3) 613 – 652.
33. Sharp BL. Pneumatic nebulizers and spray chambers for inductively coupled plasma mass spectrometry, A review. Part 2 Spray chambers. *J Anal At Spectrom* 1988 (3) 939 – 963.
34. Mora J, Maestre S, Hernandis V, Todoli JL. Liquid sample introduction in plasma spectrometry. *Trends Anal Chem* 2003 (22) 123 – 132.
35. Fisher A, Hill SJ. Instrumentation for ICP-AES, in *Inductively coupled plasma spectrometry and its applications*. SJ Hill (Ed). Boca Rotan; CRC Press: 1999.
36. Heitkemper DT, Platek SF, Wolnik KA. Elemental and microscopic analysis in the 1993 soft drink/ syringe product tampering incidents. *J For Sci* 1995 (40) 664 – 669.
37. Marumo Y, Inoue T, Seta S. Analysis of inorganic impurities in seized methamphetamine samples. *For Sci Intl* 1994 (69) 89 – 95.
38. Tanaka T, Hara K, Tanimoto A, Kentaro K, Kita T, Tanaka N, Takayasu T. Determination of arsenic in blood and stomach contents by inductively coupled plasma/ mass spectrometry (ICP/MS). *For Sci Intl* 1996 (81) 43 – 50.

39. Dufosse T, Touron P. Comparison of bullet alloys by chemical analysis: Use of the ICP-MS method. *For Sci Intl* 1998 (91) 197 – 206.
40. Spence LD, Baker AT, Byrne JP. Characterization of document paper using elemental compositions determined by inductively coupled plasma mass spectrometry. *J Anal At Spectrom* 2000 (15) 813 – 819.
41. Lundell GEF. The chemical analysis of things as they are. *Anal Ed Ind Eng Chem* 1933 (5) 221 – 225.
42. Gunther D, Jackson SE, Longerich HP. Laser ablation and ark/ spark solid sample introduction into inductively coupled plasma mass spectrometers. *Spectrochim Acta B* 1999 (54) 381 – 409.
43. Gunther D, Horn I, Hattendorf B. Recent trends and developments in laser ablation-ICP-mass spectrometry. *Fres J Anal Chem* 2000 (368) 4 – 14.
44. Russo RE, Mao X, Liu H, Gonzalez J, Mao SS. Laser ablation in analytical chemistry – A review. *Talanta* 2002 (57) 425 – 451.
45. Russo RE, Mao XL, Liu C, Gonzalez J. Laser assisted plasma spectrochemistry: Laser ablation. *J Anal At Spectrom* 2004 (19) 1084 – 1089.
46. Darke SA, Tyson JF. Interaction of laser radiation with solid materials and its significance to analytical spectrometry. *J Anal At Spectrom* 1993 (8) 145 – 209.
47. Stix J, Gauthier G, Ludden JN. A critical look at quantitative laser ablation ICP-MS analysis of natural and synthetic glasses. *Can Minerol* 1995 (33) 435 – 444.
48. Ducreux-Zappa M, Mermet JM. Analysis of glass by UV laser ablation inductively coupled plasma atomic emission spectrometry. Part 2. Analytical figures of merit. *Spectrochim Act B* 1996 (51) 333 – 341.
49. Arrowsmith P. Laser ablation of solids for elemental analysis by inductively coupled plasma mass spectrometry. *Anal Chem* 1987 (59) 1437 – 1444.
50. Hattendorf B, Latkoczy C, Gunther D. Laser ablation ICP-MS. *Anal Chem* 2003 341A – 347A.
51. Cromwell EF, Arrowsmith P. Semiquantitative analysis with laser ablation inductively coupled plasma mass spectrometry. *Anal Chem* 1995 (67) 131 – 138.
52. Copley, G. The composition and manufacture of glass and its domestic and industrial applications, in *Forensic Examination of Glass and Paint*. B Caddy (Ed). New York; Taylor & Francis: 2001.

53. Maloney, FJ Terence. *Glass in the Modern World: A Study in Materials Development*. London; Aldus: 1967.
54. Kempenaers L, Janssens K, Jochum KP, Vincze L, Vekemans B, Somogyi A, Drakopoulos M, Adams F. Micro-heterogeneity study of trace elements in USGS, MPI-DING and NIST glass reference materials by means of synchrotron micro-XRF. *J Anal At Spectrom* 2003 (18) 350 – 357.
55. Duckworth DC, Morton SJ, Bayne CK, Koons RD, Montero S, Almirall JR. Forensic glass analysis by ICP-MS: a multi-element assessment of discriminating power *via* analysis of variance and pairwise comparisons. *J Anal At Spectrom* 2002 (17) 662 – 668.
56. Pearce NJG, Perkins WT, Westgate JA, Gorton MP, Jackson SE, Neal CR, Chenery SP. A compilation of new and published major and trace element data for NIST SRM 610 and NIST SRM 612 glass reference materials. *Geost Newsl* 1997 (21) 115 – 144.
57. Miller JN, Miller JC. *Statistics and Chemometrics for Analytical Chemistry*, 4th ed. New York; Prentice Hall: 2000.
58. Glitter Time Resolved Software v 4. van Achterbergh, Ryan, Griffin. © McQuarrie 2001.
59. Dodds AJ. Forensic Glass Analysis by ICP-MS, Volume I: Sample Introduction Techniques [Thesis]. Davis (CA): Univ. of California, 2005.
60. US Department of Transportation Numbers, published online at [www.glasslinks.com]. Accessed June 2004.
61. Curran JM, Hicks TN, Buckleton JS. *Forensic Interpretation of Glass Evidence*. New York; CRC Press: 2000.